Title
The Thin Film Polycaprolactone Device: A platform technology for biodegradable and tunable long acting drug delivery implants.

Author
Schlesinger, Erica

Publication Date
2015

Peer reviewed|Thesis/dissertation

The Thin Film Polycaprolactone Device: A platform technology for biodegradable and tunable long acting drug delivery implants.

by

Erica B. Schlesinger

DISSERTATION

Submitted in partial satisfaction of the requirements for the degree of

DOCTOR OF PHILOSOPHY

in

Bioengineering

in the

GRADUATE DIVISION

of the

UNIVERSITY OF CALIFORNIA, SAN FRANCISCO

AND

UNIVERSITY OF CALIFORNIA, BERKELEY

Dedication

This dissertation is dedicated to my family – my sister, who I never do anything without, my brother who paved the way, and to my parents, my mother who inspired my love of science and creativity, and my father who made the pursuit of it possible.

Also to my boyfriend for his understanding and patience, and to the family and friends who were a vital source of support through the plentitude of ups, downs and "Oh No!" moments.

And to those who kept my sanity in check.

Acknowledgments

I'd like to acknowledge all of the guidance and support of my mentor and PI Tejal Desai, as well as her lab group. In particular, I'd like to acknowledge the contribution to sampling and data collection that made this work possible by Daniel Johengen, Lalitha Muthusubramaniam, and Jean Kim.

I'd like to acknowledge all of the contributions from the TIP Program team to the work on developing a subcutaneous TFPD for HIV PrEP, with special thanks to Ariane van der Straten and Ellen Leucke for all of their hard work and support in leading the initiative. In addition, this research was made possible by the generous support of the American people through the U.S. President's Emergency Plan for AIDS Relief. The contents are the responsibility of the authors and do not necessarily reflect the views of USAID, PEPFAR, or the United States Government.

I'd additionally like to acknowledge Gilead Sciences for providing Tenofovir Alafenamide Fumarate and Elvitegravir, Janssen Pharmaceuticals for providing Rilpivirine, and MAPP Pharmaceuticals for providing VRC01. Without these generous contributions, this work would not have been possible.

There is another team of people who I would like to acknowledge, but due to considerations of confidentiality, I am unable to disclose their affiliations. But, you know who you are.

The Thin Film Polycaprolactone Device: A platform technology for biodegradable and tunable long acting drug delivery implants.

By Erica B. Schlesinger

December, 2015

As healthcare costs rise, demand for reduced healthcare visits and improved efficacy, safety, and user acceptability grow. Among solutions, researchers seek to develop and commercialize long-acting controlled release drug delivery systems. The global revenue for these systems was estimated at $181.9 billion in 2013 with projected revenue growth to $212.8 billion by 2018. [1] Demand for such systems is broad and encompasses applications in the delivery of small molecule pharmaceuticals as well as biologics. Advancements in this area rely on the development of reproducible and controllable fabrication technologies and the availability of materials that are suitable for system duration and design. Such drug delivery systems benefit from an understanding of the underlying mechanisms of controlled release and from easily tunable release kinetics to accommodate pre-clinical through clinical development.

Here we introduce the Thin-Film Polycaprolactone Device (TFPD), a tunable and biodegradable long-acting implant platform technology. The platform is based on the use of porous and nonporous thin-film (< 50 µm) Polycaprolactone (PCL), a bioresorbable and biocompatible polymer, as a membrane for controlled or sustained release of an API from a reservoir. The platform is highly versatile, allowing for delivery of small and large molecules alike, in sizes relevant to both ocular and subcutaneous implants. A deep understanding of the fundamental mechanisms related to both membrane and device design leads to the use of empirical models to easily design and tune devices for any given API and indication. As this delivery platform is so diverse in its potential applications, tunability and design models are key platform features and the focus of this dissertation. The following sections lay out practical approaches to tuning PCL degradation, the fabrication and characterization of various styles of PCL thin-film membranes, the design and tunability of membranes to control release and of reservoir devices according to target product profiles for specific indications. These concepts are then applied to the early development of three long-acting implant systems: an ocular implant for protein therapeutics, a subcutaneous implant for antiretroviral HIV pre-exposure prophylaxis, and a miniaturized subcutaneous contraceptive implant.

Table of Contents

1. **List of Tables** xiii
2. List of Figures xiv
3. **Introduction** 1
Figure 1 Pharmacokinetic profiles representative of different drug delivery profiles 2
4. Polycaprolactone the Polymer 4
4.1. Introduction 4
4.2. Polycaprolactone degradation 5
Figure 2 Schematic of PCL Degradation. 6
Table 1 Predicted PCL degradation time 7
Figure 3 Accelerated degradation of PCL MW blends. 8
Table 2 Projected degradation time for PCL MW blends 9
4.3. Polycaprolactone membrane fabrication 10
4.3.1. Fabrication techniques 10
4.3.1.1. *Nonporous PCL membranes* (nonporous PCL) 10
4.3.1.2. *Nanotemplated PCL membranes* (nanoPCL) 10
4.3.1.3. *Microporous PCL membranes* (mpPCL) 10
4.3.2. Characterization 11
5. **TFPD Membrane Design** 12
5.1. Introduction 12
5.1.1. TFPD schematics 12
Figure 4 TFPD system design schematics. 13
5.1.2. Principles of small molecule diffusion 13
5.1.2.1. Equation 1 Fickian diffusion through a membrane 14
5.1.2.2. Equation 2 Effective diffusion coefficient for a porous membrane 14
5.1.3. Principles of Macomolecule (protein) Diffusion 14
Figure 5 Macromolecule diffusion through porous membranes. 15
5.1.3.1. Fickian diffusion 15
5.1.3.2. Knudsen diffusion 16
5.1.3.3. Single file diffusion 16
5.2. Membrane Design for Small Molecule Pharmaceuticals 17
5.2.1. Introduction 17
5.2.2. Theoretical and empirical equations describing matrix and reservoir designs 17

5.2.2.1. Matrix System 17
Table 3 Physical properties and sources of pharmaceuticals 18
Table 4 Matrix system equation variables (Equation 3) 19
5.2.2.2. Reservoir System 19
Table 5 Reservoir system equation variables (Equation 4) 20
5.2.2.3. Empirical Fits 20
Figure 6 Example of release data and empirical fit. 20
Figure 7 **:** Empirical parameters describing transport of pharmaceuticals in TFPD. 22
5.2.3. Physicochemical properties impact diffusion 23
Figure 8 Correlations between drug properties and empirical diffusion parameters. 24
5.2.4. Predictive models using physicochemical properties to estimate diffusion parameters 25
Figure 9 Predicted and experimental values of empirical parameters 26
Figure 10: Predicted and experimental release profile for Timolol from a TFPD. 28
Figure 11 Predicted and experimental release profile for (LNG) from a PCL matrix film. 29
Figure 12 Predicted and experimental release profile for Primaquine from a TFPD 30
5.2.5. Effect of porosity on diffusion 31
Figure 13 Membrane porosity increases permeability for model pharmaceuticals. 32
Figure 14 Membrane porosity decreases permeability for highly hydrophobic Rilpivirine HCl. 32
5.2.6. Impact of PCL molecular weight on diffusion 33
Figure 15 PCL molecular weight distribution does not affect membrane permeability. 33
5.3. Membrane Design for Macromolecules (Protein Therapeutics) 34
5.3.1. Introduction 34
Figure 16 Scanning Electron Microscope images of nanoPCL and mpPCL cross-sections. 35
5.3.2. NanoPCL Membrane Design 35
Figure 17 Protein release rate from nanoPCL depends on molecule characteristics. 36
Figure 18 Protein release from nanoPCL TFPD is limited by macromolecule excipients. 37
5.3.3. mpPCL Membrane Design 37
Figure 19 Sustained protein release from mpPCL TFPD. 38
Figure 20 Characterizing release profile for therapeutic protein released from mpPCL TFPD. 38
Figure 21 Characterizing release profile for therapeutic mAb released from mpPCL TFPD. 39
Figure 22 Protein release from mpPCL TFPD in the presence of macromolecule excipients. 40
5.3.4. Tuning Release (mpPCL membranes) 40
Figure 23 mpPCL membrane thickness does not impact protein release. 41

6. TFPD Device Design 42
6.1. Introduction 42
6.2. The Target Product Profile 42
6.3. Design Components 44
6.3.1. *Membrane selection* 44
6.3.2. *Device form* 44
6.3.3. *Reservoir Formulation* 45
6.4. Device Design for Small Molecule Pharmaceuticals 46
6.4.1. Release rate is proportional to surface area 46
6.4.2. Release rate is inversely proportion to membrane thickness 47
6.4.3. Formulation excipients 47
6.5. Device Design for Biologics (proteins) 48
6.5.1. Reservoir Concentration 49
Figure 24 mAb release rate from mpPCL TFPD is proportional to reservoir loading 49
Figure 25 Reservoir hydration volume depends on device size. 50
6.5.2. Membrane surface area 50
6.5.3. Applying empirical correlations to a device design model 51
Figure 26 mpPCL window device design model for mAb release. 52
7. Materials & Methods 53
7.1. Definitions 53
7.2. General Procedures 53
7.2.1. PCL Film Fabrication & Characterization – nonporous (npPCL) 53
7.2.2. *PCL Film Fabrication – nanoporous (nanoPCL)* 53
7.2.3. PCL Film Fabrication & Characterization – microporous (mpPCL) 54
7.2.4. Device fabrication (nonporous PCL/mpPCL combination devices) 55
Figure 27 PCL thin film reservoir device fabrication schematic.. 55
7.2.5. Device fabrication (nonporous PCL) 56
7.2.6. *Release Testing* 56
7.3. Accelerated PCL Degradation Specific 57
7.3.1. *Accelerated Degradation* 57
7.3.2. *GPC Analysis* 57
7.4. Pharmaceutical Membrane Design Specific 57
7.4.1. Matrix system film fabrication 57

7.4.2. *Matrix system samples* 58
7.4.3. Reservoir system samples 58
7.4.4. Data analysis 59
7.5. Ocular implant case-study specific: 59
7.5.1. Film Fabrication & Characterization 59
7.5.2. *Device Fabrication & Characterization* 60
7.5.3. Stability studies (nonPCL) 60
7.5.4. Release studies 61
7.5.5. PEG3350 solubility studies 61
7.5.5.1. Study 1 61
7.5.5.2. Study 2 62
7.5.5.3. Study 3 62
7.5.5.4. Study 4 62
7.6. HIV PrEP Subcutaneous Implant Case-Study Specific 63
7.6.1. Antiretroviral formulation and loading: 63
7.6.1.1. Elvitegravir 63
7.6.1.2. Rilpivirine HCl 63
7.6.1.3. Tenofovir Alafenimide Fumarate 64
7.6.2.1. Elvitegravir 64
7.6.2.2. Rilpivirine 64
7.6.2.3. Tenofovir Alafenimide Fumarate 65
7.6.3. Antiretroviral release studies 65
8. Case Study I: A TFPD as an Ocular Implant for Long-Acting Delivery of Protein Therapeutics 67
8.1. Introduction 67
8.2. Protein Formulation 69
8.2.1. *Introduction* 69
Figure 28 Protein stability in PCL thin film reservoir device.. 72
8.2.2. *Formulation Approach 1: Chitosan* 72
8.2.2.1. *Introduction* 72
8.2.2.2. *Chitosan load:* 73
Figure 29 Protein stability of chitosan:protein formulations in PCL thin film reservoir device.. 74
8.2.2.3. Chitosan molecular weight: 74
Figure 30 Impact of Chitosan MW on Protein Stability.. 75

Figure 31 Stability profile for protein released from mpPCL TFPD. 75
Figure 32 Impact of chitosan molecular weight on protein release from mpPCL TFPD. 76
8.2.2.4. Protein stability with chitosan formulation 76
Figure 33 Stability profiles of protein released from mpPCL reservoir devices 77
8.2.2.5. Conclusion 77
8.2.3. *Formulation Approach 2: Polyethylene Glycol (PEG)* 78
8.2.3.1. Introduction 78
8.2.3.2. PEG3350 Load (concentration) 78
Figure 34 Limiting protein solubility with PEG3350. 79
8.2.3.3. Protein stability with PEG3350 formulation 80
Figure 35 Stability profiles of protein release from PCL devices. 80
8.2.3.4. Conclusion 81
8.2.4. Conclusion 81
8.3. Release Rates & Membrane Design 81
8.3.1. Introduction 81
Figure 36 Protein release from nanoPCL devices with excipients. 82
Figure 37 Protein release from mpPCL devices with excipients 83
8.3.2. Device Design 84
8.3.2.1. Device Design: PEG3350 Formulation 85
Table 6 Key parameters for device design utilizing PEG3350 formulation 85
Figure 38 Device design flow-chart for mpPCL protein devices with PEG3350 formulation 85
Figure 39 Empirical correlations relating critical device parameters to critical system parameters for mpPCL protein devices with PEG3350 formulation. 86
8.3.2.2. Device Design: Chitosan Formulation 87
Table 7 Key parameters for device design utilizing chitosan formulation 87
Figure 40 Device design flow-chart for mpPCL protein devices with chitosan formulation 88
Figure 41 Empirical correlations relating critical device parameters to critical system parameters for mpPCL protein devices with chitosan formulation 88
Figure 42 Impact of pH on protein release from mpPCL protein device with chitosan formulation.. 89
8.4. Prototype Devices 90
8.4.1. *Prototype Devices: PEG3350* 90
Table 8 PEG3350 formulation prototype device design parameters 90

Figure 43 Comparison of prototype mpPCL protein device and system parameters to empirical correlations for PEG3350 formulation. 90
Figure 44 Evaluation of mpPCL protein prototypes devices with PEG3350 formulation. 91
8.4.2. *Prototype Devices: Chitosan* 91
Table 9 Key design parameters of chitosan prototype devices 92
Figure 45 Comparing critical device and system parameters for mpPCL protein prototype devices with chitosan formulation to empirical correlations 92
Figure 46 Evaluation of mpPCL protein prototype devices with chitosan formulation. 93
8.5. Conclusion 93
9. Case Study II: A TFPD as a Subcutaneous Implant for HIV PrEP 95
9.1. **Introduction** 95
Table 10 Target Product Profile 96
9.2. **Elvitegravir** 99
9.2.1. Background 99
Figure 47 Elvitegravir chemical structure 99
9.2.2. Elvitegravir dosing 99
Table 11 Elvitegravir dosing estimates 102
9.2.3. Elvitegravir release from TFPD 102
Figure 48 Elvitegravir release rate from TFPD is proportional to device surface area. 103
9.2.4. Conclusions 103
9.3. **Rilpivirine** 105
9.3.1. Background 105
Figure 49 Rilpivirine chemical structure 105
9.3.2. *Rilpivirine dosing* 106
Table 12 Rilpivirine-LA subcutaneous injection constant-rate subcutaneous dosing estimates 106
9.3.3. Rilpirivine release from TFPD 106
9.3.3.1. Rilpivirine HCl 107
9.3.3.2. Rilpivirine HCl + PEG300 108
Figure 50 Membrane controlled release of Rilpivirine HCl + PEG300. 108
9.3.3.3. Rilpivirine + Hydroxypropyl β Cyclodextrin (HP-β-CD) 109
9.3.3.4. Rilpivirine + Polysorbate-20 (PS20) 110
9.3.3.5. Rilpivirine-LA Nanosuspension 110
9.3.4. *Conclusion* 111
Figure 51 Rilpivirine HCl release rates from TFPD. 112

9.4. **Tenofovir Alafenimide Fumarate** 112
9.4.1. Background 112
9.4.2. TAF Dosing 113
9.4.3. TAF release from TFPD 114
9.4.3.1. Short-term screening studies 114
9.4.3.1.1. TAF Release 115
Figure 52 TAF release vs surface area. 115
9.4.3.1.2. TAF Formulation with PEG300 116
Figure 53 Membrane controlled release of TAF with PEG300 formulation. 116
Figure 54 Membrane controlled release of TAF with PEG300 formulation. 118
Figure 55 Impact of PEG300 on TAF release from TFPD.. 119
9.4.3.2. Prototype Studies 119
9.4.3.2.1. Prototype devices targeting specific release rates 120
Figure 56 TAF TFPD Prototypes. 120
Figure 57 TAF TFPD Prototype Results 121
9.4.3.2.2. TAF Stability in Device Reservoir 122
9.4.3.2.3. Pre-clinical Prototype Devices 123
Table 13 Device designs for pre-clinical rat prototypes 124
Table 14 Device characterization and performance for pre-clinical rat prototypes. 125
Figure 58 TAF Release from pre-clinical rat prototypes. 125
9.4.4. Shipping & Terminal (gamma) Sterilization 125
Table 15 Shipping & Gamma Sterilization Study Design 126
Table 16 Shipping & Sterilization Study Results 127
Figure 59 Impact of shipping & sterilization on PCL molecular weight distribution. 128
Figure 60 Impact of shipping & sterilization on device performance 128
9.4.5. Conclusion 129
9.5. **Conclusion** 130
10. Case Study III: A TFPD as a Subcutaneous Implant for Contraception 132
10.1. **Introduction** 132
10.2. **Levenorgestrel (LNG) Dosing** 133
10.3. **LNG release from TFPD** 133
10.3.1. *Short term screening studies* 133
Figure 61 LNG release from TFPD is proportional to membrane surface area. 134

Figure 62 LNG release from TFPD is inversely proportional to membrane thickness. 135
Figure 63 Co-formulation of LNG with PEG300 slightly decreases release rate from TFPD. 135
10.3.2. *Prototype studies* 135
Figure 64 LNG TFPD contraceptive implant prototypes.. 136
10.4. **Conclusion** 137
11. References 138

1. **List of Tables**

Table 1 Predicted PCL degradation time..... 7

Table 2 Projected degradation time for PCL MW blends 9

Table 3 Physical properties and sources of pharmaceuticals 18

Table 4 Matrix system equation variables (Equation 3) 19

Table 5 Reservoir system equation variables (Equation 4)..... 20

Table 6 Key parameters for device design utilizing PEG3350 formulation..... 85

Table 10 Target Product Profile 96

Table 11 Elvitegravir dosing estimates 102

Table 12 Rilpivirine-LA subcutaneous constant-rate subcutaneous dosing estimates. 106

Table 13 Device designs for pre-clinical rat prototypes. 124

Table 14 Device characterization and performance for pre-clinical rat prototypes. 125

Table 15 Shipping & Gamma Sterilization Study Design..... 126

Table 16 Shipping & Sterilization Study Results..... 127

2. List of Figures

Figure 1 Pharmacokinetic profiles representative of different drug delivery profiles. 2
Figure 2 Schematic of PCL Degradation.. 6
Figure 3 Accelerated degradation of PCL MW blends. 8
Figure 4 TFPD system design schematics..... 13
Figure 5 Macromolecule diffusion through porous membranes..... 15
Figure 6 Example of release data and empirical fit..... 20
Figure 7 **:** Empirical parameters describing transport of representative pharmaceuticals in TFPD..... 22
Figure 10: Predicted and experimental release profile for Timolol from a TFPD 28
Figure 11 Predicted and experimental release profile for LNG from a PCL matrix film. 29
Figure 12 Predicted and experimental release profile for Primaquine from a TFPD 30
Figure 13 Membrane porosity increases permeability for model pharmaceuticals.. 32
Figure 14 Membrane porosity decreases permeability for highly hydrophobic Rilpivirine HCl..... 32
Figure 15 PCL molecular weight distribution does not affect membrane permeability. 33
Figure 16 Scanning Electron Microscope images of nanoPCL and mpPCL cross-sections..... 35
Figure 17 Protein release rate from nanoPCL depends on molecule characteristics. 36
Figure 18 Protein release from nanoPCL TFPD is limited by macromolecule excipients. 37
Figure 19 Sustained protein release from mpPCL TFPD. 38
Figure 20 Characterizing release profile for therapeutic protein released from mpPCL TFPD. 38
Figure 21 Characterizing release profile for therapeutic mAb sustained released from mpPCL TFPD.. 39
Figure 22 Protein release from mpPCL TFPD in the presence of macromolecule excipients..... 40
Figure 23 mpPCL membrane thickness does not impact protein release. 41
Figure 24 mAb release rate from mpPCLTFPD is proportional to reservoir loading concentration.. 49
Figure 25 Reservoir hydration volume depends on device size.. 50
Figure 26 mpPCL window Device Design Model for mAb release from a representative TFPD 52
Figure 27 PCL thin film reservoir device fabrication schematic. 55
Figure 28 Protein stability in PCL thin film reservoir device.. 72
Figure 29 Protein stability of chitosan:protein formulations in PCL TFPD..... 74
Figure 30 Impact of Chitosan MW on Protein Stability.. 75
Figure 31 Stability profile for protein released from mpPCL TFPD. 75
Figure 32 Impact of chitosan molecular weight on protein release from mpPCL TFPD..... 76
Figure 33 Stability profiles of protein released from mpPCL reservoir devices 77

Figure 34 Limiting protein solubility with PEG3350. 79
Figure 35 Stability profiles of protein release from PCL devices. 80
Figure 36 Protein release from nanoPCL devices with excipients. 82
Figure 37 Protein release from mpPCL devices with excipients. 83
Figure 38 Device design flow-chart for mpPCL protein devices with PEG3350 formulation 85
Figure 39 Empirical correlations relating critical device parameters to critical system parameters for mpPCL protein devices with PEG3350 formulation. 86
Figure 40 Device design flow-chart for mpPCL protein devices with chitosan formulation 88
Figure 41 Empirical correlations relating critical device parameters to critical system parameters for mpPCL protein devices with chitosan formulation 88
Figure 42 Impact of pH on protein release from mpPCL protein device with chitosan formulation. 89
Figure 43 Comparison of prototype mpPCL protein device and system parameters to empirical correlations for PEG3350 formulation. 90
Figure 44 Evaluation of mpPCL protein prototypes devices with PEG3350 formulation. 91
Figure 45 Comparing critical device and system parameters for mpPCL protein prototype devices with chitosan formulation to empirical correlations 92
Figure 46 Evaluation of mpPCL protein prototype devices with chitosan formulation. 93
Figure 47 Elvitegravir chemical structure 99
Figure 48 Elvitegravir release rate from TFPD is proportional to device surface area. 103
Figure 49 Rilpivirine chemical structure 105
Figure 50 Membrane controlled release of Rilpivirine HCl + PEG300. 108
Figure 51 Rilpivirine HCl release rates from TFPD. 112
Figure 52 TAF release vs surface area. 115
Figure 53 Membrane controlled release of TAF with PEG300 formulation. 116
Figure 54 Membrane controlled release of TAF with PEG300 formulation. 118
Figure 55 Impact of PEG300 on TAF release from TFPD. 119
Figure 56 TAF TFPD Prototypes 120
Figure 57 TAF TFPD Prototype Results 121
Figure 58 TAF Release from pre-clinical rat prototypes. 125
Figure 59 Impact of shipping & sterilization on PCL molecular weight distribution. 128
Figure 60 Impact of shipping & sterilization on device performance 128
Figure 61 LNG release from TFPD is proportional to membrane surface area 134

Figure 62 LNG release from TFPD is inversely proportional to membrane thickness.. 135
Figure 63 Co-formulation of LNG with PEG300 (2:1 w/w) slightly decreases release rate from TFPD. ... 135
Figure 64 LNG TFPD contraceptive implant prototypes. 136

3. Introduction

As healthcare costs rise, demand for reduced hospital or clinic visits and improved efficacy, safety, and user acceptability grow. Among solutions, companies and researchers seek to develop and commercialize long-acting controlled release drug delivery systems. The global revenue for these systems in 2013 is estimated at $181.9 billion with projected revenue growth to $212.8 billion by 2018. [1] Enhanced drug uptake or permeability, advantageous pharmacokinetic profiles, and less frequent dosing aim to address issues of patient compliance, bioavailability, safety, and efficacy. Demand for such systems is broad and encompasses applications in the delivery of small molecules, peptides and proteins, and genetic material. The most common drug delivery routes of administration include oral, subcutaneous, ocular, and pulmonary. Therapeutic durations range from days to years, and systems may be comprised of inorganic materials or polymers, some of which are biodegradable. Advancements in this area rely on the development of reproducible and controllable fabrication technologies, and the availability of materials that are biocompatible and appropriate for system duration and design. Furthermore, novel long-acting drug delivery systems benefit from an understanding of the underlying mechanisms of controlled release and the capacity for tunable release to accommodate pre-clinical through clinical development. There are many examples of long acting drug delivery systems commercially available for indications ranging from heroin (Vivitrol®, Alkermes, Inc. Dublin, Ireland) or nicotine addiction (Nicoderm® CQ ®, GlaxoSmithKline Consumer Healthcare, LP Moon Township, PA) to uveitis (Retisert ®, Bausch & Lomb, Rochester, NY).

Long acting drug delivery systems are typically characterized by controlled or sustained release of a therapeutic and can be in the form of an implant, patch, or injectable system, among others. Characterized by continuous dosing rather than regular bolus dosing as is experienced with oral doses, long acting drug delivery systems exhibit a preferable pharmacokinetic profile (Figure 1), avoiding peaks and troughs and minimizing both super- and sub-therapeutic concentrations. The

most favorable pharmacokinetic profile is achieved with constant rate continuous dosing tuned to achieve constant, steady-state plasma or tissue concentrations comfortably within the therapeutic window. (Figure 1)

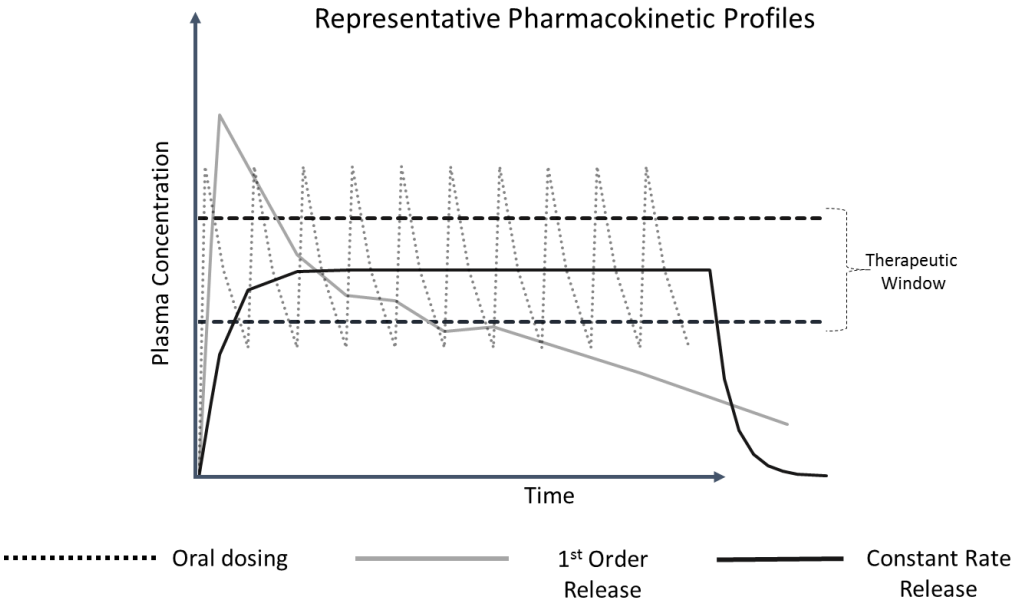

Figure 1 Pharmacokinetic profiles representative of different drug delivery profiles. Oral dosing shows peaks and troughs characterized by an exponential decay in plasma concentration between each bolus dose; 1st order release shows a similar exponential decay in plasma concentration but sustained over an extended period of time relative to regular oral dosing; constant rate release achieves a constant steady state plasma concentration throughout duration of administration. Constant rate dosing is the most efficient dosing strategy, avoiding high concentration peaks that can be associated with toxicity as well as sub-therapeutic concentrations.

As they come in a variety of forms with different routes of administration, it is expected that long acting drug delivery systems are comprised of a range of materials. For example, while injectable depots may consist of active pharmaceutical ingredients (API) encapsulated within microparticles or simply of nanocrystal suspensions of the API, implants may be comprised of inorganic materials, non-biodegradable polymers, or biodegradale polymers. Universal requirements for material choice in a long acting drug delivery system include biocompatibility as well as compatibility with the API. For biodegradable materials, compatibility is essential for both the starting material as well as the degradation products. Based on the breadth of products available commercially as well as those in

development, there are many acceptable materials and designs for long acting delivery systems, but from a safety perspective, and particularly relevant to implants, a system that is retrievable throughout the duration of administration, yet does not require removal, is ideal. Such a system would allow for removal in the case of adverse events, yet would not require follow-up visits nor an additional medical procedure for removal.

A great example of long acting drug delivery, and perhaps the most commonly known example, is in contraceptives. For example, systemically administered hormonal contraceptives, traditionally administered as daily oral doses, are now available as long acting depot injections with durations up to 3-6 months or subdermal implants lasting up to 5 years. [2] Other long-acting contraceptive systems delivering hormones locally and systemically include intravaginal rings (NuvaRing ®, Merck & Co., Inc., Kenilworth, NJ) and intrauterine devices (IUD) (Mirena ® & Skyla ®, Bayer HealthCare Pharmaceuticals Inc., Whippany, NJ). The continued development and commercial success of multiple approaches to long acting contraception highlights the need for and benefit of such systems, including improved efficacy, user compliance and preference, and the potential for reduced side effects. These long-acting contraceptives, particularly those that are user-independent such as the implant or IUD are proven to be more effective in preventing unwanted pregnancies than the oral pill. [3] Furthermore, the variety in route of administration and product duration in contraceptive products demonstrates the importance of user preference on the relevance of a long acting drug delivery approach. Between 2007 and 2009, the Contraceptive CHOICE Project investigated women's preferences for contraception, reporting that, when given the choice, 70% of women would choose a long-acting contraceptive over a short-acting method. [4] The challenges, successes, and lessons learned in the development of long acting contraceptives can be used to guide the development and commercialization of future long acting delivery systems for any indication.

Here we introduce a platform for a tunable and biodegradable long acting implant, called the Thin-Film Polycaprolactone Device (TFPD). The platform is based on the use of porous and nonporous thin-film (< 50 µm) Polycaprolactone (PCL), a bioresorbable and biocompatible polymer [5], as a membrane for controlled or sustained release of an API from a reservoir. The platform is highly versatile, allowing for delivery of small and large molecules alike in sizes relevant to both ocular and subcutaneous implants. A deep understanding of the fundamental mechanisms related to both membrane and device design leads to the use of empirical models to easily design and tune devices for any given API and indication. As this delivery platform is so diverse in its potential applications, this is a key platform feature and the focus of this thesis. The sections of this thesis lay out fundamental understanding and approaches to the tunability of PCL degradation, the fabrication and characterization of various styles of PCL thin-film membranes, the design and tunability of PCL membranes to control release of therapeutics, and the design and tunability of reservoir devices according to target product profiles for specific indications. These fundamentals and design concepts are then applied to the proof-of-concept and early development of three long acting implants for specific indications: an ocular implant for protein therapeutics, a subcutaneous implant for antiretroviral HIV pre-exposure prophylaxis, and a miniaturized subcutaneous contraceptive implant.

4. Polycaprolactone the Polymer

4.1. Introduction

Polycaprolactone is a semi-crystalline aliphatic polyester commercially available at the lab-scale in molecular weights ranging from 2kDa – 80kDa. It is both bioresorbable and biocompatible and has been used in several FDA approved systems including sutures (Monocryl® by Ethicon, a part of the Johnson & Johnson family of companies) and root canal fillings (Resilon ™). [1] Additionally, PCL is reported in development for use in many biomedical applications in the

fields of tissue engineering and drug delivery. [2] [3] [4] PCL has a glass transition temperature of -60˚C and a melting temperature of 60˚C. While insoluble in water, PCL is readily soluble in many organic solvents.

Due to its physical properties and tunable bulk degradation on the order of months to years, PCL is an ideal candidate for a thin film polymer membrane controlled drug delivery system. Thin film PCL membranes are semipermeable, allowing water and low molecular weight molecules to pass directly through the membrane while obstructing the passage of large molecules and undissolved particles. However, it is also possible to introduce porosity into PCL membranes, rendering the membrane permeable to large and small molecules alike.

4.2. Polycaprolactone degradation

Polycaprolactone is suitable for long acting biodegradable polymeric drug delivery systems because its degradation is tunable on the order of months to years. Based on numerous studies, both *in vitro* and *in vivo*, PCL is understood to degrade via bulk erosion through non-enzymatic hydrolysis until a critical chain length of 3-5 kDa is reached, allowing for further intracellular degradation. [5] However, as has been reported for PCL films, fragmentation and loss of mechanical integrity occur when PCL molecular weight reaches 8-13 kDa. [5] [6] A schematic illustrating the bulk degradation of PCL film on the macro and molecular scale is shown in Figure 2. Whereas many biodegradale or bioresorbable polymeric drug delivery systems utilize surface erosion as a mechanism to control drug release, the TFPD relies upon the bulk erosion of PCL to maintain an intact membrane throughout the duration of administration, after which the membrane fully degrades. The integrity of the membrane throughout administration is critical both for achieving consistent membrane controlled drug release, as well as for the retrievability of the TFPD implant. Therefore, the desired time frame

for PCL fragmentation and complete degradation in the TFPD depends on the specific application.

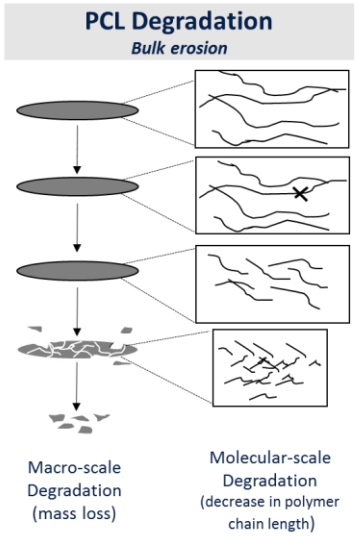

Figure 2 Schematic of PCL Degradation. PCL undergoes bulk erosion; on the macro-scale, the bulk material maintains its mechanical integrity and exhibits no mass loss even as random chain scission occurs until the average chain length reaches a critical point (13kDa) upon which fragmentation occurs.

According to results published in 1981 by Pitt, et. al., PCL hydrolysis is catalyzed by carboxylic acid end groups produced as a result of chain scission. Thus the rate of degradation is relative to the concentration of carboxylic acid, which is inversely proportional to chain length or molecular weight and can be described by the equation:

$$d[M_n]/d\mathrm{t} = -\mathrm{k}'[M_n]$$

Integrating this rate of degradation gives the following equation describing PCL molecular weight as a function of time:

$$M_n = M_n^o e^{-k\prime t}$$

Based on experimental observations by Pitt, et. al., this equation holds true for an extended period of degradation until a critical point upon which it is hypothesized that an additional mechanism of degradation characterized by a loss of mass in addition to a decrease in

molecular weight becomes significant. Based on the equation above and the empirically derived rate constant for *in vivo* subdermal PCL degradation, the time to fragmentation (M_n = 13kDa) and time to dissolution (M_n = 3-5 kDa) can be calculated and are dependent upon the starting molecular weight (Table 1).

Table 1 Predicted PCL degradation time.

	Fragmentation	Dissolution
Mn	**Months until Mn=13kDa**	**Months until Mn=5000kDa**
80000	21	32
50000	15	25
36000	12	23
27200	9	20
14000	1	12

The existing body of published work on PCL degradation provides a solid understanding of mechanism and empirical models for predicting PCL degradation *in vivo*. While in theory the dependence of PCL degradation time on starting molecular weight provides an easy method for tuning the degradation in a drug delivery system, the practical application of this concept results in some difficulties. Based on Table 1, a PCL system designed to maintain its physical integrity for one year should be comprised of PCL with a molecular weight of 36 kDa. However, 36 kDa PCL is not commercially available for lab scale use without a custom order; while this is not necessarily a problem at larger scale where raw materials can be custom produced and could also be overcome by lab scale production of PCL, it increases the complexity and cost for basic research. The lack of availability of PCL at precise molecular weights poses logistical difficulties, but even more disrupting to tuning PCL degradation is the fact that as PCL molecular weight decreases, the ability to cast, handle, and fabricate TFPDs from PCL thin films also decreases. For example, solvent casting a 14 kDa PCL results in a thin film coating the surface upon which it is cast, but the film can not be removed from this surface intact. A 45 kDa PCL film 10-30 µm thick can be cast and handled, but as the film tends to be more brittle than

an 80 kDa film, there is often failure during sealing and subsequent handling of the device. This drastically limits the ability to tune degradation of the TFPD.

All published work to date and the previous section of this report considers PCL degradation as a function of PCL molecular weight assuming a normal distribution. In light of the limitations in TFPD fabrication for low molecular weight PCL and the commercial availability of PCL in only a select few molecular weights, degradation and TFPD fabrication were investigated for bi- or tri-modal distributions of PCL molecular weights. Interestingly, based on accelerated *in vitro* degradation studies, the rate of PCL degradation was unaffected by differences in molecular weight distribution and depended solely on the number average molecular weight (Figure 3).

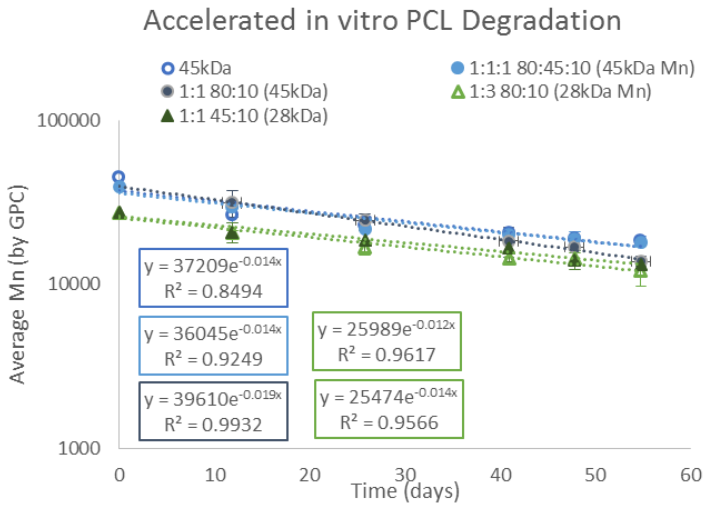

Figure 3 Accelerated degradation of PCL MW blends. Degradation profiles are comparable for PCL MW blends with the same number average molecular weight, regardless of molecular weight distribution.

While only investigated under accelerated conditions *in vitro,* previously published correlations between accelerated *in vitro*, *in vitro*, and *in vivo* PCL degradation indicate that under appropriate conditions for which bulk erosion is observed (and not surface erosion as evidenced by a loss of mass in the bulk material rather than a decrease in molecular weight), the mechanisms and trends in PCL degradation are consistent between accelerated and non-

accelerated conditions. Therefore, that no significant difference in degradation is observed under accelerated conditions for different molecular weight distributions, suggests that PCL degradation *in vivo* will also depend only on the average PCL molecular weight. As a result, PCL cast from blends of PCL with different molecular weights can be used to tune degradation. Table 2 describes some examples of how commercially available PCL can be blended together to tune degradation based on these principles. *In vivo d*egradation times are predicted based on the average PCL molecular weight and the rate constant shown to be independent of molecular weight by Pitt et. al.; again, based on results from the *in vitro* accelerated studies, the molecular weight distribution is not expected to impact this rate constant.

Table 2 Projected degradation time for PCL MW blends

Weight Fraction				Fragmentation	Dissolution
10 kDa	45 kDa	80 kDa	Average Mn (kDa)	Months until Mn=13 kDa	Months until Mn=5 kDa
	0.5	0.5	62.5	17	27
0.5		0.5	45	13	24
0.66		0.33	33	10	20
0.75		0.25	27.5	8	19
0.9		0.1	17	3	13

In addition to providing a practical solution for tuning PCL degradation, multi-modal distributions of PCL molecular weight also result in films suitable for TFPD fabrication with lower average molecular weights than possible with a normal distribution. For example, as previously described, a TFPD fabricated from 45 kDa PCL (normal distribution) has poor seal integrity and often results in device failure, yet a bi-modal distribution of 50% (w/w) 80kDa and 50% (w/w) 10kDa PCL results in a film that is less fragile and TFPDs with better seal integrity. In a more extreme example, while casting a 14 kDa PCL (normal distribution) solution does not produce an intact film, a 10% 80kDa and 90% 10kDa PCL blend does.[1]

[1] Work with this PCL blend (10:90 80kDa:10kDa) was completed by Jean Kim at UCSF.

While additional work to verify the use of multi-modal distributions of PCL to tune degradation *in vivo* and application of these blends to the fabrication and function of TFPD is needed, these early results demonstrate the possibility of this approach to tune degradation.

4.3. Polycaprolactone membrane fabrication

4.3.1. Fabrication techniques

4.3.1.1. *Nonporous PCL membranes* (nonporous PCL)

Nonporous PCL membranes can be fabricated using a number of approaches including solvent casting and hot melt extrusion. For the work presented here, all membranes were fabricated using solvent casting methods. PCL can be solvent cast from solutions in organic solvents including but not limited to, 2,2,2-trifluoroethanol, dichloromethane, and toluene. Thin films can be solvent cast from these solutions using either a spin-coater, a square wet film applicator, or a wire-wound wet film applicator rod. Both the solvent choice, solution concentration, casting surface, and application parameters (i.e. spin-speed and duration, applicator clearance) impact the resulting membrane thickness. Devices can be successfully fabricated with membrane thicknesses down to 5 µm.

4.3.1.2. *Nanotemplated PCL membranes* (nanoPCL)

Nanotemplated PCL membranes are fabricated using a sacrificial ZnO nanorod template according to the protocol developed by Bernards, et. al. [7]

4.3.1.3. *Microporous PCL membranes* (mpPCL)

Microporous PCL membranes are fabricated via solvent casting through the addition of a water soluble porogen to the casting solution. After casting, films are submerged in deionized water to leach the PEG that is dispersed throughout the PCL film, leaving behind a tortuous network of pores. The concentration, size, and choice of porogen define the

resulting pore structure and size. Based on the work published by Bernards et. al. using PEG as a porogen to create a microporous backing layer to the nanotemplated PCL membranes, the work presented here only considers PEG as a porogen.

4.3.2.Characterization

There are several measurements that are critical to characterize when using polymer membranes for membrane controlled drug release. The first critical parameter is membrane thickness. The work presented here uses membranes no less than 5 µm and no greater than 50 µm thick. Film thickness in this range, for porous and nonporous films alike, can be measured using either a profilometer or micrometer. When using a profilometer, it is important to flatly secure the film to a hard surface for an accurate measurement; this is easiest to achieve prior to removing the film from the surface on which it is cast. As the profilometer tip scores the surface of the film, it is not recommended to use the film for device fabrication after analyzing via profilometry. On the other hand, if film thickness is measured using a precision micrometer, there is no damage to the film (if the operator is careful not to twist or tear the film) and direct measurements of the films used to fabricate devices can be made.

For porous films, it is important to characterize porosity. An SEM image of the film surface or cross section will provide a qualitative tool in evaluating pore structure and size. A bulk measurement of % porosity based on density can also be helpful in characterizing and comparing between films. By comparing the density of a porous film to the density of nonporous PCL, the void volume or overall pore volume can be calculated. A more detailed description of this calculation can be found in the Materials & Methods.

5. TFPD Membrane Design

5.1. Introduction

5.1.1. TFPD schematics

Figure 4 shows schematics for several TFPD systems including a matrix system in which the drug is dispersed throughout the polymer membrane and two reservoir systems, one with a nonporous PCL membrane and one with a porous membrane. The major focus of the work presented here is on the TFPD reservoir system. The thin film PCL reservoir device consists of a semi-permeable thin film membrane enclosing a solid core of drug substance. Upon implantation, or submersion in release media for *in vitro* experiments, biological fluid or release media permeate through the PCL membrane, hydrating the device reservoir and dissolving all or part of the reservoir contents. Dissolved drug is then able to diffuse through the PCL membrane for release into the surrounding bulk fluid. As discussed in section 4.3.1 on PCL membrane fabrication, there are several variations of PCL membrane that can be used to fabricate the TFPD. TFPDs to deliver small molecule pharmaceuticals can leverage both porous and nonporous PCL, but porous PCL is required for the release of biologics. The membrane choice and design effect the release rate and profile shape.

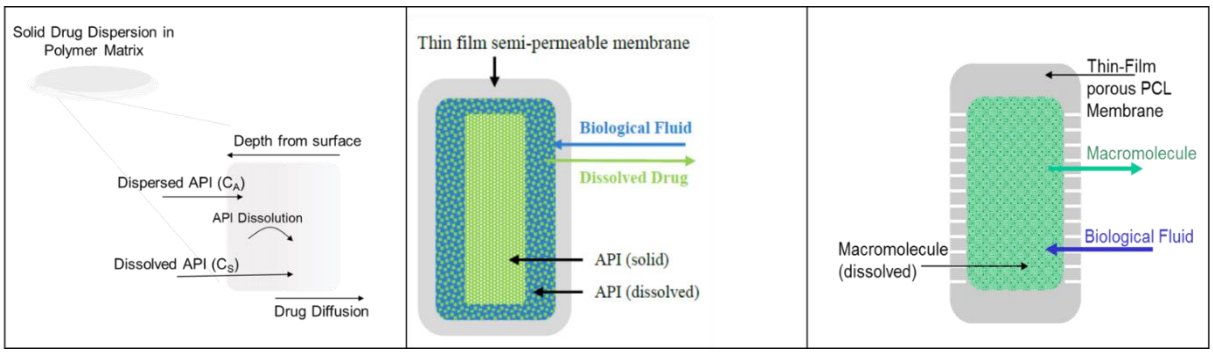

Figure 4 TFPD system design schematics. (Left) A matrix in which drug (API, active pharmaceutical ingredient) is dispersed within the polymer matrix. For drug release in this system, drug must first partition from solid state in the polymer matrix to dissolve in release media, followed by diffusion through the matrix to be released into the bulk fluid. (Center) A nonporous thin film membrane controlled reservoir system in which drug (API) is loaded as a solid into the reservoir. Upon hydration, drug is dissolved within the reservoir and diffuses through the membrane into the surrounding bulk media. (Righ) A thin film membrane controlled release system with membrane porosity allows for release of macromolecules. Upon hydration, macromolecules are dissolved in the device reservoir and then diffuse through the porous membrane to be released into the surrounding fluid.

5.1.2. Principles of small molecule diffusion

In all TFPD reservoir systems considered here, drug release through the PCL membrane is driven by the concentration gradient between the device reservoir and the surrounding bulk fluid in which drug concentration is negligible (as is typically the case *in vivo*). Equation 1 describes concentration dependent diffusion through a membrane. [8] Flux, or in the case of the TFPD, drug release, is directly proportion to the membrane surface and inversely proportional to membrane thickness. Release of small molecules is also dependent upon effective diffusion and partition coefficients (D' and k) which depend on both the physicochemical properties of the drug and membrane as well as membrane structure. In the case of a porous membrane, the effective diffusion coefficient depends on characteristics of the porous membrane such as porosity (void volume), tortuosity (effective path length), and constrictivity (inversely proportional to relative size of molecule to pore) and can be further described by Equation 2. [9]

If sink conditions exist and the concentration of drug outside of the device reservoir is negligible, then release rate is also directly proportional to the concentration of drug in the device

reservoir. Constant rate release of small molecules can therefore be achieved by maintaining a saturated solution of drug within the device reservoir; this is achieved by loading significantly higher quantities of drug into the core of the device than are soluble within the reservoir volume. As long as solid drug remains, the reservoir solution remains saturated, and release is constant. When drug depletes below saturation, release is no longer linear and the release rate will decrease proportionally to reservoir concentration.

5.1.2.1. Equation 1 Fickian diffusion through a membrane. (J) Flux; (A) membrane surface area; (D') effective diffusion coefficient; (k) partition coefficient; (C_R) reservoir concentration; (C_B) bulk concentration; (l) membrane thickness.

$$J = \frac{A*D'*k*(C_R - C_B)}{l}$$

5.1.2.2. Equation 2 Effective diffusion coefficient for a porous membrane. (ε) % porosity; (δ) constrictivity; (τ) tortuosity.

$$D'_{eff} = \frac{\varepsilon * \delta}{\tau}$$

5.1.3. Principles of Macomolecule (protein) Diffusion

In the case of protein release through porous membranes, the pore size relative to the hydrodynamic diameter of the molecule determines the type of diffusion that occurs and as a result the shape of the release profile. The three relevant diffusion regimes are discussed below and illustrated in Figure 5.

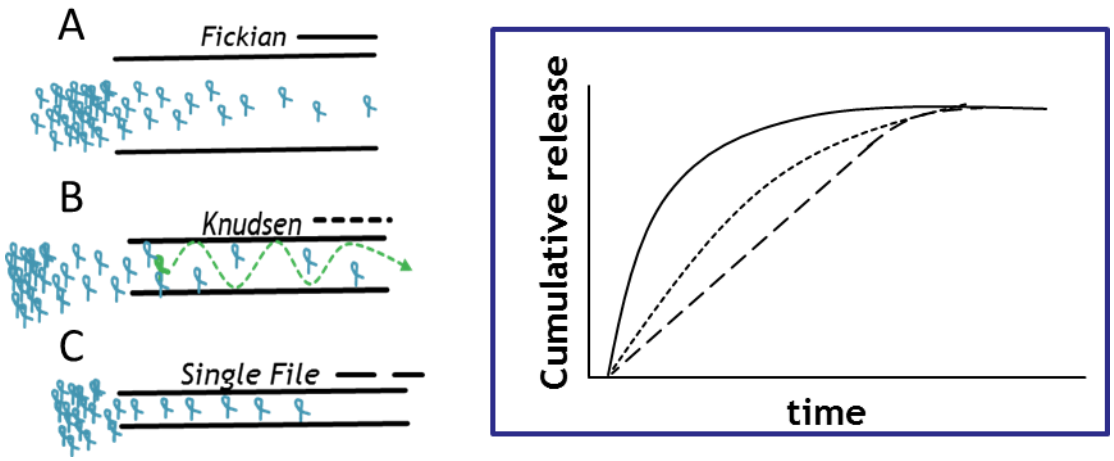

Figure 5 Macromolecule diffusion through porous membranes. In Fickian diffusion (A), pore size does not inhibit diffusion and molecules diffuse in a concentration dependent manner resulting in a first order release profile. In Knudsen diffusion (B), pore size is restrictive and diffusing molecules interact with the pore walls as frequently or more frequently than with other molecules, leading to sustained release profile, less than first order, yet not necessarily constant rate. Actual diffusion kinetics depend on the ratio of pore size to the molecule's hydrodynamic radius and mean free path for diffusion. In single file diffusion (C), pore size is less than 2-times the hydrodynamic diameter of the molecule, inhibiting multiple molecules to pass simultaneously. Single file diffusion results in concentration independent, constant-rate release.

5.1.3.1. Fickian diffusion

Fickian diffusion describes diffusion that is driven purely by the concentration gradient. Kinetic interactions between molecules in solution dominate, driving the dispersion of molecules from regions of high concentration to low. This typically occurs when the hydrodynamic diameter of the molecule is significantly smaller than the size of the pore or channel through which it is passing and the probability of a molecule encountering another molecule is significantly higher than the probability of a molecule interacting with another system feature, in this case the polymer. (Figure 5) This occurs when the mean free path of the molecule is significantly shorter than the diameter of the pore or space through which it is passing (K_n[2] < 0.01). [10] In Fickian diffusion, the release rate is directly proportional to concentration. When reservoir concentration is not constant and changes as drug depletes, the release profile for Fickian diffusion is expected to be 1st order.[3]

[2] Kn = mean free path of molecule / pore diameter

[3] 1st order diffusion in terms of the amount released is described by the equation: $A = A_{Total}(1-e^{-kt})$

5.1.3.2. Knudsen diffusion

As pore or channel size decreases, the probability of a molecule in solution encountering the polymer surface increases. When the mean free path of a molecule in solution is 100 times greater than the diameter of the pore or channel (Kn > 100) [9], the interaction between molecule and polymer begins to define release kinetics. In this scenario, a single molecule is on average more likely to encounter the polymer than another molecule, creating a "ping-pong" like effect as illustrated in Figure 5b. In this way, the porous network through the polymer impacts permeability by more than just increasing the path-length through which a molecule must pass to reach the other side of the membrane, but rather restricts the motion of the molecule within the pathway. The extent to which this motion is restricted is likely determined by both the Kn as well as physicochemical properties affecting interactions between the protein and polymer such as polar surface area, charge, or hydrogen bonding. All of these phenomena effect both the release profile shape and magnitude of release.

5.1.3.3. Single file diffusion

Single file diffusion occurs when the channel or pore diameter is less than twice the hydrodynamic diameter of the diffusing molecule. In this scenario, only a single molecule at a time may pass through the channel, thus restricting diffusion to "single file."(Figure 5c) Constrained by the pore diameter, solute molecules are unable to pass by one another, restricting diffusion through the pore to a single molecule at a time regardless of the concentration gradient driving force [11] [12]. When applied to a reservoir device, membranes effecting single file diffusion not only result in a linear release profile, but also result in a release rate independent of reservoir concentration. This is in contrast to what is

observed in sustained release systems that may exhibit near linear release profiles but with release rates proportional to reservoir concentration.

5.2. Membrane Design for Small Molecule Pharmaceuticals

5.2.1. Introduction

A primary challenge in developing drug-delivery devices is to control the drug release rate and profile. There are a number of different mechanisms for controlling drug release depending on the delivery system, but these mechanisms depend on both device design and the drug's physical properties. [13] [14] [15] Understanding how the physical properties of a drug affect its release rate in a given system is crucial for tailoring the device design to achieve a target release profile. [13] [16] [14] [17] [18] [15] Therefore, we investigated the effect of drug properties (LogP, molecular weight, solubility, and pKa) on diffusion and release in monolithic dispersion matrix as well as membrane-controlled reservoir systems. In addition to developing empirical and predictive models describing drug release profiles, we identified key physicochemical properties of pharmaceuticals affecting partition into and diffusion through PCL membranes. Insight into how different drugs behave in these simple thin-film systems will aid in the design of multi-component drug-delivery systems and the easy translation of the technology for delivering new therapeutics

5.2.2. Theoretical and empirical equations describing matrix and reservoir designs [19]

5.2.2.1. Matrix System

Release of a drug from the matrix system is represented in two phases when drug loading results in a drug concentration in the solid dispersion matrix greater than the drug solubility in release buffer. A set of empirical equations was defined to fit experimental data for drug

release from a PCL matrix. The equation for the first phase, while drug loading remains high, is based on the Higuchi equation for drug dispersed in a solid matrix (Equation 3 Top). The second phase, when drug load is less, is based on an approximation of the non-steady state solution for a monolithic solution under sink conditions [15] (Equation 3 Bottom). The transition between these two phases can be determined empirically and will depend on initial drug loading and drug solubility. For this study, setting the transition point at 60% release resulted in an empirical fit suitable for all samples.

Table 3 Physical properties and sources of pharmaceuticals

API	Form	Supplier/Catalog#	MW API[15]	MW DP[15]	Cs API (mg/L)[15,21-25]	Cs DP (mg/L)[15,21-25]	LogP[15]	pKa[15]
Caffeine	Caffeine	Sigma/C0705	194	194	16005	16005	-0.07	10.4
Diltiazem	Diltiazem HCl	Sigma/D2521	415	451	464	50000	2.8	8.2
Diclofenac	Diclofenac Na	Sigma/D6899	296	318	17.8	1771	4.51	4.15
Famotidine	Famotidine	Sigma/F6889	337	337	999	999	-0.64	8.38
Hydrocortisone	Hydrocortisone	Sigma/H0888	363	363	319	319	1.61	12.58
Labetalol	Labetalol HCl	Sigma/L1011	328	364	117	10100	3.09	8.05
Ranitidine	Ranitidine HCl	Fluka/P500026	314	350	24700	1800	0.27	8.08
Verapamil	Verapamil HCl	Sigma/V4629	455	491	4	45500	3.9	8.92
Ibuprofen	Ibuprofen	Sigma/I4883	206	206	470	470	3.5	4.91
Atenolol	Atenolol	Sigma/A7655	266	266	13300	13300	0.16	9.6
Metoprolol	MetoprololTartrate	VWR/AAJ61920-06	267	685		16900	1.88	9.67
Aspirin	Aspirin	Sigma/A5376	180	180	4608	4608	1.19	3.49

Error! Reference source not found. contains a description of the variables used in these quations. Parameters A, L, f_d, m and C_A are design parameters and empirical parameters D and Y' as well as solubility are drug-specific. In theoretical equations [18], C_s and D are the solubility and diffusion coefficient of the dissolved drug in release buffer within the polymer matrix. In the empirical equation, the aqueous solubility of the active pharmaceutical ingredient at 25°C is used for C_s. Y' is an empirical correction factor to account for the difference between solubility in an aqueous solution at 25°C and solubility within the polymer matrix under experimental conditions as well as any other deviations from the

theoretical equation. For each matrix sample, all parameters except for D and Y were calculated or determined based on matrix characterization and system design. D and Y' were then calculated empirically, using Equation 3, from plots of cumulative mass fraction released versus the square root of time and the natural log of cumulative mass fraction released versus time.

Equation 3

$$\left[{}^{M}/_{M_T} = \left((\boldsymbol{D} * \boldsymbol{Y}')^{\frac{1}{2}} * A * \left((2C_A - C_S)C_S\right)^{\frac{1}{2}} * t^{\frac{1}{2}}\right)/f_d * m \; ; \; {}^{M}/_{M_T} < \mathbf{0.6}\right]$$

$$\left[{}^{M}/_{M_T} = 1 - {}^{8}/_{\pi^2} \exp\left[-\pi^2 \boldsymbol{Dt}/_{L^2}\right] ; \; {}^{M}/_{M_T} > 0.6\right]$$

Table 4 Matrix system equation variables (Equation 3)

	Parameter	Units	Description
	M/M_T	Unitless	Fraction of drug released relative to total drug load
Design Parameters	A	mm^2	Surface area
	L	mm	Membrane thickness
	f_d	Unitless	Mass fraction of drug in film
	m	mg	Total film mass
	C_A	mg/L	Drug concentration as mass of drug per unit volume of film
Drug property	C_S	mg/L	Solubility of active pharmaceutical ingredient at 25°C
Drug-specific empirical parameters	D	mm^2/hr	Diffusion coefficient; dissolved drug through PCL matrix
	Y'	Unitless	Empirical correction factor

5.2.2.2. Reservoir System

Based on the solution to diffusion equations describing mass transport through a slab from a constant activity source under sink conditions, the empirical Equation 4 describes the release rate of drug from a membrane-controlled reservoir system, in which solid drug remains in the reservoir. [18] Table 5 defines each variable contained in Equation 4. The empirical parameter "Dk" is calculated from the slope of a cumulative mass versus time plot

using measured design parameters (A,L) for each device and solubility measurements from literature (Table 3).

Equation 4 Steady state flux through a membrane with a constant activity source and sink conditions. [19]

$$J = {A * \mathbf{Dk} * C_S^{DP}}/{L}$$

Table 5 Reservoir system equation variables (Equation 4)

	Parameter	Units	Description
	J	mg/hr	Mass flux of drug through membrane
Design Parameters	A	mm^2	Surface area
	L	mm	Membrane thickness
Drug property	C_S^{DP}	mg/L	Solubility of drug product at 25°C
Drug-specific empirical parameters	Dk	mm^2/hr	Combined diffusion coefficient (dissolved drug through PCL matrix) and partition coefficient (partition into PCL membrane)

5.2.2.3. Empirical Fits

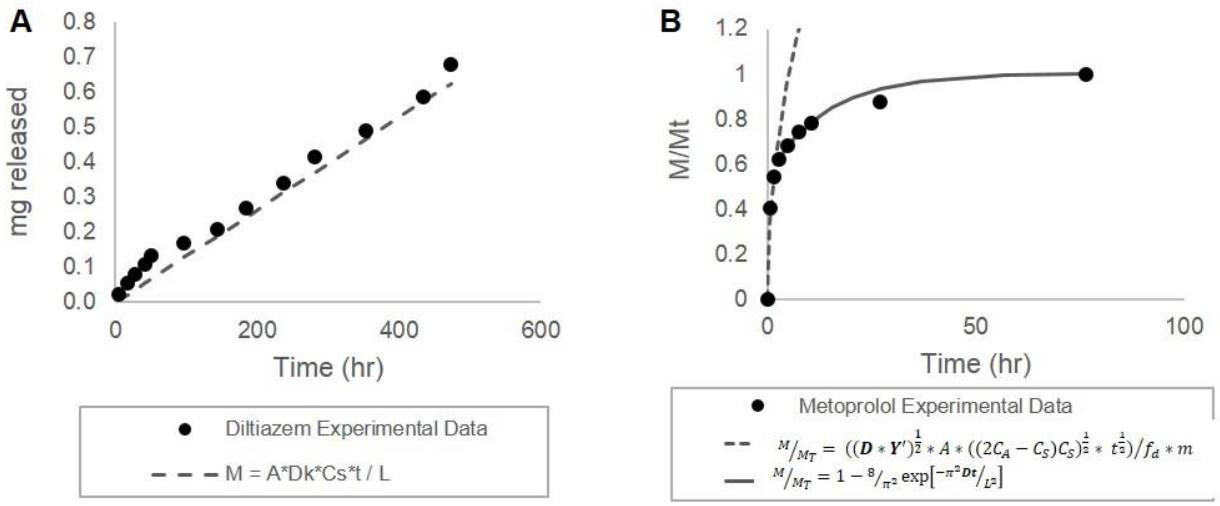

*Figure 6 Example of release data and empirical fit. The cumulative release profile for reservoir devices is linear after an initial burst release (A, Diltiazem). Data fit is based on the equation M = A***Dk***Cs^{DP}*t / L and the combined parameter Dk is determined empirically. Release in the matrix system (B, Metoprolol) is described as fraction released and is fit with two equations*

$$\left[{}^{M}/_{M_T} = ((\boldsymbol{D} * \boldsymbol{Y'})^{\frac{1}{2}} * A * ((2C_A - C_S{}^{API})C_S{}^{API})^{\frac{1}{2}} * t^{\frac{1}{2}})/f_d * m \,;\, {}^{M}/_{M_T} < \mathbf{0.6}\right] \left[{}^{M}/_{M_T} = 1 - {8}/{\pi^2}\, exp\left[{-\pi^2 \boldsymbol{Dt}}/{L^2}\right];\, {}^{M}/_{M_T} > 0.6\right]$$

and two empirical parameters (D', Y'). Data sets are from a single release experiment and fits are based on average empirical parameters from full data set (n=2-5) [19].

Figure 6 illustrates representative release profiles and empirical fits that describe matrix and reservoir systems. Data points represent typical release from a single device and the empirical fits represent average empirical values from triplicate devices. Empirical fits and parameters are defined in equations 3 and 4, for the matrix and reservoir systems respectively. Calculated empirical parameters for each system are tabulated in Table 4 and Table 5. Empirical values calculated from different device designs are averaged for each drug and represented in Figure 7 with error bars representing one standard deviation. Dk, D' and Y' are independent of design parameters and differ between drugs as depicted in Figure 7, which compares these empirical parameters on a log scale. As shown in Figure 7, the empirical equations accurately model the release profiles from these systems, and the empirical parameters describe the diffusion characteristics of a drug within or through the PCL matrix normalized for device design.

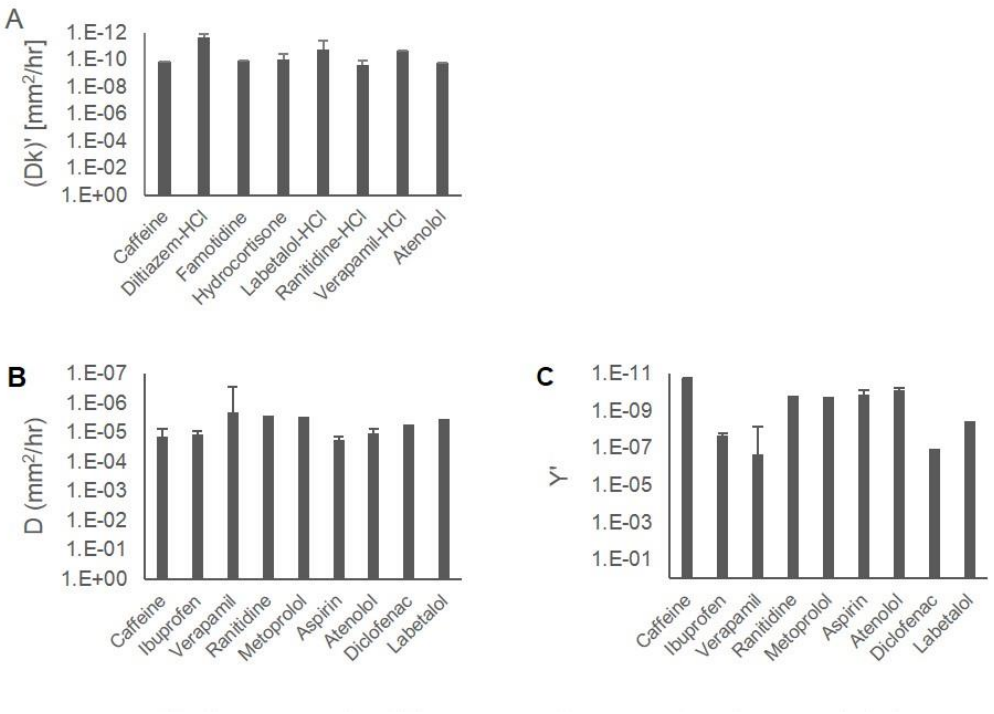

Figure 7 : Empirical parameters describing transport of representative pharmaceuticals in a PCL reservoir system (A) and PCL matrix (B, C). Empirical parameters are drug specific and represent the diffusion and partition of drug through and into a PCL membrane. Release profiles from a given system depend on empirical parameters, drug solubility and device dimensions. [19]

In the reservoir system, dissolved drug in the reservoir, driven by a concentration gradient between reservoir and bulk, partitions into the polymer membrane and then diffuses through the membrane into the bulk fluid. The diffusion coefficient (**D**) is a measure of the rate of diffusion of dissolved drug through the polymer matrix and the partition coefficient (**k**) is a measure of the molecules affinity for the polymer membrane relative to the aqueous bulk. In the empirical analysis for the reservoir system, D and k are calculated as a single parameter and cannot be determined independently. In the matrix system, solid dispersed drug in the polymer matrix partitions and dissolves in the fluid permeating into the matrix, driven by the difference in concentration between drug in the solid matrix and the saturated drug concentration in the permeating fluid. The dissolved drug then diffuses through the polymer matrix and releases into the surrounding bulk fluid. A more thorough explanation

of the theoretical equations and solutions to diffusion equations in these systems can be found in a 2012 review by Siepmann and Siepmann in the Journal of Controlled Release [18]. The diffusion coefficient (**D**'), the same as in the reservoir system, is a measure of diffusion rate of dissolved drug through the polymer matrix. **Y'** is included in the empirical equation for the matrix system as a scaling factor to adjust for using drug solubility in a bulk fluid rather than the actual saturated drug concentration in the polymer matrix.

5.2.3. Physicochemical properties impact diffusion [19]

These empirical parameters differ for different drugs (Figure 7) and are related to the interaction between the drug molecule and the polymer. Correlations between empirical diffusion parameters and drug properties suggest the nature of these interactions and their relative impact on drug release. Figure 8 shows relevant correlations for both the matrix and reservoir systems. Diffusion coefficients are known to be dependent on molecular size, and as expected, in both the matrix and reservoir system, there is a similar trend of increasing D (i.e. faster diffusion) with decreasing molecular weight. D cannot be distinguished independent of k in the reservoir system, but as the empirical **D** in both systems describes the rate of diffusion for dissolved drug through PCL matrix, it is likely that the trend with MW observed for Dk is driven by the dependence of D on MW. There is also a strong logarithmic correlation (correlation coefficient = 0.79) between Dk in the reservoir system and LogP. This is attributed to the partition of drug from the reservoir into the membrane as described by k. Since PCL is a hydrophobic polymer, the drug must partition from a hydrophilic to hydrophobic environment. The P in LogP is also a measure of drug partition between a hydrophobic and hydrophilic phase, and thus a linear correlation between P and k is expected.

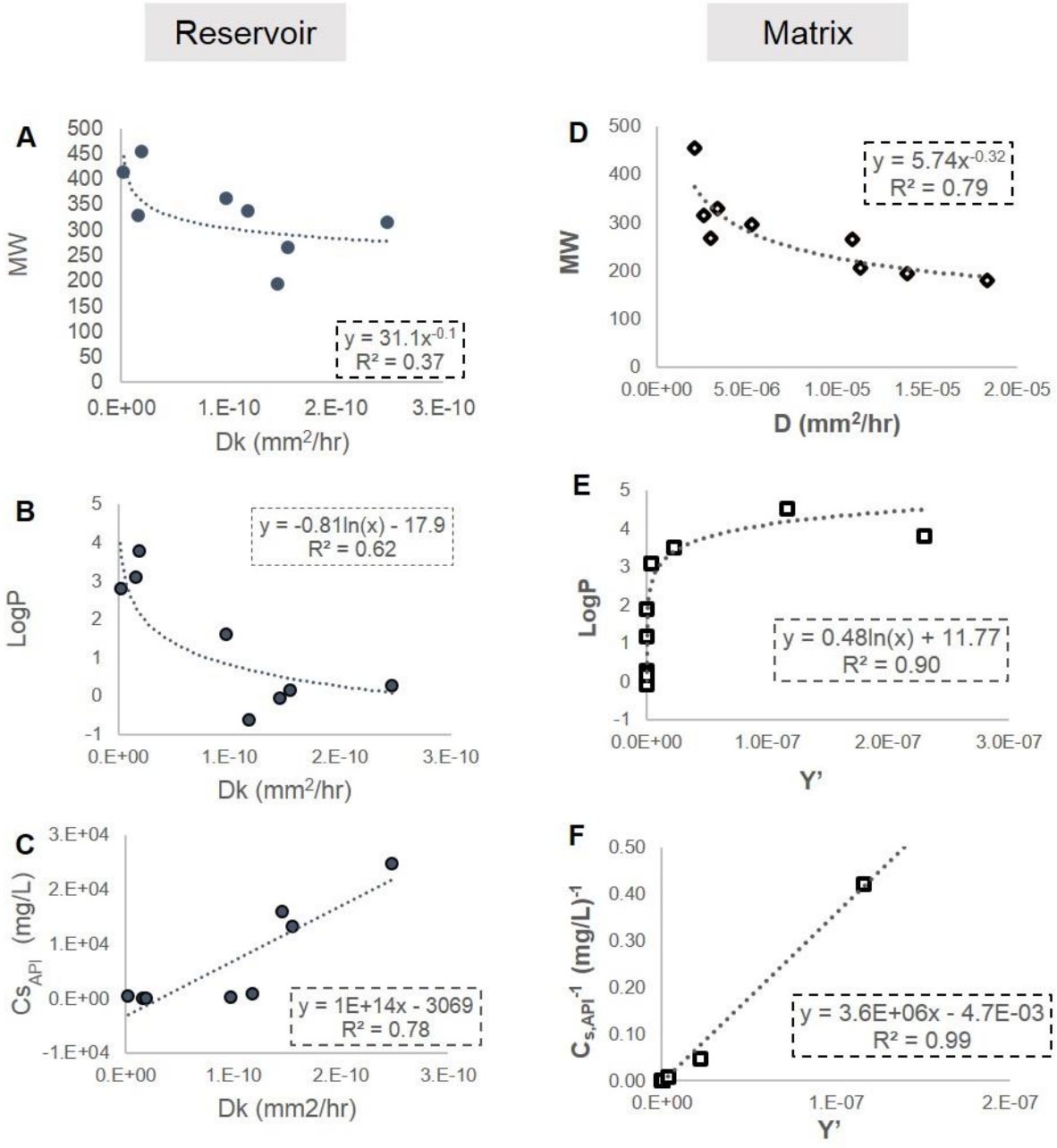

Figure 8 Correlations between drug properties and empirical diffusion parameters. Diffusion coefficient (D) shows a weak negative correlation to molecular weight in both systems (A,D). In the reservoir system (A,B,C), the combined empirical parameter Dk [$M = ADkC_S t$] is inversely correlated to API solubility (aq, 25°C) and proportional to the partition coefficient "P" as illustrated by the logarithmic correlation between LogP and Dk (B). D and k can not be independently determined from reservoir system release data. In the matrix system, described by the empirical equations $[{}^{M}/_{M_T} = ((\boldsymbol{D} * \boldsymbol{Y'})^{\frac{1}{2}} * A * ((2C_A - C_S)C_S)^{\frac{1}{2}} * t^{\frac{1}{2}})/f_d * m$; ${}^{M}/_{M_T} < 0.6]$ $[{}^{M}/_{M_T} = 1 - {}^{8}/_{\pi^2} exp[{}^{-\pi^2 \boldsymbol{Dt}}/_{L^2}$; ${}^{M}/_{M_T} > 0.6]$ *Y' shows similar yet opposite correlations to Dk in the reservoir system in that it is inversely correlated to drug solubility(F) and negatively proportional to the partition coefficient "P" (E). [19]*

Interestingly, in the matrix system, Y' shows a negative logarithmic correlation with LogP. This can be explained due to solid drug in a matrix dispersion partitioning from the hydrophobic environment into the more hydrophilic environment of the permeating fluid. Thus in the matrix system, molecules with larger LogP and a greater affinity for hydrophobic environments will have a smaller Y', whereas in the reservoir, more hydrophobic drugs will have a larger Dk and more readily enter into the polymer membrane. Y' appears to encompass an effective partition coefficient in the empirical model presented here to describe release from the PCL matrix system.

Y' in the matrix system and Dk in the reservoir system show opposite correlations with solubility. While these correlations are significant (correlation coefficient greater than 0.7), they are likely influenced by the inherent relationship between drug solubility and LogP. It should be noted that the correlation coefficient for Dk with MW in the reservoir system is only 0.6 and is weak compared to the correlation between Dk and LogP attributed to the partition coefficient (k). This suggests that in the PCL membrane controlled reservoir system, drug release is more strongly influenced by the partition of drug from hydrophilic aqueous bulk to hydrophobic polymer membrane than by the diffusion of drug within the membrane.

5.2.4.Predictive models using physicochemical properties to estimate diffusion parameters [19]

Equation 5 Predictive models for empirical diffusion parameters based on physicochemical properties of drug [19]

$$\mathrm{Dk} = 6.0\mathrm{E}-11 * \exp(-0.85\mathrm{LogP}) + 7.0\mathrm{E}-15 * \mathrm{C_S^{API}} + 1.0\mathrm{E}-11$$
$$\mathrm{D}' = 112 * \mathrm{MW}^{-3}$$
$$\mathrm{Y}' = {}^{6.0\mathrm{E}-08}/_{\mathrm{C_S^{API}} + 7.5\mathrm{E}-12 * \exp(2.08 * \mathrm{LogP})}$$

As described in our methods, we have developed a model to predict empirical parameters based on physicochemical properties of drugs. Equation 5 predicts empirical parameters **D'** and **Y'** in a PCL matrix system and **Dk** in a PCL reservoir system. Figure 9 compares the predicted empirical parameters to experimental empirical parameters in both the matrix and reservoir systems. The predictive models were built to minimize relative residual error (RRE). The average RRE in the reservoir system in the final model is 1.2, with Diltiazem-HCl as an outlier with an RRE of 8.1. Excluding Diltiazem-HCl, the RRE of the remaining 7 drugs falls to 0.2. The RREs for predicted parameters in the matrix system are 0.3 and 0.6 for D' and Y' respectively.

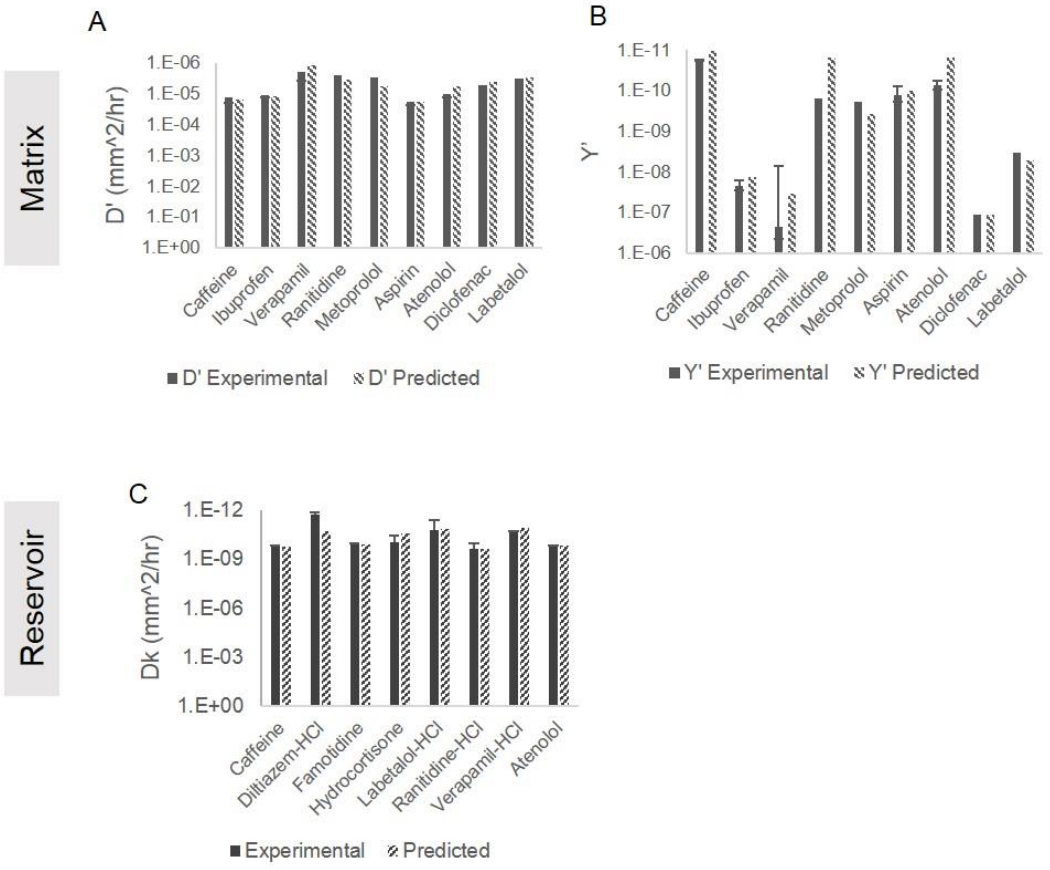

Figure 9 Predicted and experimental values of empirical parameters [19]

The models presented here are useful in early system design as well as evaluation of a PCL thin-film device for delivering a given drug at a target rate and dose. For example, we can use the predictive model to calculate Dk for Timolol [Solubility = 2.740 g/L [24], MW =316.42 [25], LogP = 1.83 [25], and pKa = 9.21 [25]; Dk = 4.18E-11mm^2/hr] and Equation 4 to model release from a reservoir device loaded with Timolol Maleate [Solubility = 100 g/L, [26] MW = 432.49 [25]] to design a device with suitable dimensions and a target release rate of 10-30 μg/day [27] for long-acting glaucoma treatment. Based on the predictive and empirical models, a 2x3mm rectangular device (12mm^2 surface area) made with a 70 μm thick PCL membrane will achieve a release rate of 17 μg Timolol/day. The duration of drug release depends on the mass loaded into the device reservoir; here we demonstrate a 15 day device with a total drug load of 300 μg Timolol (410 μg Timolol Maleate). The predicted linear release rate and experimental results in Figure 10 demonstrate that the models accurately predict the linear release rate from the reservoir device. As drug depletes and the total mass in the reservoir falls below the solubility limit, the release kinetics reflect 1st order Fickian diffusion. Due to the small reservoir volume, the mass released in this non-linear phase is small (< 40 μg).

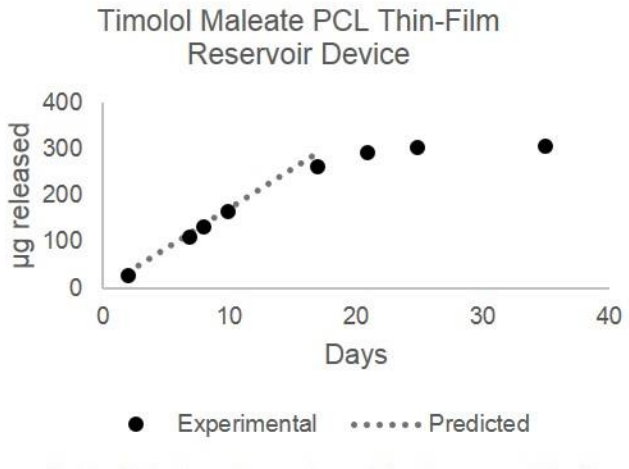

Figure 8: Predicted and experimental release profile for Timolol from a Timolol-Maleate loaded PCL reservoir device. Device dimensions are 2x3mm rectangle with a 70um thick membrane and 0.4mg Timolol-Maleate (0.3mg Timolol) load. Device was designed using predictive modeling and empirical equations for a 17ug/day Timolol release rate with dimensions appropriate for front of the eye delivery. [19]

In another example, we designed a PCL matrix system as a potential on-demand vaginal film releasing the contraceptive levonorgestrel. In this case, we use the predictive model to calculate D', 3.69E-06 mm^2/hr, and Y', 5.03E-08, based on levonorgestrel drug properties (MW = 312, LogP = 3.8, pKa = 13, solubility = 2 mg/L). [25] To target a 1 to 2 day sustained-release profile with 5-10 µg of total drug release, we designed a 6 mm-diameter PCL film, 38 µm thick with 0.8% drug loading by mass. Figure 11 shows the predicted and experimental release profile for this system. As previously described, the release profile for a matrix system is defined as a percent-released, therefore, the mass of levonorgestrel release from this film can be easily scaled with film diameter depending on desired dosing.

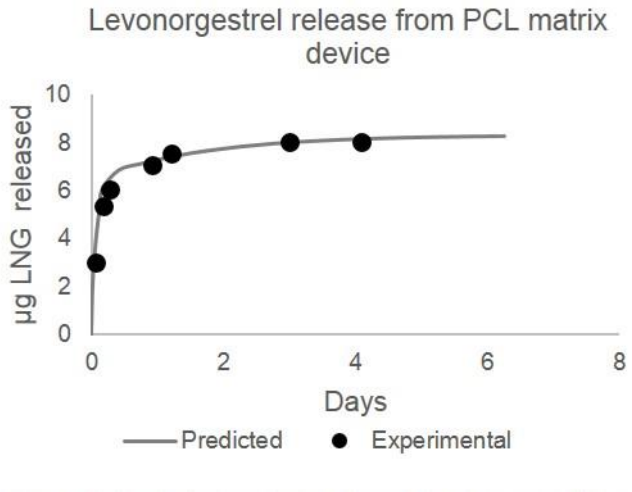

Figure 9 Predicted and experimental release profile for Levonorgestrel (LNG) from a PCL matrix film. Film dimensions are 6mm diameter, 38µm thick, with a 0.8% mass loading of LNG. Device was designed using predictive modeling and empirical equations for a 5-10ug sustained release for 1-2 days as a potential on-demand vaginal film contraceptive. [19]

Finally, we applied the predictive and empirical models to design a PCL thin-film device for long-acting malaria prophylaxis. Based on a basic pharmacokinetic model taking into account oral bioavailability, plasma half-life, volume of distribution and minimum and maximum plasma concentrations for steady-state oral dosing of primaquine bisphosphate [24], we estimated a target constant-rate release of 12-24 mg/day to achieve 50-100 ng/ml plasma concentration for effective malaria prophylaxis. Based on the properties of primaquine (MW = 259, LogP = 2.1, pKa = 10.2, API-solubility = 56.4 mg/L, drug product (primaquine bisphosphate) solubility = 166.7g/L) [24] [21], Dk was predicted (2.05E-11 mm^2/h) and the empirical model for release from a constant-activity reservoir device was used to design a PCL thin-film device targeting 16 mg/day release with a 4 µm thick membrane, 800 mm^2 (40 mmx10 mm rectangle) surface area, and 175 mg primaquine phosphate (99 mg primaquine) load for 10 days of drug release. Figure 12 illustrates the predicted linear release rate and experimental data from this device.

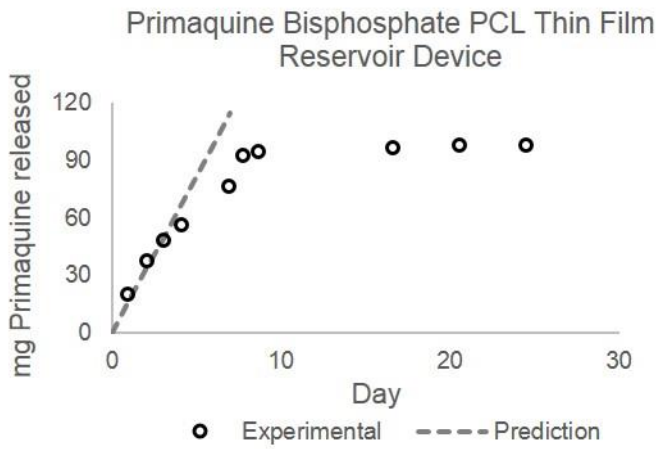

Figure 10 Predicted and experimental release profile for Primaquine from a Primaquine bisphosphate loaded PCL reservoir device. Device dimensions are 10x40mm rectangle with a 4um thick membrane and 175mg primaquine bisposhpate (99mg primaquine) load. Device was designed using predictive modeling and empirical equations for a 16mg/day release rate. [19]

The empirical models presented here describe a systematic approach to easily determine empirical parameters that define a drug's release profile from a PCL thin-film matrix and a PCL thin-film reservoir device. These empirical parameters, D' and Y' for the matrix and Dk for the reservoir, are specific to the PCL system and to each drug. Once determined, these parameters allow for easy system design and scale-up or scale-down to achieve a target release rate and quantity for a given drug. Additionally, these parameters depend on a drug's physicochemical properties, indicating that the mass transport of drug from the matrix system into the release buffer is not only affected by concentration gradients as described in the diffusion equation, but also by interactions between drug molecules and polymer. Diffusion rate of dissolved drug through the polymer in both the matrix and reservoir system depends on molecular weight, with larger molecules diffusing more slowly. In the reservoir system, the partition of drug into the polymer membrane depends on LogP and solubility, with more hydrophobic (larger LogP and lower solubility) drugs partitioning faster. Conversely, in the matrix system, drug partition from the solid polymer matrix to the permeating fluid depends on LogP and solubility with

opposite correlations to those observed in the reservoir system. In the matrix system, hydrophilic drugs partition more rapidly from the polymer matrix.

5.2.5. Effect of porosity on diffusion

Small molecule pharmaceuticals have hydrodynamic radii on the order of 1 nm or less and thus are expected to diffuse with limited or negligible steric hindrance through the porous structure of mpPCL. As a result, the introduction of porosity to the PCL membrane is anticipated to increase release rate for a given surface area and membrane thickness as dissolved drug can diffuse via the porous pathway. As Figure 13 describes, there is a drastic increase in the membrane permeability of two representative small molecules, metoprolol and atenolol, for mpPCL relative to nonporous PCL. As is evidenced by the much larger increase in atenolol permeability relative to metoprolol permeability, the magnitude of the increase in permeability depends on the hydrophobicity of the molecule. This is attributed to the greater partition of the more lipophilic metoprolol (logP 1.88) into the PCL membrane compared to the more hydrophilic atenolol (logP 0.16). With a smaller partition and a greater fraction of drug remaining in the aqueous phase, atenolol appreciates a more significant boost in permeability from the aqueous pathway presented by the porous structure. Interestingly, and rather unexpectedly, for Rilpivirine HCl, a very hydrophobic molecule (logP 4.86) with limited solubility (< 1 μg/ml), permeability in the mpPCL membrane is actually less than the nonporous membrane (Figure 14). While consistently observed for Rilpivirine HCl with and without solubilizing formulation excipients, this phenomenon has not been observed for other molecules with high logP.

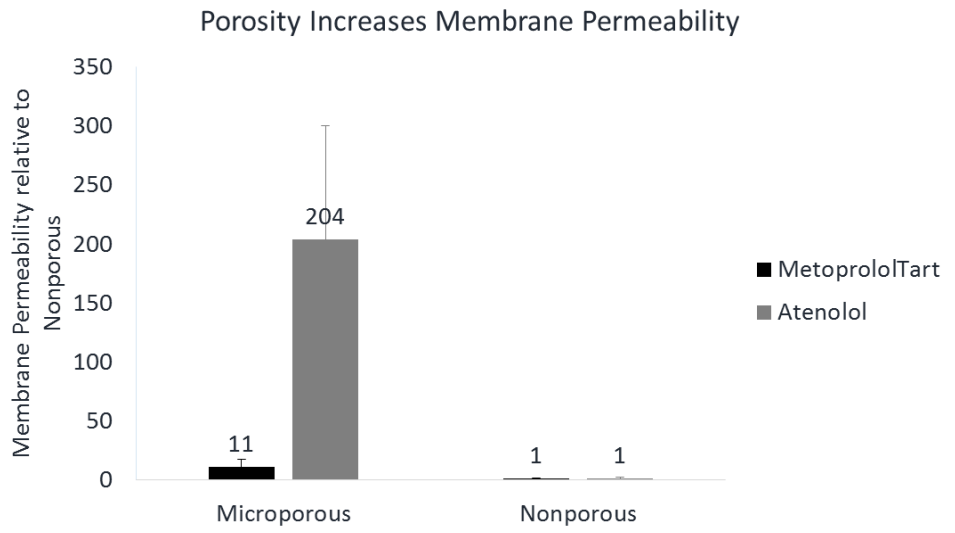

Figure 11 Membrane porosity increases permeability for model pharmaceuticals. Magnitude of increase in membrane permeability depends on molecular properties such as hydrophobicity; metoprolol (logP 1.88), with greater hydrophobicity than atenolol (logP 0.16), experiences a lesser increase in permeability with a porous membrane than atenolol as a greater fraction of metoprolol is expected to partition from the aqueous phase into the PCL.

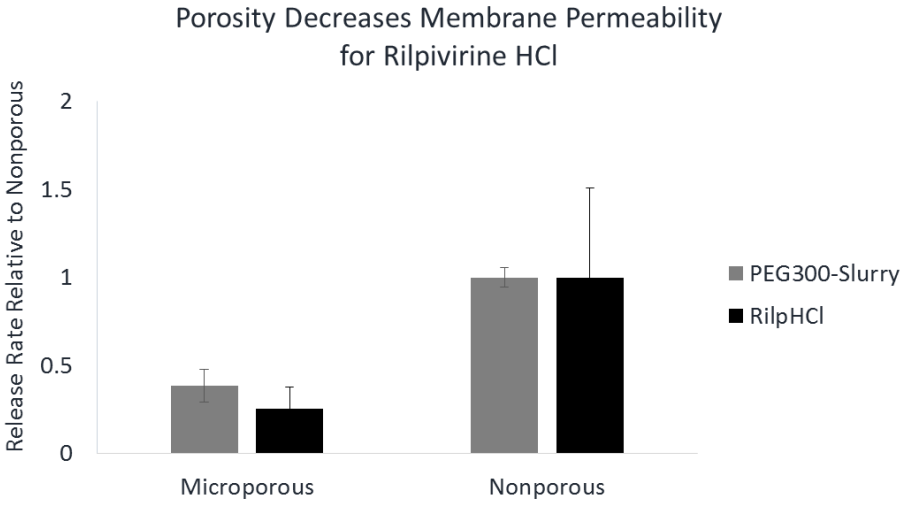

Figure 12 Membrane porosity decreases permeability for highly hydrophobic Rilpivirine HCl (logP 4.86, < 1 µg/ml solubility).

5.2.6. Impact of PCL molecular weight on diffusion

As described in the section on tuning PCL degradation, blends of PCL with different molecular weights can be used to produce membranes that are suitable for device fabrication with average molecular weights that, when comprised of a normal molecular weight distribution, are not suitable for device fabrication (i.e. do not form intact films or do not have sufficient integrity for effective sealing and device handling). With respect to this approach for tuning PCL degradation, it is important to understand how differences in PCL molecular weight distributions impact membrane permeability. Evaluation of membrane permeability for two molecules representative of the standard pharmaceutical space, one with high LogP (metoprolol, logP 1.88) and one with low LogP (atenolol, logP 0.16) illustrates no statistically significant difference ($p=0.9$ and $p=0.29$ respectively) in membrane permeability for devices fabricated from two different PCL molecular weight distributions, both resulting in an average molecular weight of 45 kDa. (Figure 15) It is important to note that a PCL film cast from a normal distribution with 45 kDa average molecular weight resulted in defective devices due to poor film and seal integrity.

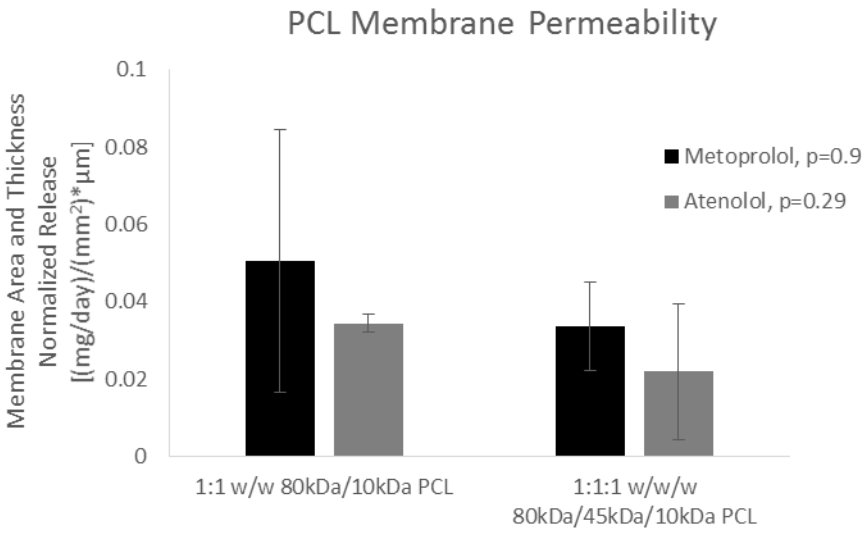

Figure 13 PCL molecular weight distribution does not affect membrane permeability. Atenolol permeability data collected by Jean Kim, UCSF.

5.3. Membrane Design for Macromolecules (Protein Therapeutics)

5.3.1. Introduction

Macromolecules such as proteins require pores to pass through a PCL film. Two categories of porous PCL films are presented here: nanotemplated PCL (nanoPCL) and microporous PCL (mpPCL). The nanoPCL membrane is characterized by a layer of 20-nm channels roughly 500 nm deep with a microporous backing layer 20-30 μm thick with a tortuous network of pores 1-2 μm in diameter. (Figure 16) The development and fabrication of this nanoPCL membrane and its use in achieving single-file diffusion of protein molecules was described by Bernards et. al. in 2010. [7] In short, the nano-channels are created by casting a submicron PCL film over a sacrificial ZnO nanorod template followed by a microporous backing layer. The diameter and density of the nanochannels are defined by the ZnO nanorod template. Leveraging similar recipes and procedures used to create the microporous backing layer that provides support to the nanochannel membrane, the mpPCL membrane is introduced here. The mpPCL membrane is fabricated by solvent casting a co-solution of PCL and PEG onto a glass surface. PEG, the porogen and a water soluble polymer, is then leached from the PCL membrane by submersion in deionized water, leaving behind a network of pores. Pore size, density, and structure are determined by the porogen, in this case 2.05 kDa PEG, the relative concentration of porogen to PCL, the solvent used for casting, and the casting surface. The standard protocol used for mpPCL films in this body of work is a 1:1 ratio PCL 80kDa to PEG 2.05 kDa cast in TFE onto a polished glass surface. As a cross-section of a typical mpPCL film depicts (Figure 16), pores are roughly 1 μm in diameter. While not directly observable or quantifiable, this suggests that inter-porous pathways are less than 1 μm. Differences in the pore structure and size observed in nanoPCL and mpPCL lead to different protein release kinetics from a porous TFPD.

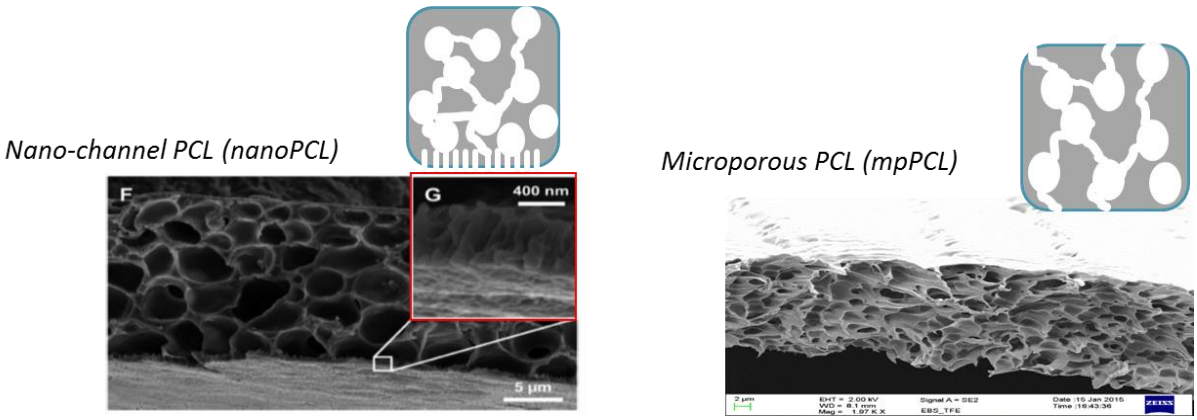

Figure 14 Scanning Electron Microscope images of nanoPCL and mpPCL cross-sections. NanoPCL membranes (left) are characterized by a thin layer of nano-channel pores (20 nm in diameter) backed by a layer of larger pores (1-3 µm diameter) for structural support. In nanoPCL, molecular diffusion is limited by the length, diameter, and density of the nano-channels. mpPCL (right) does not contain the nano-channel layer, but has a similar pore structure and size to the backing layer on the nanoPCL membrane. In mpPCL, molecular diffusion is limited by the size and extent of the connections between the large pores visualized in these cross-sectional images.

5.3.2. NanoPCL Membrane Design

The hydrodynamic diameter of an antibody is on the order of 10 nm, and thus with pore sizes averaging 20 nm in diameter, the nanoPCL membrane exhibits single file diffusion. This results in linear release of protein from a nanoPCL device with release rates independent of reservoir concentration. [11] While independent of concentration, release rate will depend on the size of the protein and may also depend on other properties such as charge, polar surface area, or capacity for hydrogen bonding.[4] (Figure 17) Protein release rates are on the order of 1µg/day per mm^2 surface area of nanoPCL membrane. While these release rates are relevant for protein therapeutics requiring doses on the order of micrograms per day, these slow rates preclude proteins requiring higher doses. Furthermore, the achievable release rate will be determined by limitations in device size. For example, an ocular sized device may only have a surface area up to 50 mm^2, whereas a subcutaneous sized device may be sized up to 250 mm^2.

[4] Dependence of protein release rates in nanoPCL membranes on molecular properties is suggested by results presented in Figure 17, but not explored further in the work presented here.

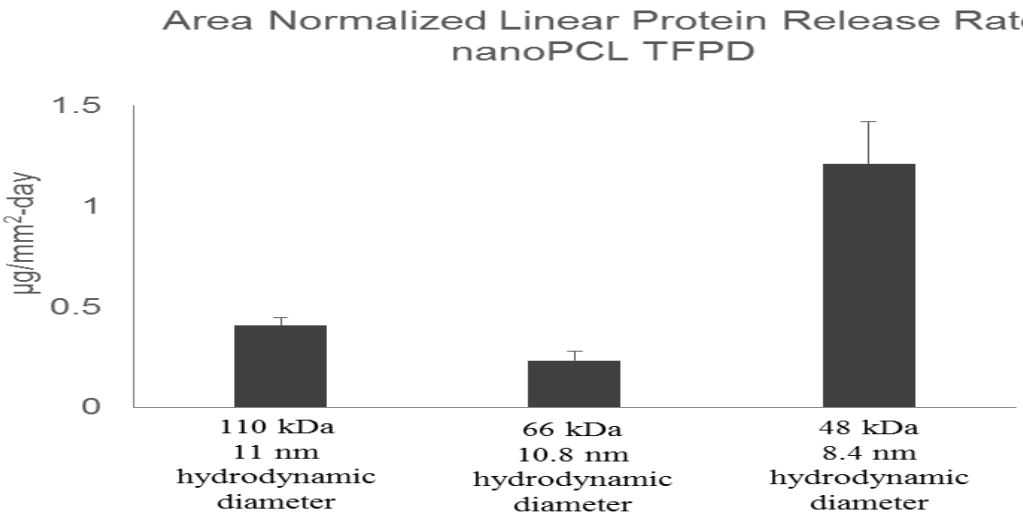

Figure 15 Protein release rate from nanoPCL depends on molecule characteristics. Size alone does not account for differences in release rates observed for different protein molecules.

As is discussed in more detail in the device design section (Section 6), protein stability is a common challenge in the design of long-acting delivery systems. While liquid protein formulations typically make use of small molecule excipients, one approach to protein formulation in the TFPD reservoir system is the use of macromolecule excipients that do not readily deplete through the PCL membrane. While this approach shows promise for improving protein stability, these macromolecule excipients limit protein release through the nanoPCL membrane to less than 0.1µg/day per mm^2 surface area of nanoPCL membrane. (Figure 18) With such slow release rates, nanoPCL TFPDs utilizing macromolecular excipients are not likely to be feasible for achieving effective doses.

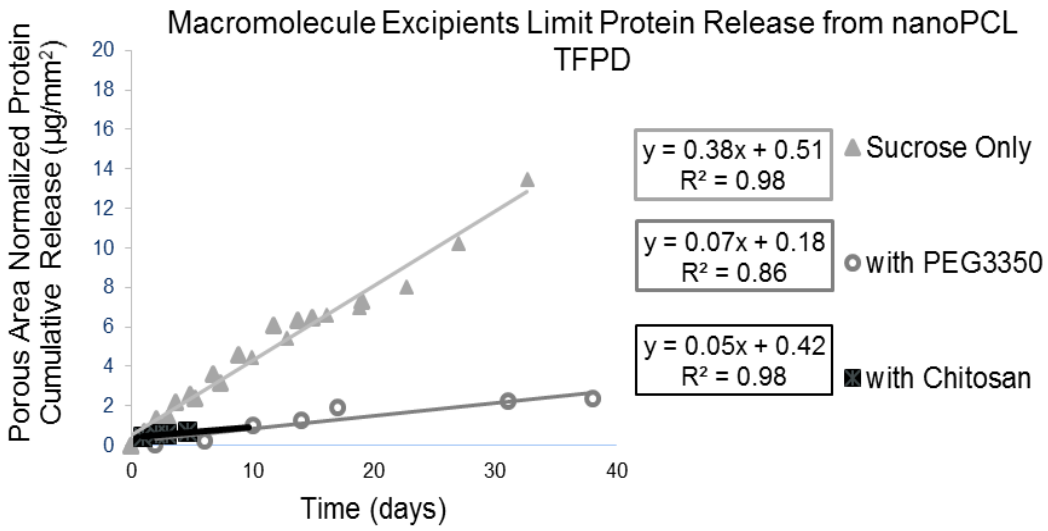

Figure 16 Protein release from nanoPCL TFPD is limited by macromolecule excipients. Upon addition of PEG3350 or Chitosan to the device reservoir, protein release is reduced by more than 5x.

5.3.3. mpPCL Membrane Design

While not achieving single-file diffusion, the mpPCL membrane controls protein diffusion, resulting in a sustained release profile with kinetics falling between zero and first order, suggesting Knudsen diffusion. Figure 19 illustrates release profiles for two different therapeutic proteins[5], demonstrating variations in the sustained release profile. Examining the release profiles closer shows that the therapeutic protein in Figure 20 has a near linear release profile up to about 80% followed by a second release phase with rates slowly decreasing (linear with respect to $t^{0.28}$) until depletion. The therapeutic mAb demonstrates a sustained release profile linear with respect to the square root of time (Figure 21) until depletion.

[5] Identification of therapeutic protein is redacted due to confidentiality. Therapeutic mAb is VRC01, a broadly neutralizing HIV antibody

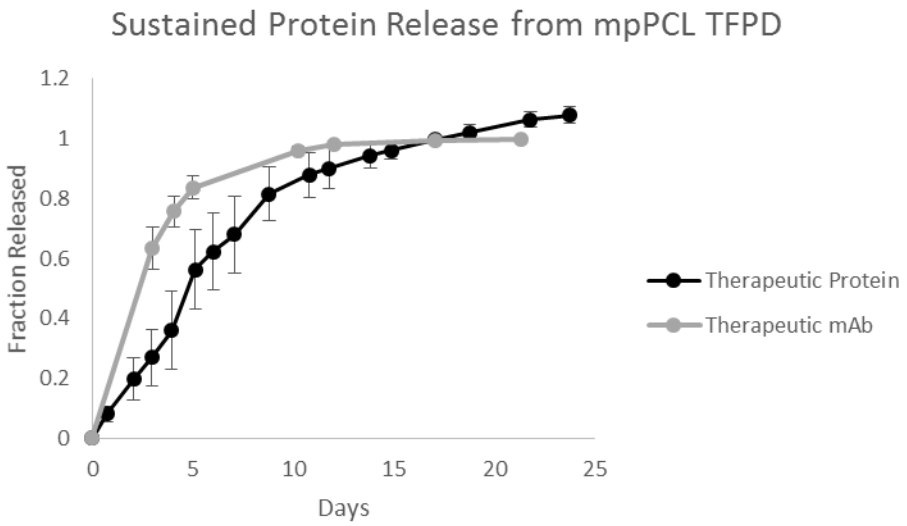

Figure 17 Sustained protein release from mpPCL TFPD. Release profiles for therapeutic proteins from mpPCL TFPD are less than 1st order, but not constant-rate, with a slowing in release as reservoir concentration decreases. While both are sustained release, exact profile shape is molecule dependent.

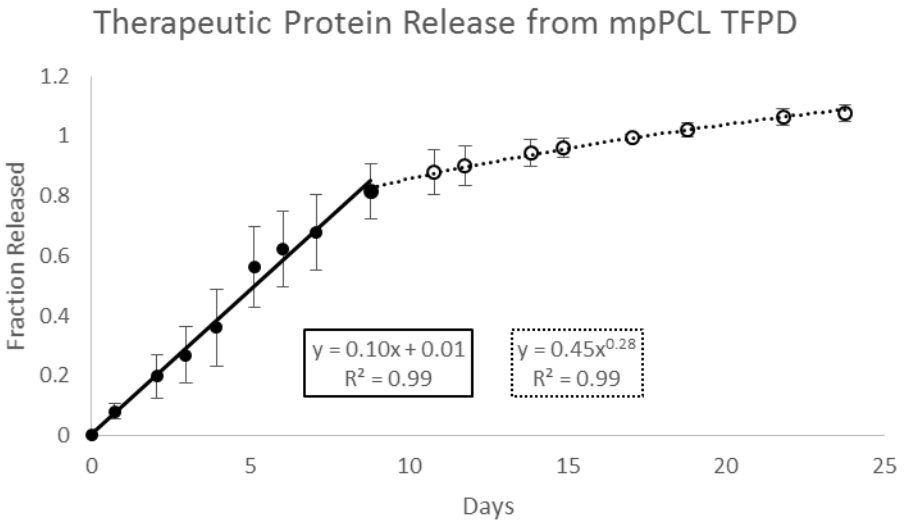

Figure 18 Characterizing release profile for therapeutic protein released from mpPCL TFPD. Release profile of a therapeutic protein from the mpPCL TFPD is bi-phasic, with an intial linear release up to 80% release, followed by a sustained release as the device depletes.

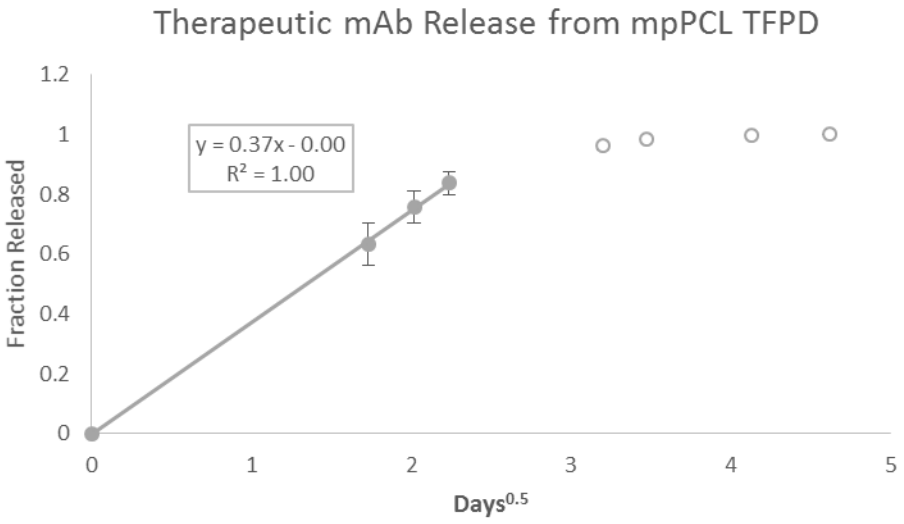

Figure 19 Characterizing release profile for therapeutic mAb sustained released from mpPCL TFPD. For this therapeutic mAb, release from the TFPD is linear with respect to the square root of time.

While the mpPCL membrane does sustain protein release, it does not result in concentration independent release as the rate of diffusion is still dependent on the concentration gradient through the porous membrane. The impact of reservoir concentration on protein release rates is discussed in more detail in the section on device design. Even though release rates from the mpPCL membrane are not perfectly linear nor concentration independent, they are significantly faster than with the nanoPCL membranes (> 1 µg/day per mm^2 surface area, depending on reservoir concentration), allowing for higher dosing and more flexibility in device design. Furthermore, as is illustrated in Figure 22, while macromolecule excipients do reduce diffusion in mpPCL, release rates are high enough to be therapeutically relevant for a reasonably sized device.[6]

[6] Additional information provided in Case Study I which further investigates protein formulation for an ocular implant.

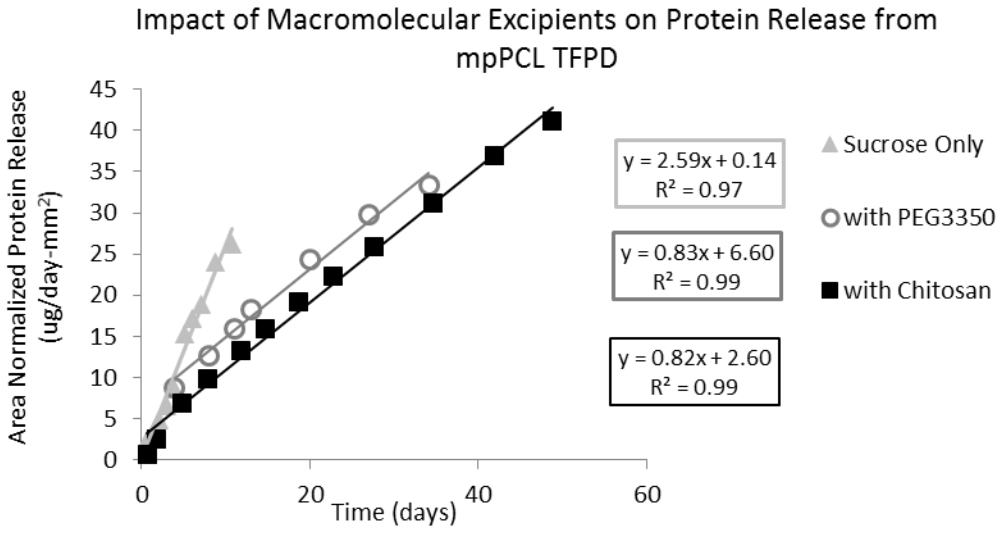

Figure 20 Protein release from mpPCL TFPD in the presence of macromolecule excipients. Similar to the nanoPCL, release rates are reduced upon addition of excipients PEG3350 or Chitosan to the device reservoir. However, with the significantly faster release from the mpPCL TFPD compared to the nanoPCL TFPD, adequate release is achievable in the presence of these excipients.

5.3.4. Tuning Release (mpPCL membranes)

As a platform technology for a range of drug delivery applications, it is desirable to be able to tune drug release from the TFPD. This was particularly important when replacing the nanoPCL membranes with mpPCL membranes for developing an ocular implant (Case Study I) as the mpPCL membranes have significantly faster release rates. While not an extensive investigation into altering membrane properties, two approaches to using membrane design to reduce release rate were tested. Based on the diffusion equations presented in Section 5.1.2, if diffusion through the tortuous pore structure of the mpPCL membrane is the limiting step for diffusion, release rates should be decrease as membrane thickness increases. However, as shown in Figure 23, increasing membrane thickness from 20 to 100 µm has no impact on protein release. This suggests that the bulk membrane and its porous structure are not the rate limiting step for diffusion. There are two hypothesized explanations for this, one is that, similar to the nanoPCL membranes, diffusion through the submicron pores connecting the micron sized pores

observed in the mpPCL cross section is rate-limiting or that the membrane surface is rate-limiting.

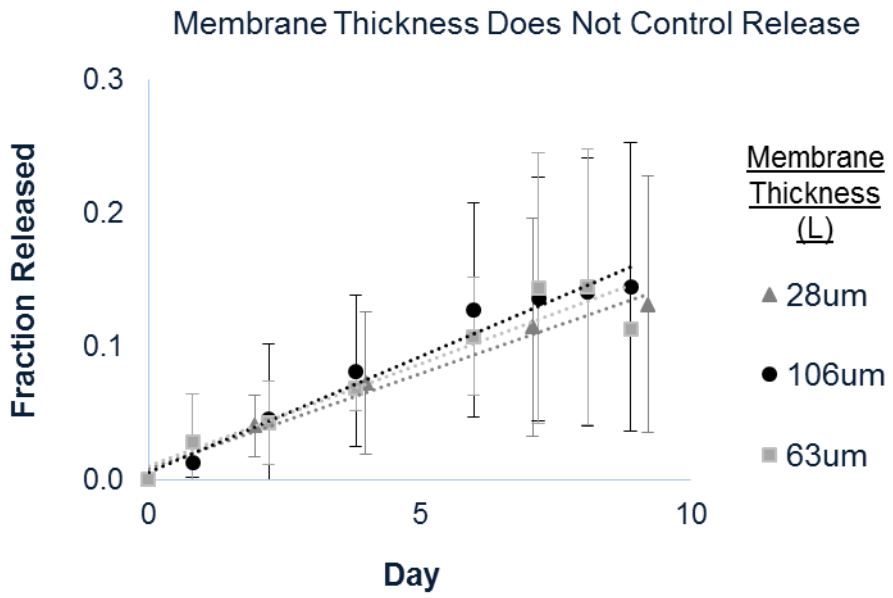

Figure 21 mpPCL membrane thickness does not impact protein release.

Another approach to tuning release rate is to alter pore size and/or structure. Pore structure is defined by the choice of porogen, relative concentration between porogen and polymer in the casting solution, casting surface, and process control such as % humidity, temperature, etc. However, in the context of the work presented here, major changes to membrane pore structure were avoided to prevent loss of the desired sustained protein release profile. In a simple attempt to reduce pore density while maintaining a comparable pore structure, the concentration of porogen was reduced. While this resulted in porous films with decreased porosity (less than 10% compared to the typical 50% porosity in mpPCL films fabricated from the "standard" recipe), protein release from these films was negligible and further investigation into reduced porosity films was abandoned.

As will be discussed further in the device design section (Section 6.5.2), rather than altering membrane properties to tune release rates, devices were fabricated with a combined nonporous and mpPCL membrane design, allowing for the adjustment of porous surface area to tune release rates while maintaining the sustained release profiles characteristic of the mpPCL membranes presented here.

6. TFPD Device Design

6.1. Introduction

Aside from the membrane, there are several aspects of TFPD design that are key for developing a system suitable for long-acting delivery of a therapeutic for a given indication. Device design is defined as membrane selection, device form, and reservoir formulation, all of which are dependent on the target indication and API. This section will generally describe how each of these components is considered in the development of a TFPD system for either small molecule pharmaceuticals or biologics; the proceeding case studies further illustrate the use of these concepts to design devices for specific indications.

6.2. The Target Product Profile

In designing a TFPD for a specific indication, it is critical to develop a target product profile for the system prior to starting device design. The target product profile should at a minimum consist of limitations or targets in device size and shape, API release rates, device duration, and acceptable storage conditions.

The device size and shape will be defined by the route of administration and user acceptability; for example an ocular device must fit within the intraocular space, while a subcutaneous device can be

significantly larger. Additionally, device form may be limited by methods of insertion as both size and shape may determine if the implant can be inserted without the need for sutures or anesthesia. Depending on the indication and site of implantation, what is acceptable may differ.

API release rates depend on the pharmacokinetic profile for the API delivered from a constant-rate implant as well as the drug efficacy. While for new and untested APIs this may be difficult to estimate, the development of TFPD systems is often relevant for molecules for which preclinical or clinical data are already available, albeit for a different route of administration or dosing regimen. Depending on what data are available, there are a number of different methods using very basic pharmacokinetic principles and models for estimating target release dosing, examples of which are given in Case Study II and Case Study III. There are two important concepts to remember in these evaluations. First, that when basing estimates on data from oral administration, that implants will likely by-pass the first-pass hepatic clearance. Second, that there is a pharmacokinetic benefit obtained from a constant rate release compared to a regular bolus or oral dosing regimen. While estimates at this stage may be very rough, it is critical to understand the range of dosing relevant to the target indication in order to develop a device capable of API release in this range.

Targets for device duration as part of the target product profile are dependent upon the indication, the current standard of care, and user acceptability. Take contraceptive implants as an example, particularly with the availability of multiple contraceptive methods, contraceptive implants requiring multiple rods as large as 2mm in diameter by 40mm long may be acceptable for a 5 year duration, but not acceptable for only 3 months of contraception. Additionally, implants must be desirable relative to the current standard of care; if the available regimen is an oral dose once a week and the implant offers only a one month duration but must be inserted into the eye, all other things being

equal, this is not likely to be the general user's preference. So based on these ideas and the clinical need, the target duration of the device should be defined in the target product profile before device development.

Acceptable storage conditions depend on the indication and target patient population. For example, in Case Study II, the product profile for an HIV PrEP implant with a target patient population in Sub-Saharan Africa is defined as storage conditions that do not require a cold chain. However, in Case Study I looking at the development of an ocular implant that will be administered in hospital clinics in the developed world, a cold chain requirement for storage is not an undue burden. While the testing of storage conditions may come well after the early device design, it is important to know the limitations on device design, API form, and reservoir formulation that may be defined by these storage conditions.

6.3. Design Components

6.3.1. *Membrane selection*

Section 5 describes the different variations of PCL membranes and their resulting release profiles for pharmaceuticals or biologics. Based on the principles outlined in the membrane design section, a membrane should be selected that is suitable to deliver the API of interest with the desired release profile. Furthermore, a membrane should be developed that is most capable of releasing the API at release rates relevant to the given indication; as is discussed in the proceeding sections, achieving target release rates also depends on device form and reservoir formulation.

6.3.2. *Device form*

The size and shape of the device, defined by the site of implantation and user acceptability, in turn defines the reservoir volume, device surface area, and the potential methods or protocols for insertion. The reservoir volume is a key device parameter for device design as it both defines the loading capacity as well as reservoir concentration which will be discussed further in the following sections. Release rates scale with membrane surface area; while the combination of membranes with different characteristics allows us to reduce the effective surface area for drug release, the upper limit for effective surface area and thus drug release rate is defined by the device form. As discussed in the target product profile, the device form may also dictate how and where the device may be inserted and whether or not the procedure requires anesthesia or surgery.

Furthermore, device duration is dependent on both device form, release rates, and polymer degradation. Device form defines reservoir volume, and thus the API loading capacity. The maximum duration is therefore a function of API loading capacity and release rate as long as the polymer degradation does not result in fragmentation before drug depletion.

6.3.3. *Reservoir Formulation*

Formulation excipients may be added to the device reservoir for several reasons. In the case of pharmaceuticals, solubilizing excipients may be used to increase the rate of dissolution or to increase drug solubility in the device reservoir. If the rate of dissolution in the device reservoir for an API is not faster than the rate of release, dissolution will define the release profile. (Figure 52) If this is the case, excipients that increase the rate of dissolution may be added to achieve membrane controlled release. As is illustrated in Case Study II, increasing the solubility of an API in the device reservoir increases the concentration gradient, the driving force for diffusion, thus

increasing release rates. (Figure 51) In some cases, the same excipients that increase solubility may also increase the rate of dissolution. For both pharmaceuticals as well as proteins, formulation excipients may be added to the device reservoir to increase API stability. This is particularly relevant for protein formulation as high concentrations in the device reservoir (> 100 mg/ml in most cases) create an unstable environment for proteins in solution under physiological conditions. Two approaches to protein formulation in the device reservoir are discussed in Case Study I. As is highlighted by the case studies, it is important to remember in designing a TFPD that any change to reservoir formulation may impact release rates and thus the device design or membrane selection must be altered accordingly. (Figure 18)

6.4. Device Design for Small Molecule Pharmaceuticals

Case study II and III describe the application of the ideas presented in this section on device design to the development of TFPD systems for specific indications. The basic design for small molecule API TFPDs hinges upon the excess loading of API into the device reservoir, well above the solubility limit, maintaining a saturated solution in the reservoir throughout the majority of the duration of administration. With a constant concentration and driving force for diffusion, constant rate membrane controlled release is achieved until API depletes below the saturated concentration. This section will summarize the key tools used in device design for these systems.

6.4.1. Release rate is proportional to surface area

As is shown in Figure 53 and Figure 54 and described in Equation 4 Steady state flux through a membrane with a constant activity source and sink conditions. , release rates are proportional to membrane surface area. This is one tool in device design used to tune release rate and is particularly useful when scaling devices for pre-clinical animal studies in which both the device

size and release rate need to be adjusted to accommodate the animals smaller size. Additionally, demonstrating the proportional relationship between membrane surface area and release rate also indicates that the TFPD exhibits membrane controlled release. A non-linear relationship between release rate and surface area may indicate a dissolution controlled release. (Figure 52)

6.4.2. Release rate is inversely proportion to membrane thickness

As described by Equation 1 and Equation 4, release rate in a membrane controlled reservoir device is inversely proportional to membrane thickness. This provides a means of tuning release rate that is orthogonal to membrane surface area. For example, if a reduction in device size and thus membrane surface area is not desirable due to the loss in loading capacity, membrane thickness can be increased to effectively reduce drug release. However, there is a practical limit to reducing membrane thickness and membranes less than 5 μm are not practical for handling. Furthermore, it is important to validate the relationship between membrane thickness and release rate for a given range of membrane thickness; as is observed in **Error! Reference source ot found.**, as membrane thickness is increased for this particular system, a critical point is reached after which increasing membrane thickness no longer reduces release rate. This suggests that at this point, membrane thickness is no longer the limiting factor for drug release. Such a phenomenon may be dependent on both the API and the film fabrication protocol and should be tested empirically.

6.4.3. Formulation excipients

Common formulating excipients to increase drug solubility or dissolution can be used to formulate API in the device reservoir. Examples of such excipients include polyethylene glycols,

cyclodextrins, polysorbates, and co-polymers such as poloxamers. The impact of formulating with these excipient depends on both the excipient concentration as well as its interaction with the given API. There is a significant body of work and experience in the pharmaceutical field using such excipients as formulation components that can be used as a guide. [25] [26] However, the effect of these excipients on API release and stability in the context of the TFPD must be evaluated empirically as the impact of excipients in controlled release systems can be complex. [27] [28] For example, while in theory increase in reservoir solubility for an API should be directly proportional to an increase in release rate, this may not always be observed. Variations can be due to the formation of complexes between API and excipient resulting in larger effective hydrodynamic radii or a change in API partition between the aqueous phase and polymer membrane.

6.5. Device Design for Biologics (proteins)

As is the case with membrane design, device design for biologics compared to pharmaceuticals is more complex. As proteins have relatively high solubilities and tendencies to form gels rather than saturated solutions the way small molecules do, the TFPD design for protein APIs does not leverage a constant reservoir concentration from a saturated solution achieving constant rate release. Instead, as previously discussed, the membrane design achieves a constant-rate or sustained protein release. This section will describe the approach to device development for mpPCL devices which have the most flexibility and tunability as TFPDs for protein delivery. The development of device designs for the mpPCL TFPD release protein API depend on a series of empirical correlations that relate device design parameters, those aspects of the system that are directly controlled in fabrication, to system design parameters, system characteristics that define performance and are indirectly controlled through the device design parameters. The following sections describe the

device design model for a representative mAb therapeutic with no additional formulating excipients. Case Study I describes the development of a similar design model when formulation excipients are considered.

6.5.1.Reservoir Concentration

While the mpPCL membrane does sustain protein release, it does not result in concentration independent release as the rate of diffusion is still dependent on the concentration gradient through the porous membrane. This is evidenced by a linear dependence between the magnitude of the release rate and the protein reservoir concentration or the protein load as compared to similarly sized devices. (Figure 24) The release rate constant for the therapeutic mAb, which exhibits a sustained release profile that is linear with respect to the square root of time, is taken as the linear release rate relative to the square root of time (as illustrated by the trendlines in Figure 21).

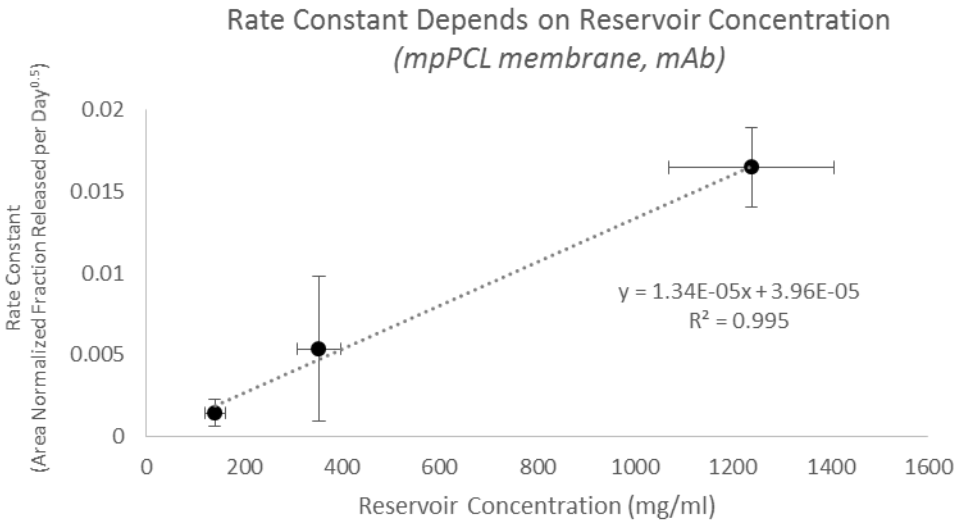

Figure 22 mAb release rate from mpPCLTFPD is proportional to reservoir loading concentration. Reservoir concentration is empirically determined and defined as the loading mass relative to reservoir hydration volume determined by mass change upon hydration.

The reservoir concentration is clearly a key factor in designing a device with a targeted release rate. The reservoir concentration as defined in the empirical correlation illustrated in Figure 24 is the initial protein loading divided by the volume of water absorbed into the device reservoir upon hydration. Thus the reservoir concentration depends on both device loading as well as reservoir hydration. For a given formulation and API, the reservoir hydration volume correlates with device size. (Figure 25) Thus, knowing the device load and device volume, both device design parameters, the resulting reservoir concentration and rate constant can be predicted.

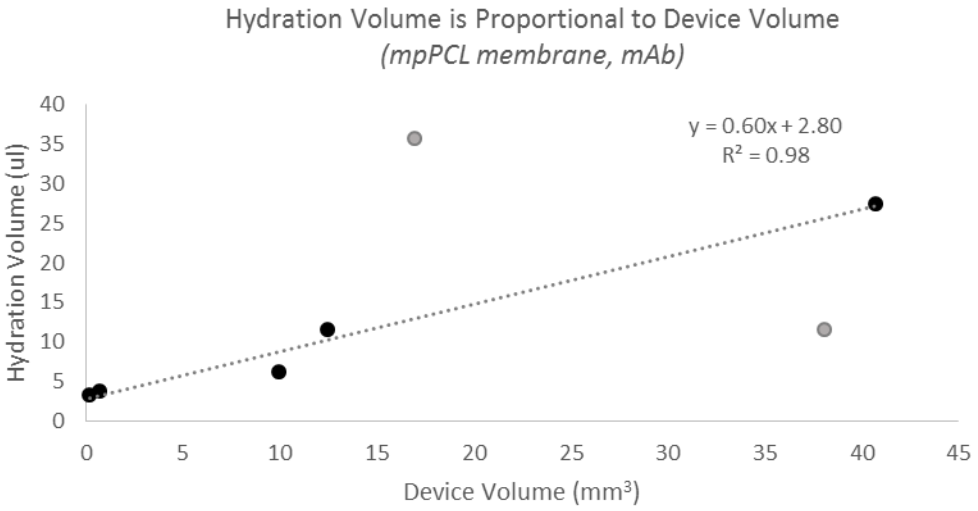

Figure 23 Reservoir hydration volume depends on device size. Gray data points are outliers and not included in trendline. Error in empirical measurement is not unexpected due to small increases in mass upon hydration and presence of air bubbles due to under-loading or large devices.

6.5.2. Membrane surface area

It should be noted that the empirical correlation presented in Figure 24 describes the rate constant as area normalized fraction released. As release rate and porous surface area are proportional to one another, membrane surface area can be used to tune the rate of protein

release. Proteins do not diffuse through a nonporous PCL membrane, and thus by combining the nonporous and mpPCL membrane, essentially creating a mpPCL "window" through which protein is released, protein release rates as a function of membrane surface area are decoupled from the overall device size. Instead of being dependent on device surface area, protein release is only dependent on the mpPCL membrane area, which can be as small as possible for fabrication (~ 3-5 mm^2 with bench scale fabrication) and as large as the total surface area of the device.

6.5.3. Applying empirical correlations to a device design model

The empirical correlations and device design principles presented here can be combined to produce a model for device design. The inputs are device design parameters (i.e. protein load, device volume, and membrane surface area) and the output is the release rate constant as fraction released per square root of time and a predicted release profile presented as cumulative mass released as a function of time. It should be noted that the translation of empirical correlations to a device design model takes into consideration the shape of the sustained release profile, which is molecule specific, as described in Section 5.0.

Figure 26 details the device design and predicted release profile up to 100 days for a subcutaneous device 2mm in diameter and 40mm long with varied mpPCL surface areas to release the mAb investigated in this section. The protein load for this device is estimated based on 90% of the theoretical loading capacity of a device this size with a protein particle density of 1.4 mg/ml.

Device Design Parameters	
Protein Load (mg)*	158
Device Volume (mm^3)	125
System Parameters	
Hydration Volume (ml)	0.078
Reservoir Concentration (mg/ml)	2025
Design Output	
Rate constant (fraction per mm^2 per $day^{0.5}$)	0.027

*based on 90% of theoretical loading capacity

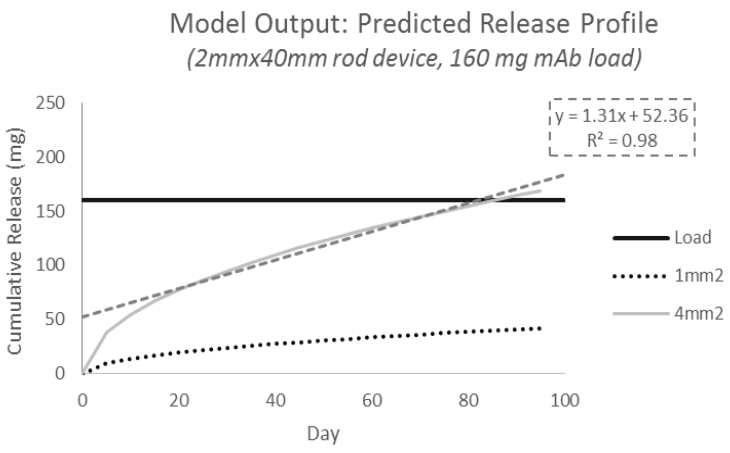

Figure 24 mpPCL window Device Design Model for mAb release from a representative TFPD designed for a subcutaneous implant. Predicted release profiles are illustrated for two different mpPCL "window" sizes.

Based on the input for device volume and the empirical correlation in Figure 25, reservoir hydration volume is predicted. From the input for protein load and the predicted reservoir hydration volume, reservoir concentration is predicted. With the predicted reservoir concentration and the empirical correlation in Figure 24, the area normalized rate constant in terms of fraction released is calculated. The rate constant can then be used to calculate a cumulative release profile by taking into consideration the total protein load and the input for mpPCL surface area. While this is only one example of a device design using this model for the mAb considered here, device design inputs could be tuned to predict release profiles or determine necessary mpPCL membrane areas targeting specific release rates for devices of different sizes and loading. Variations in this approach to developing a model for device design based upon empirical modeling are presented in Case Study I for another protein therapeutic in the presence of formulation excipients.

7. Materials & Methods

7.1. Definitions

mpPCL – microporous PCL; nanoPCL – nanoporous PCL; npPCL – nonporous PCL; PEG – polyethylene glycol; PEG3350 – polyethylene glycol average m.w. 3350; hVLM - Human vitreous-like media; a phosphate buffered saline based media, pH 7.2 ; SE-UPLC/HPLC – Size exclusion ultra performance liquid chromatography / high performance liquid chromatography ; RP-UPLC/HPLC – Reverse phase ultra performance liquid chromatography / high performance liquid chromatography; WFI – water for injection; TFPD – thin film polymer device; PDMS – polydimethylsiloxane; HP-β-CD – hydroxypropyl beta cyclodextrin; PEG300 – polyethylene glycol with 300 average molecular weight; PS20 – polysorbate 20; UV – ultraviolet

7.2. General Procedures

7.2.1. PCL Film Fabrication & Characterization – nonporous (npPCL)

Films were draw-cast onto a glass surface using a multiple clearance square applicator (Paul N. Gardner Company, Inc., Pompano Beach, FL) from an 80 to 200 mg/ml solution of PCL (average Mn 80kDa, Cat#440744 Sigma, St. Louis, MO) in dichloromethane. After drying, PCL was annealed by heating to just past melting with a heat gun and cooling at room temperature. The solution concentration and height of the draw-casting rectangle were used to obtain films of varying thickness. npPCL films were characterized for film thickness using a micrometer.

7.2.2.*PCL Film Fabrication – nanoporous (nanoPCL)*

Films were fabricated by Dan Bernards according to the following method described in the 2012 article “Nanostructured Thin Film Polymer Devices for Constant-Rate Protein Delivery” published in Nanoletters [7]: Onto a clean silicon substrate a zinc oxide seed layer is spin-cast

and nanorods, on average 20nm in diameter and 500-1000nm long, are grown hydrothermally. A thin PCL layer is spin-cast onto the ZnO template followed by a PCL and PEG mixture. Deionized water dissolves the PEG phase from a supporting layer, and sulfuric acid etches the ZnO template to generate a supported nanostructure PCL thin film.

7.2.3.PCL Film Fabrication & Characterization – microporous (mpPCL)

Films were draw-cast onto a glass surface using a multiple clearance square applicator (Paul N. Gardner Company, Inc., Pompano Beach, FL) from a 200 mg/ml PCL (average Mn 80kDa, Cat#440744 Sigma, St. Louis, MO) and 200 mg/ml PEG (m.w. 2050 Da, Cat#295906 LotBCBJ7635V, Sigma, St. Louis, MO) in 2,2,2-trifluoroethanol. After drying, deionized water was used to dissolve the PEG phase from the PCL creating a porous structure. mpPCL films were characterized for % porosity and film thickness. Film thickness was measured using a micrometer, and % porosity was determined by film density compared to PCL density according to the following equation:

$$\%\, porosity = 1 - \frac{\rho_{film}}{\rho_{PCL}}$$

PCL density is 1.125 g/ml and PCL film density is calculated using the mass of a section of film with known dimensions.

7.2.4.Device fabrication (nonporous PCL/mpPCL combination devices)

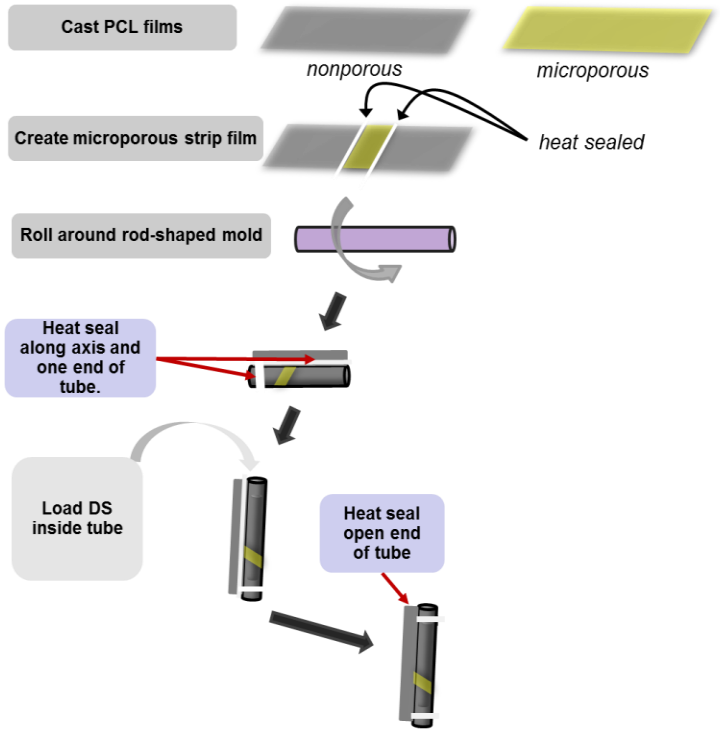

Figure 25 PCL thin film reservoir device fabrication schematic. For a mpPCL TFPD, the first step consists of splicing a mpPCL section between two nonporous PCL pieces using a heat-sealing apparatus. Next, for either a mpPCL TFPD or nonporous PCL TFPD, the film is rolled around a rod-shpaed mold with a diameter slightly smaller than the desired device diameter. The heat sealing apparatus is used to seal along the longitudinal axis of the rod. The rod is then removed (not shown) and one end of the device is sealed. Drug substance is then loaded into the open end of the tube, and the open end of the tube is then sealed.

Figure 27 illustrates the general process flow for device fabrication of a combined nonporous and mpPCL PCL device. In short, a piece of mpPCL is spliced between two pieces of nonporous PCL using heat sealing. Heat sealing is accomplished by aligning the film above a nickel-chromium wire embedded between two PDMS slabs. The wire is heated by passing a current through the wire. The film is then rolled around a cylindrical mold whose diameter is chosen based on the target device dimensions and heat sealed along the longitudinal axis of the cylinder and on one end to create a hollow cylinder with one open end. Drug substance is then loaded into the cylinder and a final seal made along the open end.

7.2.5.Device fabrication (nonporous PCL)

The same general process is followed for fabrication of purely nonporous or mpPCL devices as described in Figure 27, skipping the first step combining mpPCL and nonporous PCL. In more detail, for each device, the PCL film thickness at multiple points (> 9) was measured using a micrometer. A Nickel-Chromium wire sandwiched between two thin slabs of PDMS and attached to a DC power supply constituted a heat-sealing apparatus through which controlled current was applied (1.2A) to heat the wire. PCL film was placed over the wire, and when the wire heats, the PCL melts. To fabricate a rod-shaped device, the PCL thin film was reinforced on each end with thicker (>30um) pieces of PCL film to provide structural support to the thin-film cylinder during device loading and later sampling. This reinforcement was done by sealing the thicker piece of PCL along the edge of the membrane film, folding over the added piece of PCL and sealing again along the same line. The cylindrical device was fabricated by wrapping the PCL around a rod-shaped mold of the desired diameter and sealing the film together along the lengthwise axis first and then along one reinforced end to create a PCL tube with one end open. Empty devices were weighed prior to loading.

7.2.6.*Release Testing*

API concentrations in all samples were measured by either UV absorbance at their respective maximum wavelength using a SpectraMax M5 (Molecular Devices, Sunnyvale, CA) plate reader or by HPLC via use of a calibration curve. All release studies were done in , pH 7.4 at 37ºC in an incubator on an agitator at 120 rpm. Release buffer volume and time intervals between samples were chosen to fully submerge device and to maintain sink conditions in release buffer at less

than 1/5th of saturation. Volumes ranged from 0.5 – 10mL with sample time points ranging from 1 hr -5 days, depending on the API and device size. At each time point, the device was transferred to an aliquot of fresh release buffer. For each sample API concentration was measured and mass of API released during the time interval was calculated. For each device a cumulative mass versus time profile was used to determine the linear release rate. Linear release profiles were normalized to membrane area by dividing the release rate (mg/day) by device surface area (mm^2).

7.3. Accelerated PCL Degradation Specific

7.3.1. *Accelerated Degradation*

Films were cut into pieces roughly 1-3 in^2 fully submerged in 5-10mL of 4N Formic Acid and incubated at room temperature on an agitator. At each time point, a PCL film sample was rinsed thoroughly in DI water, blotted dry with a tissue, and further dried at room temperature for at least 24 hours, weighed, and stored under ambient conditions until further analysis.

7.3.2. *GPC Analysis*

PCL molecular weight distributions were determined via GPC. An isocratic method with THF as the running buffer was used with a series of three Styragel® GPC columns (HR5/WAT0554460, HR2/WAT044234, HR0.5/WAT044231) and an RID detector. Molecular weight analysis was completed based on polystyrene standards.

7.4. Pharmaceutical Membrane Design Specific

7.4.1.Matrix system film fabrication

Drug product was dissolved in TFE and once dissolved, 70-90 kDa PCL was added to solution at 200 mg/ml. PCL was dissolved in drug/TFE solution overnight in either a 60°C water bath or in a 37°C incubator on an orbital shaker. A drug-polymer thin-film matrix was cast onto a 3-inch diameter silicon wafer using a spin-coater *(Specialty Coating Systems, Model P6700; 30s at*

1500RPM, 30s at 2000RPM) at room temperature. The resulting film was dried under ambient conditions and film thickness was measured using a profilometer. Circular samples (28 mm diameter) were cut from films for *in vitro* release studies. For each drug and loading concentration, three films were cast and a sample was taken from each. See Table II below for a summary of analyzed samples.

7.4.2. *Matrix system samples*

Table II: Summary of PCL Matrix Samples Analyzed

Pharmaceutical	n	% Loading (w/w API/PCL)	Membrane Thickness (μm)	D‘ (mm²/hr)	Y'
Aspirin	3	3	15.8	1.3E-05	1.38E-10
	3	4	17.3	2.4E-05	8.44E-11
	3	5	19.5	1.4E-05	6.67E-11
	3	5	17.4	1.8E-05	1.65E-10
	3	6	20.2	2.2E-05	1.96E-10
Atenolol	3	4	12	1.5E-05	5.93E-11
	3	5	10.4	1.0E-05	7.49E-11
	3	7	19.5	7.8E-06	9.88E-11
	3	7	7.7	1.0E-05	6.52E-11
Caffeine	3	2	8.6	8.2E-06	*
	3	3	10.2	7.9E-06	*
	3	4	10.4	1.7E-05	*
	3	5	19.5	1.3E-05	1.84E-11
	3	7	13.2	2.3E-05	1.75E-11
Diclofenac-Na	3	4	19.5	5.3E-06	1.16E-07
Ibuprofen	3	3	16.2	1.0E-05	1.99E-08
	3	4	14.7	1.4E-05	1.82E-08
	3	5	19.8	1.0E-05	2.87E-08
Labetalol-HCl	3	5	19.5	3.4E-06	3.41E-09
Metoprolol Tartrate	3	16	20.3	3.0E-06	1.82E-10
Ranitidine-HCl	3	9	19.5	2.6E-06	1.54E-10
Verapamil-HCl	3	4	13.7	1.2E-06	6.29E-08
	3	6	14.5	1.1E-06	1.01E-07
	3	11	13.6	1.2E-06	5.52E-07
	3	12	19.2	4.8E-06	2.04E-07

** Y' not calculated for these samples. Drug loading was below Cs and data is fit with equation 1b only.*

7.4.3. Reservoir system samples

Table III: Summary of PCL Reservoir Samples Analyzed

Pharmaceutical	Area (mm^2)	Membrane Thickness (um)	Dk (mm^2/hr)
Caffeine	208	15	1.7E-11
	208	14	1.0E-11
	208	13.4	4.9E-13
	188	8.5	3.8E-10
	188	5.2	3.2E-10
Diltiazem-HCl	157	12.3	2.6E-12
	157	12.3	1.5E-12
Ranitidine-HCl	188	18.8	3.9E-10
	188	16.4	2.4E-10
	188	14.7	1.2E-10
Verapamil-HCl	188	25.5	1.9E-11
Atenolol	188	6	1.5E-10
Famotidine	190	16.2	1.7E-11
	173	16.2	2.7E-10
	173	16.2	7.1E-11
Hydrocortisone	157	10.8	5.4E-11
	157	12.3	1.4E-10
Labetalol-HCl	208	14.5	2.5E-12
	208	11.8	2.6E-11
	208	11.8	1.9E-11

7.4.4. Data analysis

For both matrix and reservoir samples, concentration in each sample was determined using a UV calibration curve for the relevant drug. Based on the release volume, mass released in each time interval and cumulatively were calculated. Matrix system release data was further processed to determine the cumulative percentage of drug released based on the total drug released. Time courses for matrix system data were continued until cumulative drug release reached a clear plateau and release could no longer be detected.

7.5. Ocular implant case-study specific:

7.5.1.Film Fabrication & Characterization

All films are prepared as described in general procedures. Devices in all experiments presented in this section are comprised of at least one of the following:

- nanoPCL films with 20nm average pore diameter

- nonporous PCL films 12-20 µm thick
- mpPCL films with 45-65% porosity, 25-35 µm thick

When combining mpPCL and nonporous PCL films in device fabrication, a nonporous PCL thickness is selected to be roughly the same mass of PCL in a given area relative to the mpPCL film. That is, for a 50% porosity mpPCL film 30 µm thick, a 15 µm nonporous PCL film is selected.

7.5.2. *Device Fabrication & Characterization*

To determine load, mass of each loaded device is compared to the mass of the empty device. Porous dimensions for a nonporous PCL / mpPCL device are measured using a caliper prior to device loading, assuming that any subsequent sealing does not affect the porous area. Overall device dimensions are determined using a caliper after loading and sealing. If final sealing steps impacted porous area, porous area is re-evaluated post-fabrication.

Devices with “sucrose only” formulation are loaded with lyophilized protein and no additional excipients. PEG3350 formulation devices are loaded with lyophilized protein and crystalline PEG3350. For studies investigating chitosan load for the chitosan formulation, solid chitosan and lyophilized protein are physically combined in solid form and loaded into the device. For all other chitosan formulation studies, chitosan and protein are co-lyophilized.

7.5.3. Stability studies (nonPCL)

Nonporous PCL devices are fabricated and loaded with protein and excipients. Devices are fully submerged in 0.5 - 1mL release media (hVLM, pH7.2) and incubated at 37˚C in polypropylene tubes. While protein release from the npPCL devices is not expected nor measured, release media is changed regularly (1-3 days) to prevent bacterial and fungal contamination. At each time point for analysis, a device is transferred to a known volume of release media and cut

open. Gently vortexing or mixing ensure that all reservoir contents are released into the media and dissolved. Protein purity is analyzed via SE-HPLC or SE-UPLC.

7.5.4. Release studies

NanoPCL or mpPCL devices are fabricated and loaded with protein and excipients. Release of protein from nanoPCL and mpPCL devices is evaluated by fully submerging devices in 0.5 – 1mL release media (hVLM, pH7.2) and incubating at 37˚C in polypropylene tubes. At each time point (1-3 days), devices are transferred into a fresh aliquot of release media; release media from the prior period of incubation is retained for analysis. Protein quantity and purity is determined in each sample via SE-HPLC or SE-UPLC, and mass of protein released for each time interval is determined. Release profiles are typically presented as cumulative release as a function of time; cumulative release is calculated by summing the quantity of protein released in each subsequent sample over a time course. Release profiles are at times also presented as normalized to porous surface area; this is calculated by dividing the cumulative release at each time point by the porous surface area measured during device fabrication and characterization.

7.5.5. PEG3350 solubility studies

Studies are conducted in glass vials, not device reservoirs, to better understand this approach of using PEG3350 to limit protein solubility and thus improve protein stability. We investigate both the precipitation of protein from solution through the addition of PEG3350 solution (designated "liquid") as well as the reconstitution of lyophilized protein combined with solid PEG3350 to recapitulate what occurs upon hydration of the reservoir device (designated "reconstituted").

7.5.5.1. Study 1

To determine the reduction in protein solubility with the addition of PEG3350 in solution, concentrated PEG3350 solutions are added to multiple protein solutions of known

concentration to target a range of final PEG3350 concentrations. A total protein content of 5 mg/ml is targeted in all final solutions. After mixing and a > 60 min equilibration period, solution is centrifuged to pellet any solid contents and supernatant is removed for analysis. Prior to SE-UPLC and RP-UPLC analysis to determine protein purity and concentration, supernatant is filtered through a 0.22 μm spin-filter.

7.5.5.2. Study 2

To determine the impact of total protein content on protein solubility with the addition of PEG3350 in solution. Study 1 protocol is repeated for protein solutions with total protein contents ranging between 10 – 45 mg/ml. For each protein concentration, four PEG3350 concentrations are evaluated.

7.5.5.3. Study 3

To determine the impact of PEG3350 concentration on protein solubility when reconstituted from lyophilized protein and crystalline PEG3350. Total protein content in reconstituted solution is targeted to be 10 mg/ml and PEG3350 target concentration in reconstituted solution is varied by PEG3350 load. WFI is used for reconstitution. Analysis of protein purity and quantity is performed as described in Study 1.

7.5.5.4. Study 4

To determine the recovery and purity of protein excluded or precipitated from solution by PEG3350. Total protein content in starting solutions is 25 mg/ml and 5 mg/ml in final solutions. Starting with either protein precipitated from solution according to the protocol in Study 1 or protein excluded from solution as described in the protocol in Study 3, solutions are diluted 5x with WFI. After 5x dilution, protein solubility based on PEG3350

concentration as determined by results of Study 1-3 is higher than the total content of protein in the samples. Thus, PEG3350 no longer limits protein solubility in this system and all protein should be recovered in solution. Protein purity and concentration is determined by SE-UPLC and RP-UPLC.

7.6. HIV PrEP Subcutaneous Implant Case-Study Specific

7.6.1.Antiretroviral formulation and loading:

7.6.1.1. Elvitegravir

Elvitegravir was graciously provided by Gilead Sciences (Foster City, CA). Elvitegravir was loading into the TFPD as a dry powder. For the preliminary screening work presented here, elvitegravir was compressed slightly upon loading, but not compressed fully into a solid pellet. After loading, devices were laid flat on the PDMS of the heat sealing apparatus and sealed. Once sealed devices were weighed to determine the total payload and device dimensions were recorded.

7.6.1.2. Rilpivirine HCl

Rilpivirine HCl and nanosuspension formulations were graciously provided by Janssen Pharmaceuticals R&D, Pharmaceutical Development and Manufacturing Sciences (Beerse, Belgium). When formulated with PEG300 or PS20, rilpivirine HCl was added to the liquid formulation excipient to create a viscous slurry that could be loaded through a P100 pipette tip into the device reservoir. When formulated with HP-β-CD, HP-β-CD was first dissolved at 60% w/w in deionized water. Rilpivirine HCl drug powder was then added to the solution to create a thick slurry to be loaded into the device reservoir in a similar manner to the PEG300 slurry formulation. While not represented in the data presented here, after loading the HP-β-CD slurry formulation into the device reservoir and prior to

making the final seal, the loaded device could be placed in a vacuum chamber overnight to dehydrate the reservoir contents leaving behind a solid dispersion of Rilpivirine HCl and HP-β-CD. The liquid nanosuspension was loaded into the device reservoir with a P100 pipette, and the lyophilized nanosuspension was loaded as a solid powder, compressed slightly upon loading, but not fully compressed into a solid pellet. After loading, devices were laid flat on the PDMS of the heat sealing apparatus and sealed. Once sealed devices were weighed to determine the total payload and device dimensions were recorded.

7.6.1.3. Tenofovir Alafenimide Fumarate

TAF was graciously provided by Gilead Sciences (Foster City, CA). When formulated with PEG300, TAF was mixed with PEG300 at desired ratios (1:2, 1:1, or 2:1 w/w) immediately prior to device loading. Devices were loaded using either a 1mL insulin syringe with the needle removed or with a P100 pipette tip. After loading, devices were laid flat on the PDMS of the heat sealing apparatus and sealed. Once sealed devices were weighed to determine the total payload and device dimensions were recorded.

7.6.2. *Antiretroviral quantification & stability analysis*

7.6.2.1. Elvitegravir

Elvitegravir was quantified using a UV-based assay (λ = 260nm) on a 96-well plate using a calibration curve. Elvitegravir stability was not analyzed. For the UV assay, all samples and standards were run in triplicate.

7.6.2.2. Rilpivirine

Rilpivirine was quantified using either a C18 RP-HPLC assay with two mobile phases and a linear gradient[7] or using a UV-based assay (λ = 300nm) on a 96-well plate using a calibration curve. For the UV assay, all samples and standards were run in triplicate. Rilpivirine stability was not analyzed.

7.6.2.3. Tenofovir Alafenimide Fumarate

TAF was quantified using a UV-based assay (λ = 260nm) on a 96-well plate using a calibration curve. All samples and standards were run in triplicate.

TAF stability in the device reservoir was evaluated by opening up a device with remaining TAF, dissolving the entire reservoir contents into release buffer, and measuring TAF purity using RP-HPLC**.** This HPLC method separates TAF from process impurities associated with TAF production as well as TAF degradation products. TAF purity is calculated as % peak area associated with TAF relative to total peak area of TAF related degradation products and product impurities.[8]

7.6.3. Antiretroviral release studies

All release studies were done in phosphate buffered saline (PBS), pH 7.4 at 37ºC in an incubator on an agitator at 120 rpm. For all rilpivirine release studies, 1% v/v PS20 was included in the release media to increase drug solubility and maintain sink conditions. Release buffer volume and time intervals between samples were chosen to fully submerge device and to maintain sink conditions in release buffer at less than 1/5th saturation. Volumes ranged from 1 – 50mL with sample time points ranging from 1 hr-5 days. At each time point, devices were transferred to fresh release buffer. For each sample, drug concentration was measured and mass of released

[7] Full analytical HPLC method provided by Janssen Pharmaceuticals.
[8] Full analytical HPCL method for TAF purity adapted from Gilead Sciences STM-2013.

during the time interval was calculated. For each device a cumulative mass versus time profile was used to determine the linear release rate. Linear release profiles were normalized to membrane area by dividing the release rate (mg/day) by device surface area (mm^2).

8. Case Study I: A TFPD as an Ocular Implant for Long-Acting Delivery of Protein Therapeutics

8.1. Introduction

Improving therapeutic delivery to the eye is both a challenging and lucrative endeavor. The size of the patient population and market are astounding. In 2010, 733 million people globally were affected by vision loss or blindness [29] . Fortunately, for many of the leading causes of vision loss there are treatments available to at least slow or halt disease progression, if not improve sight. In 2014, the market for such ophthalmic therapeutics and devices reached 36 billion USD [29] and it's only expected to grow. [30]

When delivering therapeutics to the back of the eye, there are few options available. While small molecules can potentially be applied to the front of the eye with hopes of permeation through the eye's multiple barriers, very little drug is expected to actually reach to the site of action at the back of the eye. Biologics typically do not permeate at all through the corneal epithelium. Therefore, most back of the eye therapeutics rely on direct injection. While this gets the drug where it needs to go in effective doses, it is undeniably unpleasant to receive an ocular injection and many treatments require patients to undergo this once or twice a month. As a result, patient compliance can be a major hurdle, leading to under-treatment in many cases. Additionally, ocular injections pose their own risk of complications resulting from the procedure itself, so minimizing the number of injections into the eye is critical for improving therapeutic delivery. Therefore, there is strong interest in long-acting drug delivery systems to improve patient compliance, safety, and efficacy of posterior ocular therapeutics. [31]

In this section is considered the development of a PCL thin film reservoir device as a back of the eye ocular implant for long acting delivery of protein therapeutics.[9] Currently on the market are several examples of protein therapeutics injected once or twice a month into the back of the eye to treat chronic diseases such as age related macular degeneration. Delivery of such therapeutics from a biodegradable implant such as the PCL thin film reservoir device with a 4-6 month duration would increase bioavailability and reduce the effective dose, improve patient compliance, and reduce the frequency of risky ocular injections and clinic visits. However, there are significant challenges to developing such a system, both in controlling release of the therapeutic and maintaining protein stability under physiological conditions within the device reservoir.

When developing a back of the eye implant for the controlled release delivery of a protein therapeutic, several key factors must be considered. First, the device must be reasonably sized to both fit within the intravitreal space and to be inserted without major surgery. In a human, the maximum size of such a rod shaped implant is expected to be 1mm or less in diameter and 8mm or less in length. In the context of early pre-clinical development and device design, particularly while devices are fabricated individually by hand, larger devices are used. However, as the scale down of such devices will be paramount to their future success, a thorough understanding of the fundamental principles of the device design, performance, and scaling are critical. Related to the device size are the loading capacity and duration of administration from a single device. Based on the protein therapeutics commercially available for back of the eye, doses of less than 100 μg per day are reasonable for therapeutic effect from a long acting implant. Therefore, loading capacities for 4-6 months duration will be on the order of several milligrams. For the system presented here,

[9] Due to the confidential and proprietary nature of our collaboration on this project with an industry partner, molecule names and sensitive information have been redacted from this section.

the target loading capacity is 3 mg of protein. The third factor for consideration is protein stability. As the following section describes in more detail, there are many challenges associated with maintaining the physical stability of protein in a long acting reservoir device implant. For early preclinical development of the protein therapeutic considered here, there is a minimum criteria of 75 % protein monomer after 90 days. The final key factor in device design is the target release rate and release profile. A linear or near linear release profile with minimal burst release is ideal, and release rates must be tuned to specific targets for a given therapeutic.

The research presented here describes the early development and design of an intraocular back of the eye PCL implant for long acting delivery of a protein therapeutic. In addition to introducing novel formulation techniques suitable for high concentration long acting reservoir devices, scalable and tunable device designs specific to these formulations are presented.

All experiments and devices presented in this section use a recombinant protein therapeutic relevant to ocular drug delivery. Further information regarding molecular properties and identification are proprietary and therefore redacted. The protein therapeutic will simply be referred to as "protein" throughout the section. It should be noted that fundamental principles and underlying approaches presented in this section to device design and protein formulation are relevant to and could be applied to any protein molecule.

8.2. Protein Formulation

8.2.1. *Introduction*

In a reservoir device loaded with a 4-6 month's supply of protein, protein concentrations upon reservoir hydration will be at least 100 mg/ml, if not significantly more. Furthermore, the protein must remain stable at these high concentrations in a fully hydrated environment at 37˚C

throughout the duration of administration. This is a challenge in protein formulation in itself, but making it even more challenging is the exclusion of small molecules as formulation excipients due to their rapid depletion from the device reservoir.

While there are many mechanisms of instability for protein therapeutics, the one of greatest concern for the therapeutic considered here is aggregation. While in some cases protein dimer may still be active with reduced efficacy, higher molecular weight aggregates are potentially immunogenic and typically have little or no efficacy. When in solution, proteins are susceptible to aggregation, which can either be due to non-covalent hydrophobic interactions between protein molecules or to covalent interactions such as cross-linking of disulfide bonds between intermolecular residues. High concentrations and temperatures both increase the frequency of collisions and thus interactions between molecules as well and increase protein unfolding that exposes hydrophobic regions that promote aggregation. [32] Therefore, there is typically a direct correlation between the concentration and temperature of a protein solution and its physical stability. Protein therapeutics are therefore often stored at low temperatures or as lyophilized powders. Unfortunately, when considering protein stability throughout the duration of administration of an ocular implant, temperature is defined by physiology, and protein concentration in the device reservoir is unavoidably high as it is directly related to device size and duration.

In addition to low temperatures and concentrations, excipients are often used in protein therapeutic formulations to improve stability. While excipients serve a range of purposes in stabilizing proteins in solutions, the most common approach for reducing aggregation in protein solutions relies on the principle of preferential interactions and solute exclusion [33] [34], which

is typically achieved using small molecule carbohydrates such as sucrose, trehalose, or mannitol. These molecules may also serve as cryoprotectants upon lyophilization to create a protein powder; in fact, the lyophilized protein therapeutic used in this research consists of 25% sucrose, which constitutes our “standard” formulation. [35]

While the use of these small molecule carbohydrates may be an effective formulation technique to reduce aggregation, in the case of a protein releasing reservoir device, the small molecule is expected to deplete at a significantly faster rate than the protein therapeutic as its small size will allow it to pass unhindered through the porous membrane. The impact of this is illustrated in Figure 28, which compares stability profiles for protein in a nonporous PCL reservoir device and for protein in a porous PCL reservoir device from which both protein and sucrose are released. The results presented in this figure were obtained by sampling the reservoir contents at each time point for the nonporous device and sampling the released material for the porous device. These results suggest that while sucrose may protect the protein from aggregation when it is retained in the device reservoir, the effect is lost in the porous device.

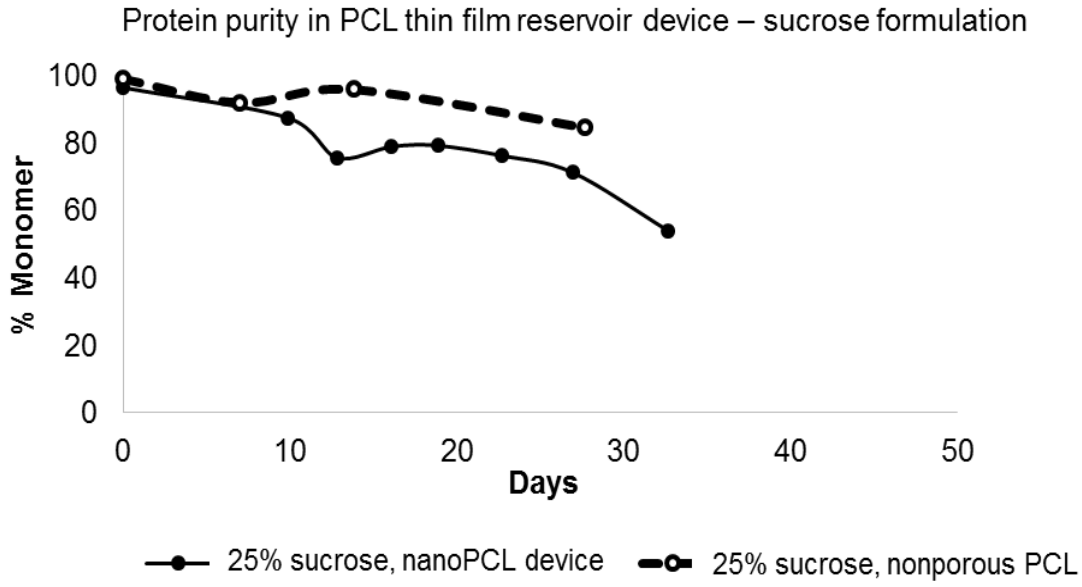

Figure 26 Protein stability in PCL thin film reservoir device. In nonporous PCL device, release of sucrose from device reservoir is limited and protein purity remains >80% after 30 days. In nanoPCL device, protein is less stable, likely due to the release of sucrose from the device reservoir.

In order to prevent rapid depletion of excipients and to achieve effective formulation within the device reservoir, two large molecule excipients were considered: polyethylene glycol, m.w. 3350 (PEG3350) and chitosan. The formulation approach for each of these excipients utilizes different principles for reducing aggregation; while chitosan offers protein stability through the formation of polyionic interactions and possible immobilization of proteins within a matrix [36], PEG3350 is used to reduce protein solubility [37], protecting the bulk of the protein by keeping it out of solution. The following sections will consider each formulation approach independently, describing in more detail the theoretical mechanism of stabilization and summarizing the observed results on protein stability in the device reservoir for each formulation.

8.2.2. *Formulation Approach 1: Chitosan*

8.2.2.1. *Introduction*

Chitosan is a linear polysaccharide with amino, hydroxyl, and acetyl functional groups and a net negative charge. [38] Chitosan is available from a variety of sources such as the breakdown of chitin from shellfish or from bioengineered fungal producers. Depending on the source and the processing, chitosan comes in a range of molecular weights and degrees of acetylation which affect its physicochemical properties such as solubility and viscosity. At low concentrations and physiological pH, chitosan is fully soluble, but at higher concentrations it forms a hydrogel matrix. Under either condition, proteins form polyionic interactions which have the potential to stabilize the protein by reducing protein-protein interactions and/or immobilizing the protein within a hydrogel matrix. [36] [39] For formulation of therapeutic protein within the reservoir of a thin film PCL reservoir device, chitosan is co-formulated in solution with protein, sucrose as a cryoprotectant, and acetate to maintain solubility and then lyophilized.

8.2.2.2. *Chitosan load:*

Chitosan and protein are prepared at two levels, a 0.05:1 mass ratio and a 1:1 mass ratio of chitosan to protein. Upon reconstitution in the device reservoir, the lower level of chitosan appears fully soluble while the higher chitosan content material forms a solid hydrogel. As is illustrated in Figure 29, the 1:1 mass ratio of chitosan to protein results in a greater than 80% purity by UP-SEC of protein in a nonporous device reservoir after more than 80 days while the lower level of chitosan drops to around 60% purity within 15 days. Based on these results, all further chitosan formulation development for the PCL reservoir device is conducted with a 1:1 mass ratio of chitosan to protein. These experiments are conducted with Ultrapure Chitosan MW 150-400 kDa 75 – 90% deacetylated.

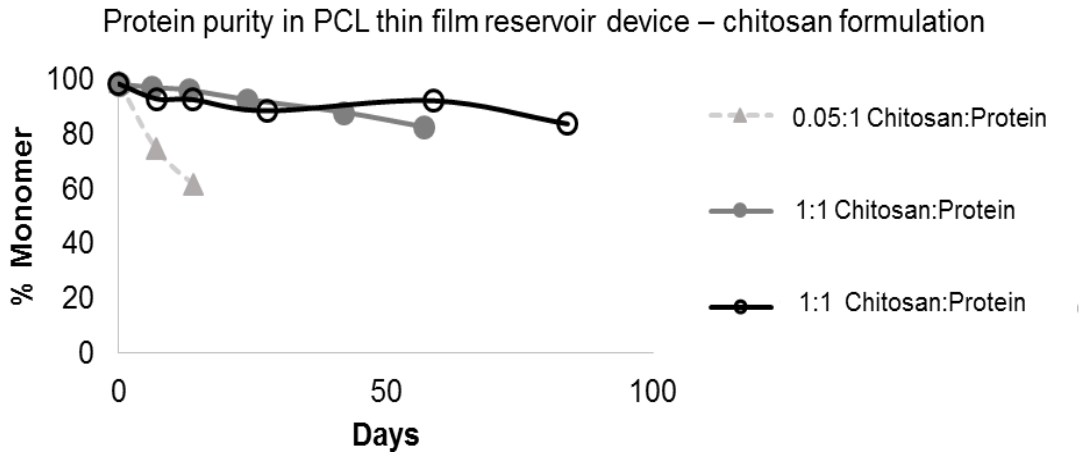

Figure 27 Protein stability of chitosan:protein formulations in PCL thin film reservoir device. 1:1 mass ratio of chitosan to protein results in improved protein stability while 0.05:1 mass ratio of chitosan:protein fails to reduce protein aggregation, resulting in significant loss of protein purity within one week.

8.2.2.3. Chitosan molecular weight:

Two experiments are used to determine the impact of chitosan molecular weight on protein stability. In all cases, lyophilized chitosan, protein, sucrose and acetate are prepared with a 1:1 mass ratio of chitosan to protein. Three different molecular weights of ultrapure chitosan are investigated[10], 14cP, 26cP, 32cP (Synolyne Pharma, Herstal, Belgium) under two conditions, dry at 50˚C, and in a hydrated device reservoir at 37˚C submerged in release media at pH 7.2. Protein stability under both conditions is evaluated as % purity by UP-SEC. As Figure 30 shows, there is no significant impact of chitosan molecular weight and protein degradation over a 1 month period. Figure 31, capturing the purity of protein released from reservoir devices for up to a month further supports that there is no difference in protein stability as a function of chitosan molecular weight. Both data sets demonstrate that there is no significant impact of chitosan molecular weight on protein stability, but it is additional important to verify that there chitosan molecular weight does not impact protein release

[10] Chitosan molecular weights from Synolyne are represented with viscosity, a common practice for polymers. The corresponding molecular weight is not provided.

from the reservoir device. Figure 32 illustrates that there is no significant difference in area normalized release rates of protein from an mpPCL reservoir device as a function of chitosan molecular weight.

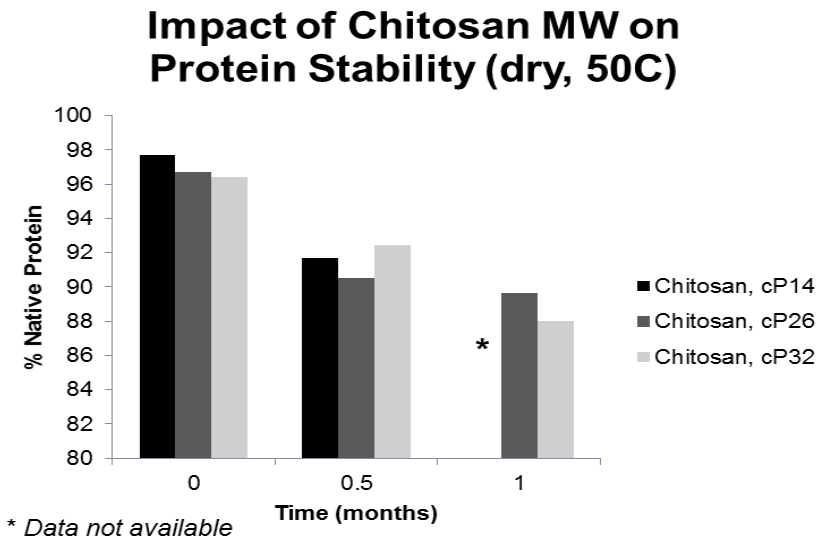

Figure 28 Impact of Chitosan MW on Protein Stability. Under dry, accelerated degradation conditions, chitosan molecular weight in a 1:1 mass ratio formulation with protein does not impact protein stability.

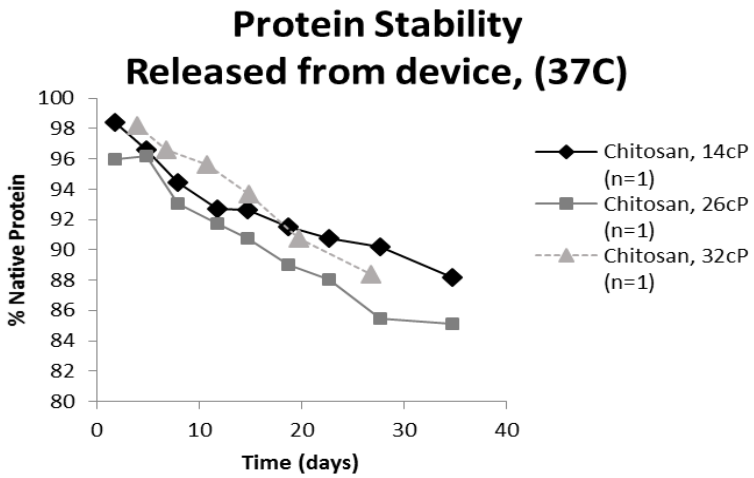

Figure 29 Stability profile for protein released from mpPCL thin film device. Chitosan molecular weight in a 1:1 mass ratio formulation with protein does not impact protein stability in mpPCL device.

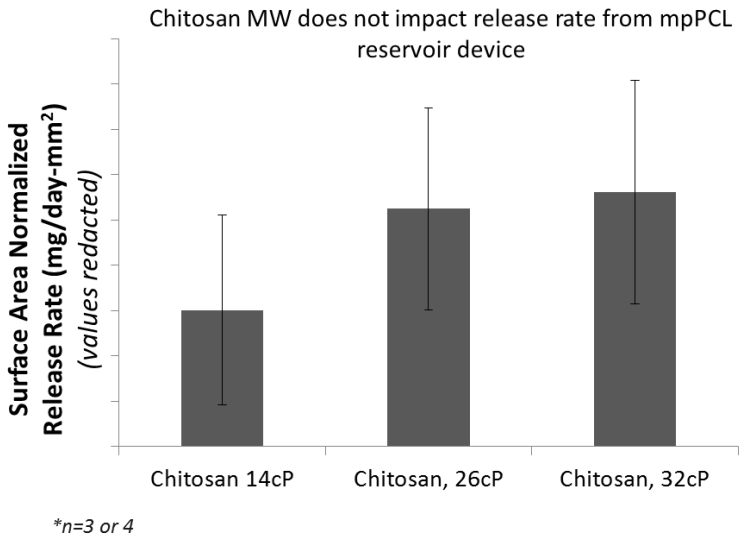

Figure 30 Impact of chitosan molecular weight on protein release from mpPCL thin film reservoir device. In a 1:1 mass ratio with protein, chitosan molecular weight does not impact protein release rates from the mpPCL device.

8.2.2.4. Protein stability with chitosan formulation

Protein stability in a mpPCL device reservoir with a 1:1 chitosan to protein formulation is highly dependent on the protein reservoir concentration. Protein reservoir concentration is estimated as protein load, calculated from a mass difference between the empty and loaded device, divided by the volume of water in the hydrated device reservoir, calculated from a mass difference between the hydrated device after > 12 hour incubation in release media and the dry device. The reservoir concentration therefore depends on device loading and size. Figure 33 shows the stability profile of protein released from the device reservoir for three different groups of devices with different protein reservoir concentrations. The rate of decrease in protein purity, due to aggregation, is greater for Group III with a 271 mg/ml average concentration than the rate of decrease in purity for Group I with a 103 mg/ml average concentration. While the use of high levels of chitosan as a formulation excipient has potential to improve protein stability, it is highly dependent on device loading and size.

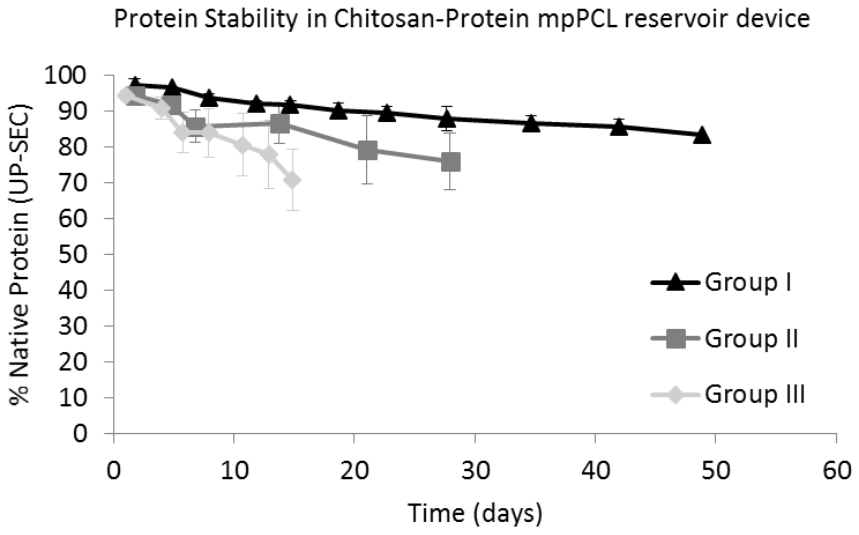

		Protein Load (mg)	Protein Res Conc (mg/ml)
Group I	n= 2	3.0 +/- 0.2	103 +/- 16
Group II	n=4	3.0 +/- 0.6	124 +/- 18
Group III	n=6	3.4 +/- 0.4	271 +/- 56

Figure 31 Stability profiles of protein released from mpPCL reservoir devices (1:1 w/w formulation with chitosan). Protein stability is inversely dependent on protein reservoir concentration.

8.2.2.5. Conclusion

A chitosan hydrogel matrix formed with a 1:1 mass ratio of chitosan to protein improves protein stability in a mpPCL reservoir device for long-acting delivery under physiological conditions. Chitosan as a charged biomolecule may stabilize the protein to reduce aggregation through the formation of polyionic interactions and immobilization of protein molecules within a hydrogel matrix. However, the utility of this formulation approach depends strongly on the protein reservoir concentration. Additionally, while chitosan can be produced from non-shellfish based sources and is used in a number of biomedical and drug delivery systems, concerns around biocompatibility and immunogenicity are a

consideration. In ocular drug delivery, chitosan has been used in topical formulations but not intra-ocularly.

8.2.3. *Formulation Approach 2: Polyethylene Glycol (PEG)*

8.2.3.1. Introduction

Polyethylene glycol (PEG) is an uncharged linear polyether available in a wide range of molecular weights. For the purposes of the experiments presented here, all work is done with a 3350 kDa molecular weight PEG (PEG3350). At low concentrations (< 10000 ppm or 10 mg/ml), PEG is used as a protein stabilizing excipient. [40] At higher concentrations, PEG is often used to precipitate proteins from solution for x-ray crystallography. [37] As a formulation approach to reduce aggregation in a device reservoir, PEG is used at high concentrations to limit protein solubility. As protein aggregation is typically correlated with protein concentration, reducing protein solubility in the hydrated device reservoir is hypothesized to reduce protein aggregation. The utility of this approach depends on the stability of the protein excluded from solution in the device reservoir.

8.2.3.2. PEG3350 Load (concentration)

The first step in developing a formulation approach using PEG3350 in the device reservoir is to determine the protein's solubility as a function of PEG3350 concentration. Figure 34 illustrates this relationship. Data presented in Figure 34 consists of two data series, one describing the precipitation of protein from solution upon addition of a PEG3350, also in solution; no sucrose is present in these solutions. The other data series describes protein solubility when lyophilized protein containing sucrose as a cryoprotectant and PEG3350 as a solid are reconstituted together; this scenario recapitulates hydration of the device reservoir. The difference in solubility observed between these data series is likely due to the

presence of sucrose. There is no loss of purity for the soluble protein in either case. In addition to evaluating the purity of protein in solution, it is also important to consider the stability of the insoluble protein. This is done by starting with a solution of high PEG3350 concentration and low protein solubility with an excess of protein. This solution is then diluted to a concentration of PEG3350 that does not limit full dissolution of the protein load, followed by analysis of the % recovery of protein that solubilizes upon dilution and the purity of protein in solution. Figure 34C tabulates these results which indicate full recovery of protein and no loss of purity.

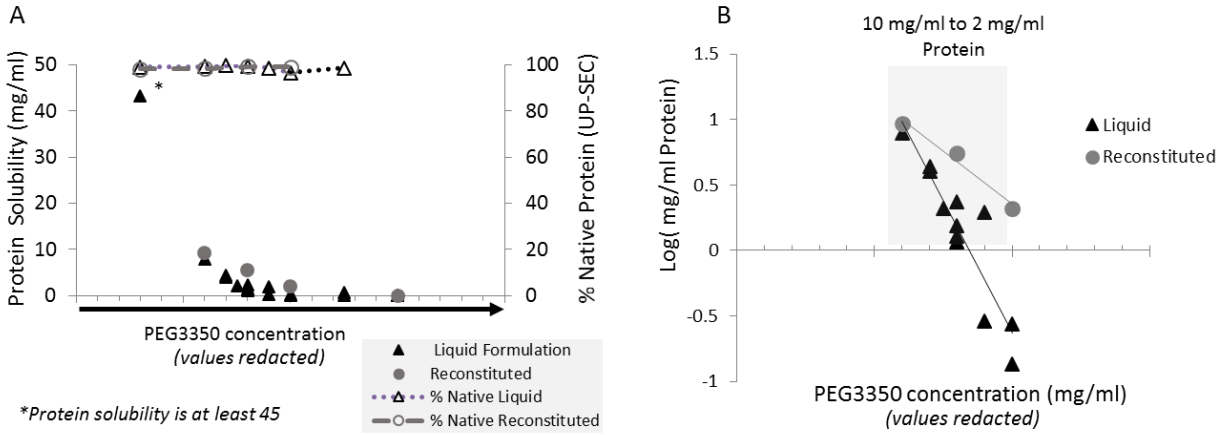

C

Analysis of Reconstituted Protein after PEG3350 Precipitation				
	%HMW	%Native	%LMW	%Recovery
Liquid	1.14	98.86	0	103
Reconstituted	1.34	98.66	0	109

Figure 32 Limiting protein solubility with PEG3350. (A) Protein solubility decreases exponentially with increasing PEG3350 concentration. There is no observed loss of purity for protein remaining in solution. (B) Data from chart (A) depicted on a log-scale highlights the exponential trend as well as the difference between the liquid formulation (no sucrose) and the reconstituted formulation (with sucrose). (C) Protein either precipitated or excluded from solution by PEG3350 is fully recoverable with no loss of purity upon dilution of PEG3350 from solution.

The correlation between protein solubility and PEG3350 concentration shown in Figure 34 is used to determine a target range for PEG3350 concentration resulting in protein solubility greater than 2 mg/ml and less than 10 mg/ml; because protein concentration is the driving

force for diffusion from the device reservoir, it is undesirable in the overall system design to limit the protein concentration to negligible. As is discussed further in the device design section, controlling the concentration of PEG3350 in the device reservoir is critical for this formulation approach. As it is the concentration of PEG3350 that is important and not the absolute load or ratio to protein, both the PEG3350 load and volume of reservoir hydration are key parameters.

8.2.3.3. Protein stability with PEG3350 formulation

Figure 35 illustrates the impact of PEG3350 on protein stability in the device reservoir. Both series in Figure 35 represent data collected from protein that is released from the device reservoir. In the PEG3350 devices, protein solubility is limited to less than 10 mg/ml based on the estimated PEG3350 concentration. After 60 days, protein purity is greater than 80%. Based on these stability results, PEG3350 shows great promise as a formulation approach for the thin film reservoir device.

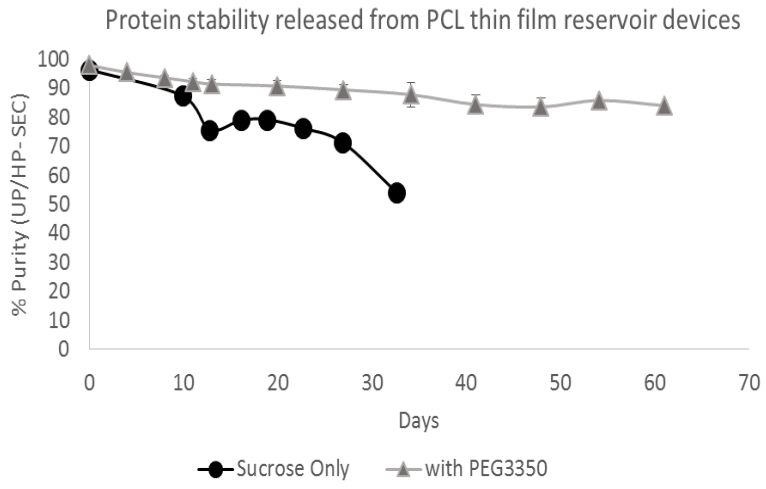

Figure 33 Stability profiles of protein release from PCL devices. PEG3350 formulation improves protein stability.

8.2.3.4. Conclusion

PEG3350 effectively reduces the solubility of a protein, decreasing the concentration of protein in solution and thus leading to a decrease in protein aggregation. With this formulation approach, protein stability depends on PEG3350 concentration, and thus protein solubility, but is otherwise independent of total protein load. PEG is a commonly used and biocompatible formulation excipient both in a variety of indications. While the work presented here only considers PEG3350, the same approach could be applied to other PEG molecules or to other nonionic polymers that effectively reduce protein solubility.

8.2.4.Conclusion

Both a chitosan hydrogel matrix and PEG3350 are potential formulations for therapeutic protein within the reservoir of a thin film PCL reservoir device. With either formulation, it is important to consider how the presence of formulation excipient will impact protein release and what additional parameters will be critical to the device design to implement the formulation approach. For example, with the chitosan hydrogel, protein stability depends on reservoir concentration, meaning that protein load and reservoir volume are key parameters in device design that will effect protein stability. With the PEG3350 formulation, protein solubility depends on PEG3350 reservoir concentration, so PEG load and reservoir volume are key device design parameters. These parameters and their role in overall device design will be discussed further in the section on device design.

8.3. Release Rates & Membrane Design

8.3.1.Introduction

In addition to protein stability, another key criteria in a long acting ocular implant is the protein release rate. It is important that the device be capable of achieving relevant release rates (not

too slow and not too fast) for device dimensions that are appropriate for the given indication. In the case of an ocular implant to deliver the protein therapeutic under consideration here, release rates need to be between 10 and 100 µg/day for a device no bigger than 1-1.5 mm diameter and 10 mm long. Ideally, the release rate will be as close to constant as possible.

As discussed in Section 5 on membrane design, a porous membrane is required for protein diffusion and a nanoPCL membrane is known to result in a concentration independent, constant rate release of protein. Due to this desirable release profile, a nanoPCL membrane is the ideal choice for this device. However, as shown in Figure 36, the use of either PEG3350 or chitosan as formulation excipients inhibits protein release through a nanoPCL membrane, resulting in release rates that are too slow to achieve 10 µg/day – 100 µg/day in an ocular sized device. In fact, based on the results presented in Figure 36, to release 10 µg/day with the PEG3350 formulation, a 1mm diameter device would need to be 40mm long. Therefore, the nano-channel membranes are not suitable for use with these formulation approaches.

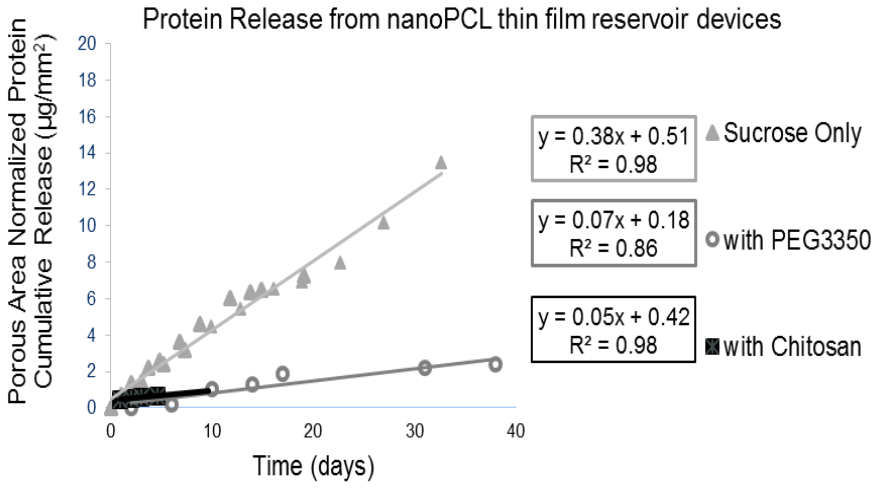

Figure 34 Protein release from nanoPCL devices. Presence of large molecule formulation excipients limits protein release.

As described in Section 5.3.3, while not truly concentration independent, mpPCL membranes restrict protein release from a device reservoir to result in a near linear release profile. With mpPCL membranes, even though PEG3350 and chitosan as formulation excipients still inhibit protein release compared to the sucrose only formulation, release is an order of magnitude faster than with the nanoPCL membranes (Figure 37). Relevant release rates (> 10 µg/day) for all formulations are therefore achievable in ocular sized mpPCL devices.

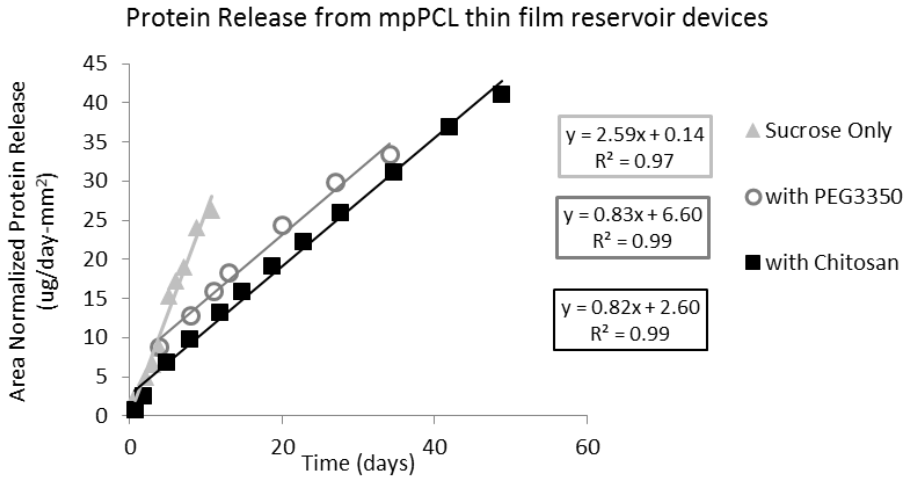

Figure 35 Protein release from mpPCL devices. Release rates are an order of magnitude faster than from nanoPCL devices. Large molecule excipients still reduce protein release, yet it is still possible to achieve relevant release rates with reasonably sized devices.

While the primary criteria is to achieve protein release within the target range, it is also desirable to develop a device platform with a tunable release rate. In the case of protein release through a mpPCL membrane, membrane thickness does not impact release rate (Section 5.3.4) and thus the most practical way to tune release rate is through surface area. In order to decouple device size from surface area for release, devices are fabricated from a combination of mpPCL and nonporous PCL. Because nonporous PCL is impermeable to large molecules such as

proteins, release rates are dependent only on the porous surface area. The schematic in Figure 37 illustrates the fabrication process to produce such devices.

8.3.2. Device Design

For successful design and fabrication of devices that meet specified design attributes, both protein formulation, release rate, and device size must be taken into consideration simultaneously. Dependent factors that are controlled during fabrication such as device size, porous area, and protein and formulation excipient load, are designated as **design parameters**. **Design attributes** are criteria specified as a target product profiles. For the case of the ocular implant under consideration in this section, the specified design attributes are:

Design Attribute	Target
Device Size	1-1.5mm D x 10mm L
Protein load	> 3 mg
Release Rate	10-100 µg/day (confidential info redacted)
Protein Stability	> 75% after 90 days under physiological conditions

System parameters are empirically measured characteristics of the system, indirectly controlled by the design parameters, on which the critical design attributes depend. This section presents models for flexible device design based on empirical correlations between system parameters and design parameters; these models allow for easy scaling of devices to meet specified criteria and are specific to the formulation.

8.3.2.1. Device Design: PEG3350 Formulation

Critical design and system parameters for mpPCL devices utilizing PEG3350 formulation are listed in Table 6. The device design flow-chart in Figure 38 illustrates how these critical parameters are used in an overall device design model. The numbers 1-4 in the flow chart represent the use of empirically derived correlations describing relationships between key parameters. These empirical correlations are shown in Figure 39.

Table 6 Key parameters for device design utilizing PEG3350 formulation

Design Attributes	Design Parameters	System Parameters
Device size	Device size	Reservoir hydration volume
Duration of administration (protein load)	Protein load	PEG3350 reservoir concentration
Release rate	PEG3350 load	Protein reservoir solubility
Protein stability	Porous Area	

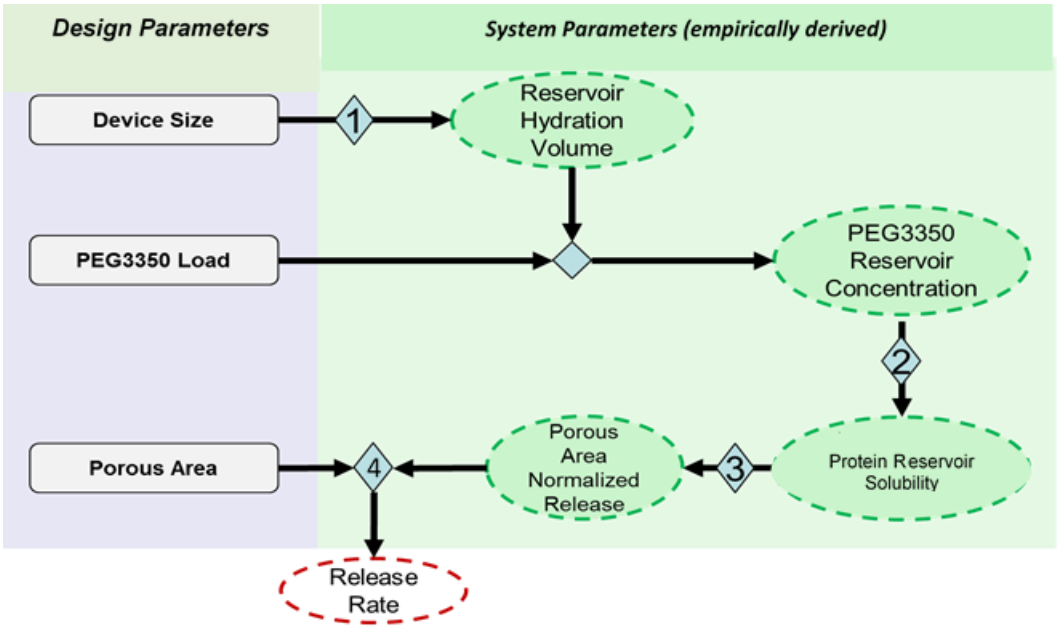

Figure 36 Device design flow-chart for mpPCL protein devices with PEG3350 formulation

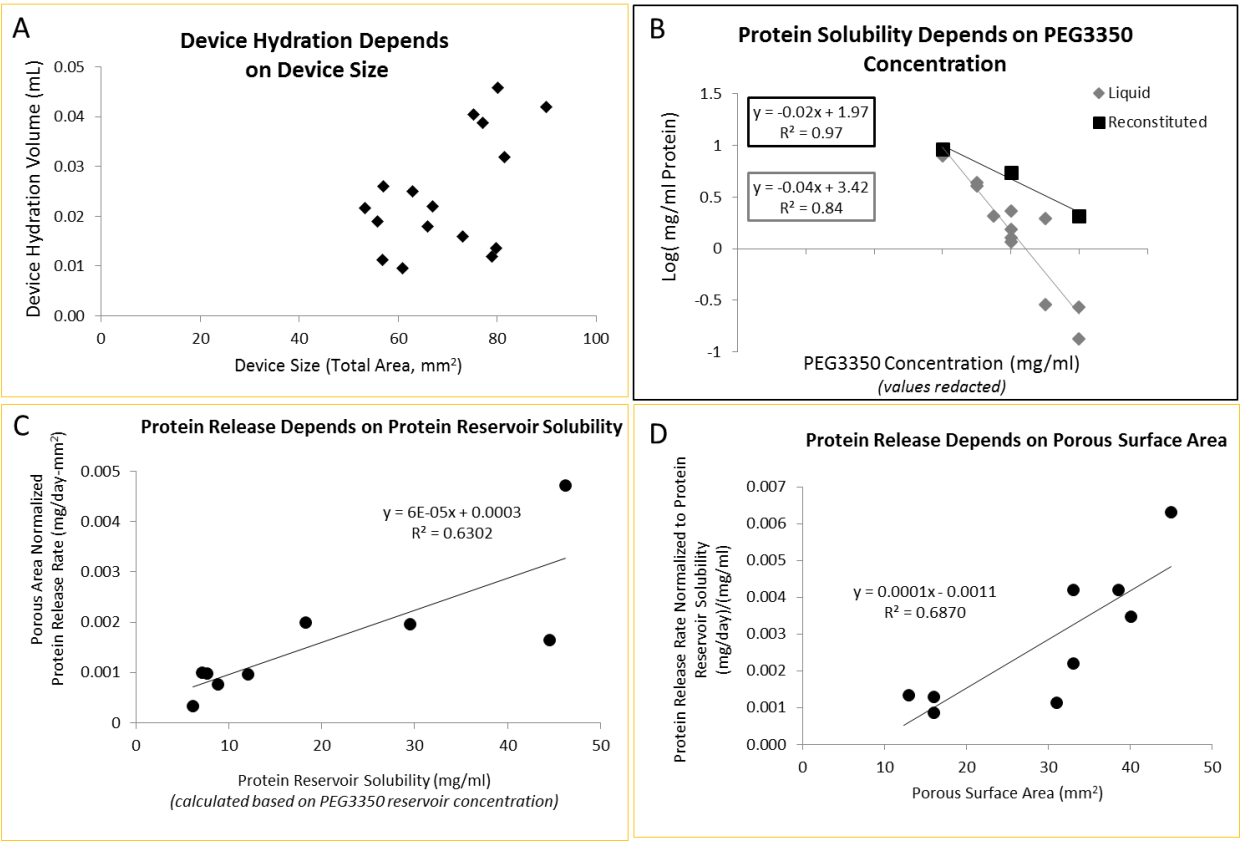

Figure 37 Empirical correlations relating critical device parameters to critical system parameters for mpPCL protein devices with PEG3350 formulation.

As previously discussed, PEG3350 formulation improves protein stability by limiting protein solubility in the device reservoir and protein solubility is a function of PEG3350 concentration. Furthermore, as protein release from the mpPCL device is dependent on the initial reservoir concentration **(**Figure 24, Section 5.3.3**)**, release rate will therefore depend indirectly on PEG3350 concentration as a function of protein reservoir solubility (Figure 39C). Therefore, PEG3350 reservoir concentration is a key parameter defining both protein release and stability. PEG3350 load is easily controlled during device fabrication, but in order to target a PEG3350 reservoir concentration, it is necessary to know the reservoir hydration volume. The reservoir hydration volume for a given formulation depends on device size; therefore, by defining the device size and correlating this to a reservoir

hydration volume using the relationship in Figure 39A, the necessary PEG3350 loading can be determined to target a specific reservoir concentration. If the PEG3350 reservoir concentration is known, the protein reservoir solubility can be calculated based on the relationship presented in Figure 39B. Based on the protein reservoir solubility, the porous area normalized release rate can be calculated (Figure 39C) and the porous area can be adjusted to target a specific release rate.

8.3.2.2. Device Design: Chitosan Formulation

Critical design and system parameters for mpPCL devices utilizing a chitosan formulation (1:1 w/w ratio with protein) are listed in Table 7. The device design flow-chart in Figure 40 illustrates how these critical parameters are used in an overall device design model. The numbers 1-3 in the flow chart represent the use of empirically derived correlations describing relationships between key parameters. These empirical correlations are shown in Figure 41.

Table 7 Key parameters for device design utilizing chitosan formulation (1:1 w/w with protein)

Design Attributes	Design Parameters	System Parameters
Device size	Device size	Reservoir hydration volume
Duration of administration (protein load)	Protein load	Protein reservoir concentration
Release rate	Porous Area	
Protein stability		

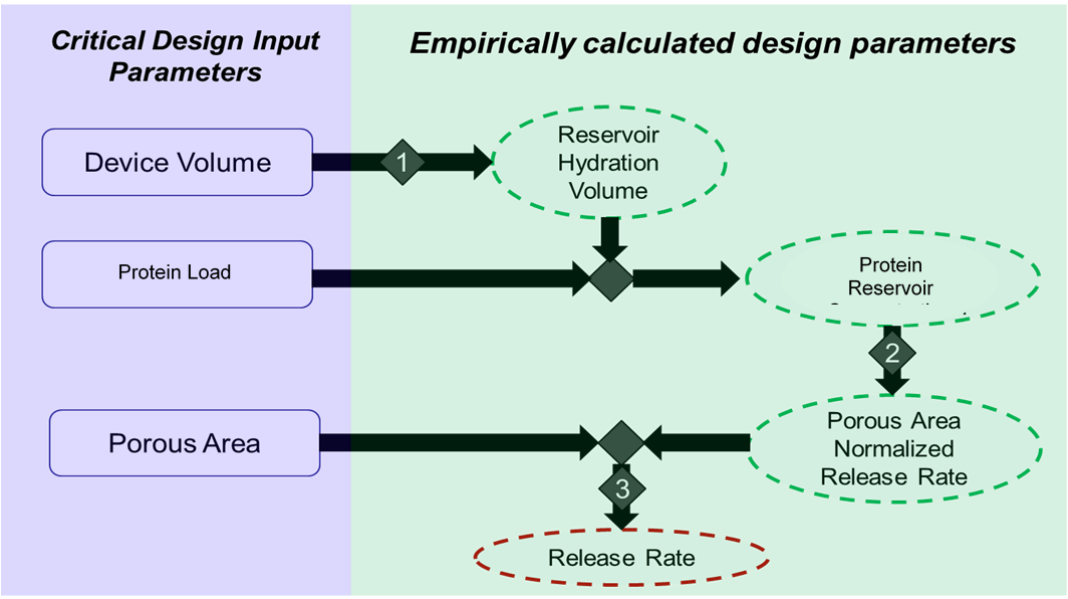

Figure 38 Device design flow-chart for mpPCL protein devices with chitosan formulation

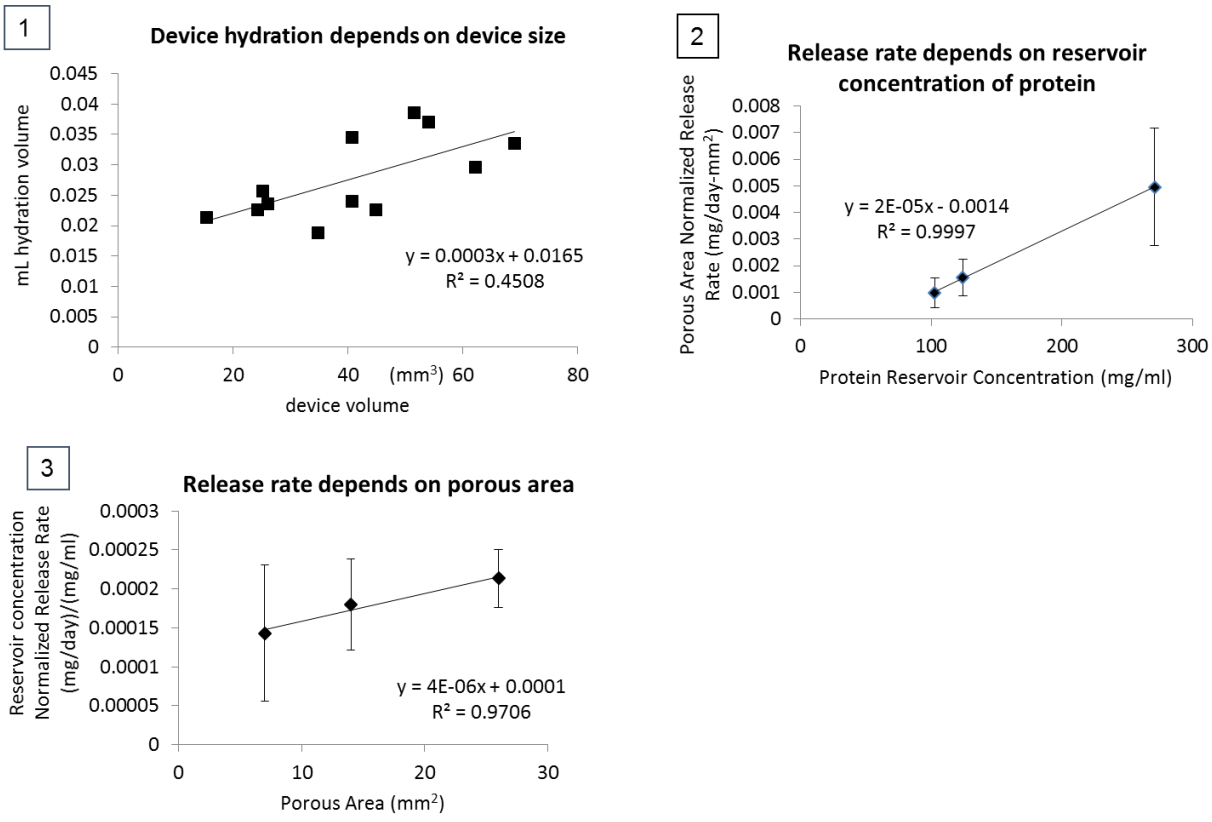

Figure 39 Empirical correlations relating critical device parameters to critical system parameters for mpPCL protein devices with chitosan formulation

For chitosan formulated devices, both protein stability and release rate are directly correlated to protein reservoir concentration. In turn, protein reservoir concentration depends on both protein load and reservoir hydration volume, which is proportional to device size. Therefore, for a given device size and protein load, a reservoir concentration can be estimated and an area normalized release rate predicted. The porous area can then be adjusted to achieve a target release rate.

The lyophilized protein-chitosan formulation contains acetate which is readily released from the device upon hydration. In *in vitro* studies, the release of acetate into release media lowers the pH which results in an increased release rate. This is evidenced by a correlation between release media pH and release rate in the first 5-10 days of sampling (Figure 42). While an important consideration for *in vitro* testing, the impact of this level of acetate released into the intra-ocular space is not expected to be significant.

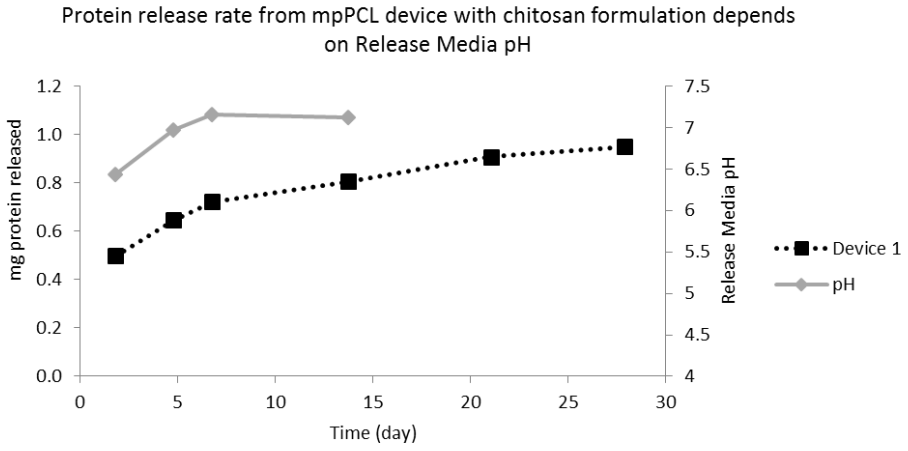

Figure 40 Impact of pH on protein release from mpPCL protein device with chitosan formulation. Release of acetate contained in lyophilized protein-chitosan formulation within first week of release study decreases pH of release media. Shape of protein release profile within first week reflects the shape observed in the release media pH profile, suggesting that pH impacts protein release.

8.4. Prototype Devices

Prototype devices serve a three-fold purpose: to demonstrate the use of the device design models, to evaluate protein stability, and to evaluate release profiles.

8.4.1. *Prototype Devices: PEG3350*

Table 8Table describes the key design parameters for five PEG3350 prototype devices. Figure 43 illustrates how the empirical correlations are used to determine critical system parameters for PEG3350 prototype devices from key design parameters. And Figure 44 shows both the stability and release profiles for the prototype devices. The release profile demonstrates near linear release for up to 60 days and about 50% release with protein stability >80% at 60 days.[11]

Table 8 PEG3350 formulation prototype device design parameters

Key Design Parameters *(n=5)*			
Device Size	**Protein Load**	**PEG3350 Load**	**Porous Area**
79 mm^2 +/- 10	3.2 mg +/- 0.4	2.6 mg +/- 0.9	40 mm^2 +/- 5

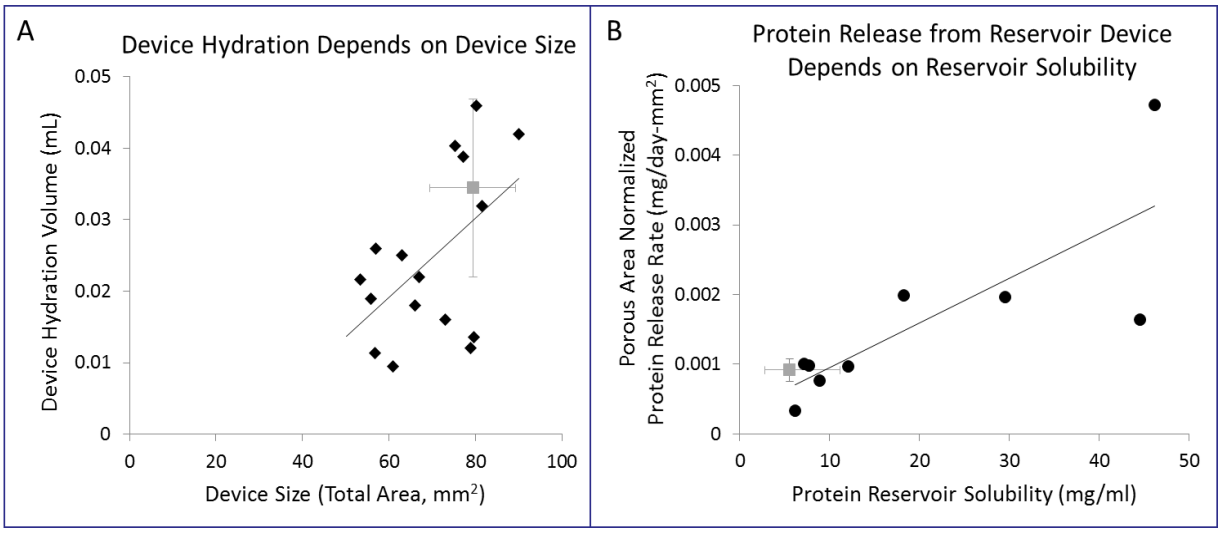

Figure 41 Comparison of prototype mpPCL protein device and system parameters to empirical correlations for PEG3350 formulation.

[11] The evaluation of these devices will continue until depletion unless contaminated.

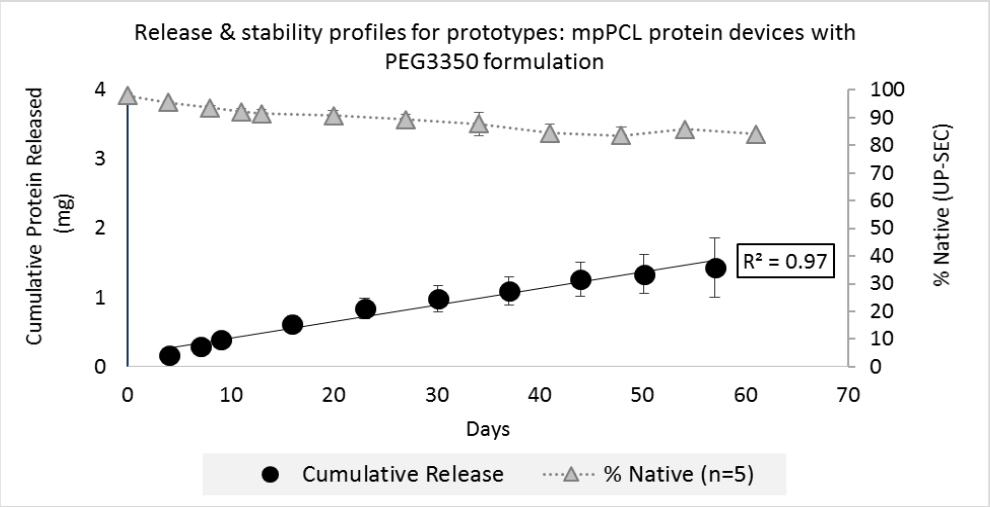

Design Attribute	Target	Prototypes
Device Size	1-1.5mm D x 10mm L	*Devices larger than target*
Protein load	> 3 mg	YES: 3.2 mg +/- 0.4 mg
Release Rate	0-100 µg/day (confidential info redacted)	YES: Exact values redacted
Protein Stability	> 75% after 90 days under physiological conditions	Pending: 84 % at 61 days

Figure 42 Evaluation of mpPCL protein prototypes devices with PEG3350 formulation.

8.4.2. *Prototype Devices: Chitosan*

Three groups of chitosan prototype devices are evaluated. Groups I (n=2) and II (n=3) are selected based on protein reservoir concentrations from devices fabricated to develop empirical correlations and are thus representative of protein release an stability for the corresponding protein reservoir concentrations, but do not demonstrate use of the design model. Group III (n=6) devices are fabricated to target specifications using the device design model. Table 9 contains the key design parameters for Group III prototype devices and Figure 45 illustrates how the empirical correlations are used to determine critical system parameters from key design parameters. Figure 46 shows both the release (A) and stability (B) profiles for the three groups of chitosan formulation prototype devices. Release rate and stability are dependent on protein

reservoir concentration. As release rate is proportional to both porous surface area and protein reservoir concentration, the porous surface area is reduced as reservoir protein concentration increases in order to achieve comparable release rates between groups of devices.

Table 9 Key design parameters of chitosan prototype devices

Key Design Parameters *(n=6)*		
Device Size	**Protein Load**	**Porous Area**
19 mm3 +/- 3.5	3.4 mg +/- 0.4	7.0 mm2 +/- 1.1

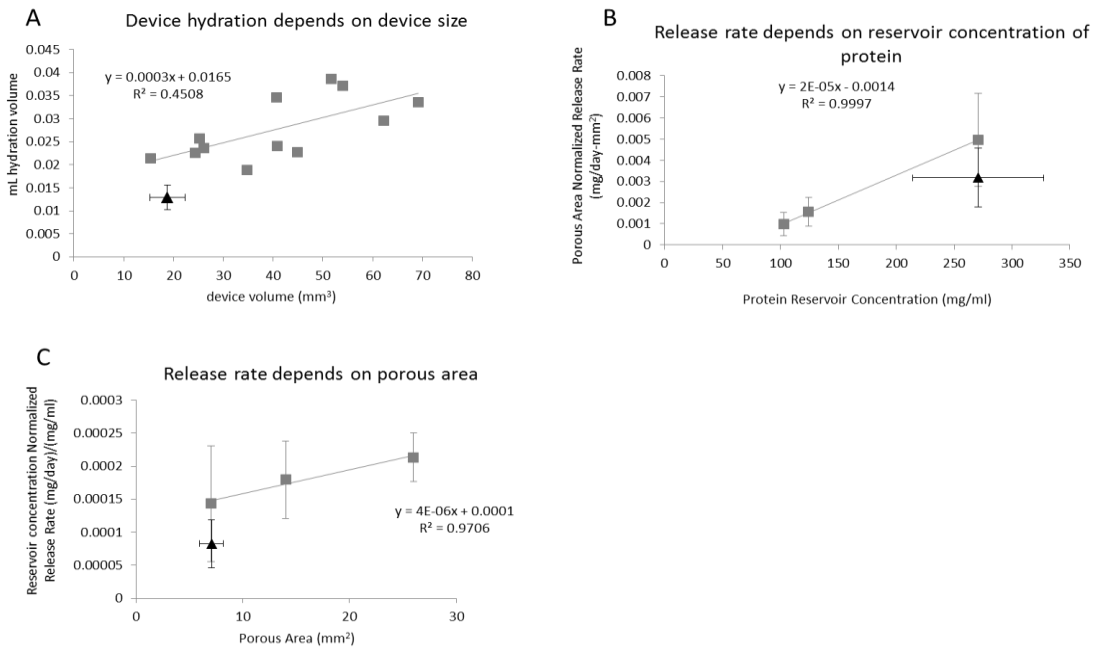

Figure 43 Comparing critical device and system parameters for mpPCL protein prototype devices with chitosan formulation (Group III) to empirical correlations

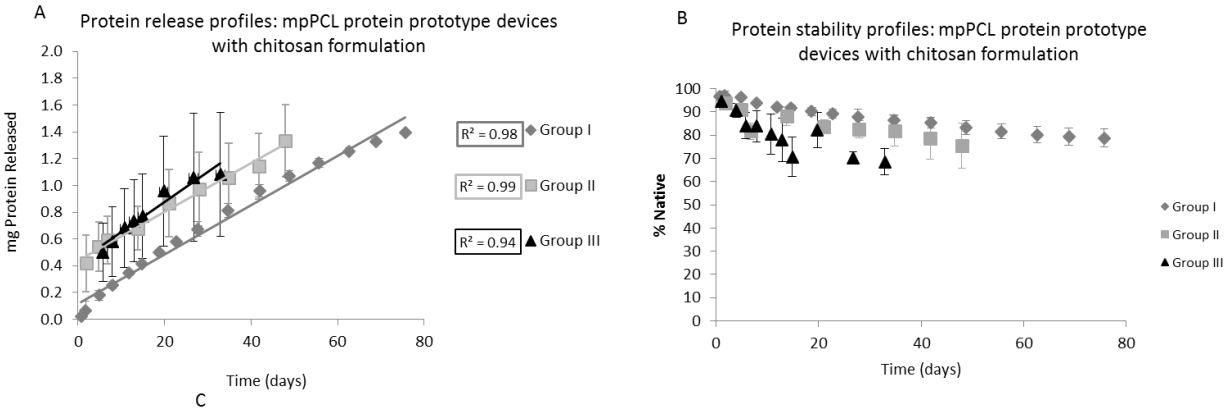

C

		Protein Load (mg)	Protein Res Conc (mg/ml)	Porous Area (mm^2)	Release Rate (ug/day)
Group I	n= 2	3.0 +/- 0.2	103 +/- 16	26 +/- 14	Redacted
Group II*	n=4	3.0 +/- 0.6	124 +/- 18	14 +/- 4	Redacted
Group III**	n=6	3.4 +/- 0.4	271 +/- 56	7 +/- 1	Redacted

*Terminated at Day 47 due to contamination ; ** Terminated at Day 33 due to contamination

Figure 44 Evaluation of mpPCL protein prototype devices with chitosan formulation. Three groups represent different reservoir concentrations as described in (C).

8.5. Conclusion

In this section the fundamentals of membrane and device design for PCL thin film reservoir devices outlined in the early chapters of this thesis are applied to the early development of a long-acting biodegradable implant for intraocular delivery of a protein therapeutic. To address the general challenge of stable protein formulation under physiological conditions in a long-acting implant, two approaches leveraging large molecule excipients are described. For both, methodology for device design resulting in targeted design attributes is presented based on empirical correlations between design parameters and critical system parameters.

The designs & formulations presented in this section are developed and tested with a specific protein relevant to intraocular drug delivery. However, the underlying principles for formulation and device design based on empirical correlations are broadly applicable and could be leveraged for the development of mpPCL implants to deliver any protein therapeutic at any device size, indication, or

route of administration. To apply this methodology to other proteins and device sizes, one must simply acquire the relevant empirical correlations relating system parameters to device parameters in the relevant ranges.

9. Case Study II: A TFPD as a Subcutaneous Implant for HIV PrEP

9.1. **Introduction**

Antiretroviral (ARV) effectiveness for HIV pre-exposure prophylaxis (PrEP) is proven, but hinges on correct and consistent use. For example, when taken daily as an oral dose, tenofovir (TFV)-based antiretrovirals show high efficacy for HIV pre-exposure prophylaxis (HIV PrEP) in men and women, but poor adherence to the regimen drastically decreases effectiveness. [41] Clinical studies with tenofovir disoproxil fumarate (TDF)/emtricitabine (FTC) and TDF alone have highlighted a strong correlation between the level of HIV PrEP effectiveness and product adherence. [42] [43] The iPrEx [44] and Partners PrEP [45] studies investigated the prophylactic effectiveness of orally administered Truvada in gay/bisexual men and heterosexual discordant couples, respectively. In these studies, Truvada reduced the risk of infection by at least 90% when taken regularly, but this level of protection declined to only 44% and 75%, respectively, when lower product adherence resulting in sub-prophylactic dosing regimens were taken into consideration. Outcomes from the VOICE and FemPrEP trials in Sub-Saharan Africa [46] [47] [48] investigating the effectiveness of TDF or TDF/FTC oral dosing regimens -further demonstrated that poor adherence to the product regimen stands as a barrier to an otherwise efficacious HIV PrEP strategy. In light of these outcomes, there is a strong interest in the development of alternative delivery strategies for antiretrovirals as HIV PrEP, that are less burdensome to the user and do not depend on user compliance.

When poor adherence is the major hurdle to an otherwise efficacious prevention approach, sustained release delivery systems can offer an alternative solution. The first long-acting pre-exposure prophylaxis (LA-PrEP) antiretroviral treatments for HIV to enter into clinical trials are both nanocrystal depot injections targeting a minimum dosing frequency of once every 2-3 months. [49]

While this approach significantly decreases dosing frequency and is user independent, neither of the two products currently in Phase II trials for an HIV PrEP indication, cabotegravir (an integrase inhibitor) and rilpivirine (a non-nucleoside reverse transcriptase inhibitor (NNRTI)), have yet been proven to be efficacious for HIV PrEP in humans. These depot formulations also have a first order dissolution profile, resulting in a pharmacokinetic profile with the potential for a significant sub-therapeutic tail. [50] [51] Additionally, as a nanocrystal solution, there is no potential for retrieval after administration in the event of adverse reactions or seroconversion. This is a particularly relevant consideration in the case of HIV where low doses of antiretroviral monotherapies given to infected individuals may result in the development of viral resistance. [52]

A thin film polycaprolactone reservoir device (TFPD) as a tunable biodegradable subcutaneous implant for long-acting constant rate delivery of antiretrovirals provides a viable solution for user independent HIV PrEP that improves on the effectiveness, acceptability, usage, and accessibility of existing microbicide systems. A simple target product profile pertaining to the technical development of such a device is described in Table 10. Acceptable size and geometry for this subcutaneous implant are based on existing subdermal contraceptive implants such as Jadelle ® (Bayer Group, Germany) or Implanon ® (Merck & Co., Inc., NJ, USA).

Table 7 Target Product Profile

Item	Target
Administration route	Subcutaneous / Subdermal
Dosage form and schedule	Single insertion every 3 months
Stability	Stable under physiological conditions for 90+ days & shelf-life >24 months without cold-chain requirement
Size / geometry	Rod-shaped, < 2.5mm diameter, <40mm length

While a thin film polycaprolactone subcutaneous device confers many of the benefits desired in long-acting HIV PrEP, the success of such a device hinges on the ability to deliver effective doses of an ARV for at least 90 days. Most antiretrovirals used for treatment have the potential to act as PrEP agents, but only the most potent will be compatible with delivery with the TFPD. Compatibility with the TFPD depends on dosing requirements, which are important both in regards to loading capacity and release rate. ARVs requiring high dosing, on the order of tens of milligrams per day or more, can immediately be rejected for compatibility with the TFPD as the loading capacity of a single subcutaneous device is not large enough for a 90 day drug load. For the more potent ARVs, compatibility with the TFPD must still be evaluated in regards to achievable release rates, which depend on the drug's physico-chemical properties and formulation. It should be noted that as most ARVs are developed for oral administration, relevant release rates for subcutaneous delivery of ARVs for PrEP must be estimated from available pharmacokinetic parameters. While these estimates may serve as a basis for evaluating ARV compatibility with the TFPD, pre-clinical studies identifying effective dosing targets from a subcutaneous implant will be necessary. Because a precise dosing target is unknown, a tunable device design is highly desirable to facilitate pre-clinical and clinical development requiring multiple animal species and doses.

This section presents the evaluation and technical development of three ARV loaded TFPDs for HIV PrEP. Elvitegravir, Rilpivirine and Tenofovir Alafenimide Fumarate, the three small-molecule ARVs evaluated, represent three different ARV drug classes, integrase inhibitors, Non-Nucleoside Reverse Transcriptase Inhibitors and Nucleoside Reverse Transcriptase Inhibitors, respectively. Each ARV will be evaluated for the following (in order):

- Is estimated dose compatible with loading capacity?
- Is drug release from the TFPD membrane controlled with a linear release profile?

- Are estimated maximum doses achieved in a maximum sized device?
- If no, can release rate be increased through ARV formulation development?
- Can release rate be tuned accurately based on empirical models?

Also presented is additional device design and development for TAF, the only ARV evaluated thus far that fulfills all requirements for compatibility with the TFPD. The ability to accurately and reproducibly produce prototype devices targeting specific and relevant release rates based on the results of small scale studies for preliminary ARV-TFPD compatibility evaluation is demonstrated with the design, fabrication, and in vitro evaluation of relevant prototype devices. Linear release and stability of TAF in these prototype devices is demonstrated up to 90 days.

9.2. **Elvitegravir**

9.2.1. Background

Elvitegravir (Figure 47) is an integrase inhibitor developed as first-line treatment for HIV. [53] It is prescribed for HAART as part of a fixed-dose combination daily oral pill. However, as a CYP3A substrate, elvitegravir is highly susceptible to extensive intestinal and first pass hepatic clearance. Co-administration with a CYP3A inhibitor (a "booster") such as ritonavir or cobicistat drastically increases absorption and extends plasma half-life from 3.5 to 9.5 hours. [54] [55] Elvitegravir efficacy as an antiretroviral depends on maintenance of effective trough concentrations in plasma defined as greater than ten times the IC95 value of 45 ng/ml. [56] [54] Thus, if not taken according to the prescribed daily regimen, Elvitegravir efficacy is compromised. In addition to being on the market as an HAART component, Elvitegravir is currently being developed as a topical gel for HIV post-exposure prophylaxis (PEP). [57]

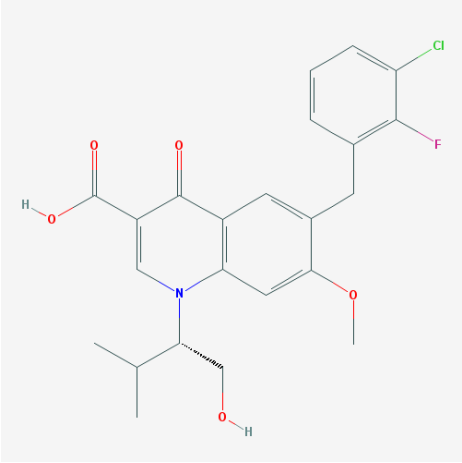

Figure 45 Elvitegravir chemical structure [53]

9.2.2. Elvitegravir dosing

The estimation of effective elvitegravir subcutaneous dosing based on oral pharmacokinetic data is complicated by the effect of co-administered boosters in the majority of elvitegravir clinical studies. As CYP3A inhibitors, these boosters not only increase intestinal absorption by

reduceing first pass hepatic clearance of elvitegravir, but they also act to extend half-life. Without booster, elvitegravir bioavailability as determined in animal models is estimated to be only about 30%. [54] With a booster, an increase in AUC up to 20-fold is observed accompanied by an increase in half-life from 3.5 to 9.5 hours. [54] Standard dosing for elvitegravir as part of an oral HAART regimen is 85 or 150 mg once daily, and with boosting, this dose and regimen result in maintenance of elvitegravir trough concentrations 6-10 times the IC95 value of 45 ng/ml. [54]

Elvitegravir delivered through a long-acting subcutaneous TFPD will not be subjected to limited intestinal absorption nor first pass hepatic clearance. While the booster is therefore not need to improve these pharmacokinetic parameters, the lack of a co-administered booster results in a 3.5 hour half-life instead of the 9.5 hour half-life expected with the booster. With the available information from clinical studies investigating elvitegravir pharmacokinetics, two approaches to estimating effective subcutaneous dosing are used.

While elvitegravir is not intended to be co-administered with a booster from the TFPD, estimating the required constant rate subcutaneous dose for elvitegravir based on pharmacokinetic parameters derived from oral dosing with a booster will indicate a dosing value less than required elvitegravir subcutaneous dosing without a booster. The pharmacokinetic parameter, CL/F (clearance divided by bioavailability), can be used to calculate a constant-rate steady state dose (k_o) to achieve a target plasma concentration (C_{target}) according to the following equation:

Equation 6

$$k_o = C_{target} * {CL}/{F}$$

For elvitegravir antiviral efficacy in treatment regimens, C_{target} is determined at greater than 450 ng/ml, or ten times the IC95. However, recent results for HIV PrEP from GSK744, an integrase inhibitor, suggest that 3 times the IC90 value are effective for PrEP. [58] Therefore, to target a plasma concentration of 135 ng/ml, or 3 times the IC95, a constant-rate subcutaneous dose of 16 mg/day is required, whereas a dose of 52 mg/day is required to target a plasma concentration of 450 ng/ml. Based on this analysis, subcutaneous dosing of elvitegravir without a booster will need to be at least greater than 16 mg/day and potentially much greater.

In a second approach for estimating elvitegravir subcutaneous dosing without a booster, a basic two-compartment model is used with a half-life of 3.5 hours, a volume of distribution of 67L [54], and 100% bioavailability. Based on this model, a constant-rate dose of 9 mg/day is needed to maintain a 135 ng/ml plasma concentration and 30 mg/day is necessary for 450 ng/ml.

Based on either estimate, the required dosing for effective HIV PrEP from subcutaneous constant rate delivery of elvitegravir is incompatible with the loading capacity of the TFPD. With a minimum dosing estimate of 9 mg/day, a 90 day device must hold 890 mg of elvitegravir. Based on the estimated density of elvitegravir (1.4 mg/mm^3) [59] and the volume of the maximum sized subcutaneous TFPD (126 mm^3), the maximum elvitegravir loading capacity is 176 mg.

However, while not yet tested clinically, a recent report investigating elvitegravir concentrations in rectal and vaginal secretions in macaques suggests that relatively low levels of elvitegravir in plasma may correlate with significantly higher concentrations in the rectal and vaginal tracts, an important finding for the use of elvitegravir for systemic PrEP. [60] A single unboosted oral dose

of 50 mg/kg in macaques resulted in equivalent plasma concentrations observed for humans receiving 800 mg of unboosted elvitegravir, but lower concentrations than observed for the standard 150 mg dose of elvitegravir with cobicistat as a booster. Based on 24 hour AUC measurements, the ratio of elvitegravir exposure the rectal and vaginal tract (determined by measurements in mucosal secretions) compared to plasma was 694 and 114 times higher. These results suggest that significantly lower plasma concentrations of unboosted elvitegravir may result in vaginal and rectal tissue concentrations high enough for effective PrEP. Based on this information, Table 8 shows estimates of subcutaneous doses, predicted plasma concentrations, and estimated vaginal tract concentrations based on a 114 fold increase in vaginal tissue concentration relative to plasma. In light of this, subcutaneous constant rate doses as low as 0.15 mg/day may result in protective concentrations (3x IC95) in the vaginal tract. A more conservative estimate of effective concentration based on 10 x IC95 (450 ng/ml) is achieved in the vaginal tract with just 0.5 mg/day.

Table 8 Elvitegravir dosing estimates

SubQ Dose (mg/day)	Estimated Plasma Concentration (ng/ml)	Estimated Vaginal Secretion Concentration (ng/ml)
0.15	1.3	148
0.5	4.5	513
1	9	1026
16	135	15390

9.2.3. Elvitegravir release from TFPD

While estimated dosing of elvitegravir based on clinical data for HAART treatment is not compatible with device loading capacity, a preliminary evaluation of release from the TFPD was conducted. Release studies were conducted for elvitegravir with no additional formulation excipients released from devices with 6 µm thick nonPCL membranes at three different device sizes (n = 3 or 4 for each size). Figure 48 illustrates the expected linear correlation between

elvitegravir release and device surface area, indicating membrane controlled release. Furthermore, based on the correlation in Figure 48, a maximum sized device with 250 mm^2 surface area and a 6 µm thick membrane will release 4.4 mg/day elvitegravir.

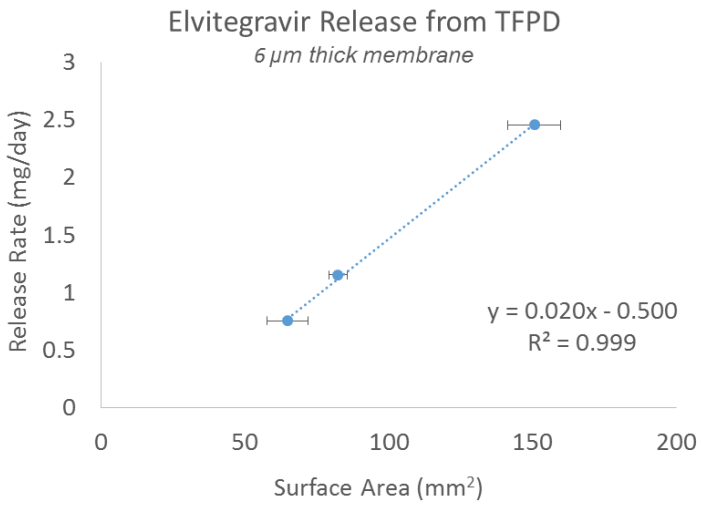

Figure 46 Elvitegravir release rate from TFPD is proportional to device surface area. Based on correlation, a maximum sized device with 250 mm^2 surface area will release elvitegravir at a rate of 4.4 mg/day. Each data point represents average release rate for 3 or 4 devices and error bars represent one standard deviation.

9.2.4. Conclusions

While elvitegravir exhibits membrane controlled release can be released from the TFPD at rates up to 4.4 mg/day with a 6 µm thick membrane, dosing estimates for subcutaneous constant rate delivery of elvitegravir for HIV PrEP based on plasma concentrations alone are, at a minimum, 9 mg/day and potentially as high as 50 mg/day. Not only are release rates not compatible with this dosing range, but the loading capacity for a maximum sized elvitegravir-TFPD is almost an order of magnitude too small. However, based on recent results suggesting a preferential distribution and possible sequestration into rectal and vaginal tissues resulting in a significantly higher elvitegravir exposure in these tissues compared to plasma, drastically lower doses of unboosted elvitegravir may be effective for HIV PrEP. Additional studies in animal models

investigating tissue distribution and protection against viral infection at steady state for unboosted elvitegravir delivered subcutaneously are needed to draw further conclusions regarding effective subcutaneous elvitegravir dosing for HIV PrEP.

9.3. **Rilpivirine**

9.3.1. Background

Rilpivirine (Figure 49), is a non-nucleoside analog reverse transcriptase inhibitor (NNRTI) developed originally for HIV treatment as an oral tablet and currently in clinical development as a long-acting injectable nanosuspension for HIV PrEP (Rilpivirine-LA). [61] As a result of these efforts to develop rilpivirine as both an oral tablet and nanosuspension, rilpivirine is available in several forms. Rilpivirine is highly insoluble and was thus developed as an HCl salt for improved solubility for oral dosing compared to the free base. While there may be a marked improvement in solubility in a pH range relevant to the gastrointestinal tract, the solubility of the HCl salt at a subcutaneously relevant pH of 7.4 remains drastically low (< 1 µg/ml). Standard dosing for rilpivirine as part of a combination therapy for HIV treatment is a 25mg daily oral dose. As a nanosuspension for long-acting HIV PrEP, rilpivirine HCl is wet-milled to produce crystal sizes less than 1 µm. [62] The nanosuspension used in clinical development is formulated as a liquid suspension with a cold-chain requirement to maintain particle size and chemical stability, but was additionally available in a lyophilized form. Doses ranging from 400 – 1200mg are currently under evaluation for rilpivirine-LA. Relatively high efficacy and low oral dosing of rilpivirine in HIV treatment make it a good candidate for a long-acting formulation if its extremely low solubility and hydrophobicity can be overcome.

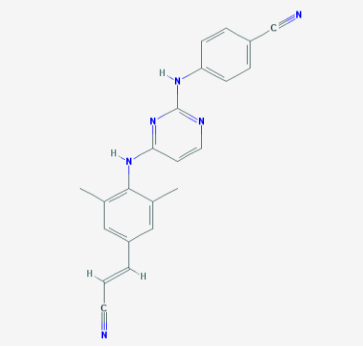

Figure 47 Rilpivirine chemical structure [75]

9.3.2. *Rilpivirine dosing*

Effective rilpivirine constant-rate dosing from a subcutaneous implant targeting is estimated based on pharmacokinetic data obtained from pre-clinical and clinical studies of Rilpivirine-LA [63] [64] [50] [61] and Equation 6. A target plasma concentration of 40 ng/ml is used based on recommendations from experts in the field, results from Rilpivirine-LA clinical studies, and it is just over 3 times the IC90 value of 12 ng/ml. Table 9 contains the relevant pharmacokinetic data used in Equation 1 and estimates of rilpirivine constant rate subcutaneous dosing required to achieve a range of target plasma concentrations. Based on these calculations, a 5.5 mg/day constant rate dose is needed to achieve a 40 ng/ml steady-state plasma concentration.

Table 9 Rilpivirine-LA subcutaneous injection PK data and constant-rate subcutaneous dosing estimates.

Rilpivirine PK data **[63]**	
Dose	400 mg
AUC	70007 ng*hr/ml
CL/F (= Dose/AUC)	5700 ml/hr
Rilpivirine Constant-Rate Dosing Estimates	
Constant Release Rate	**Plasma Concentration**
1 mg/day	8 ng/ml
2 mg/day	15 ng/ml
5.5 mg/day	40 ng/ml
8 mg/day	59 ng/ml

9.3.3. Rilpirivine release from TFPD

Initially the HCl salt form of rilpivirine was selected for evaluation of release from the TFPD as the solubility was expected to be higher than that of the free base form. However, at pH 7.4, rilpivirine HCl solubility remains extremely low at < 1 µg/ml. Low solubility combined with a high LogP results in very slow release of rilpivirine from the TFPD. In an effort to increase release rates, additional forms and formulations of rilpivirine are explored. In the TFPD, reservoir concentration which is dictated by drug solubility, is the driving force of release. In

pharmaceutical formulation it is a common practice to use solubilizing excipients to increase drug solubility; in the TFPD, it is hypothesized that solubilizing excipients to increase drug solubility will increase release rate.

9.3.3.1. Rilpivirine HCl

Rilpivirine HCl was loaded as a dry powder into TFPDs with 6 µm thick membranes, and release rates under simulated physiological conditions were evaluated (n=3). An average area normalized release rate of 7E-04 mg/day-mm^2 was measured, which translates to 0.2 mg/day in a maximum sized device. Based on a target release rate around 5 mg/day, a greater than 10-fold increase is needed. As this drastic increase in release is not achievable by adjusting PCL membrane properties alone[12], re-formulation of the drug substance was considered and Rilpivirine HCl drug powder was not evaluated further in this form.

[12] *Use of a microporous PCL membrane to release Rilpivirine HCl as both a powder and a PEG300 slurry indicate a decrease in release rate with the introduction of porosity. This is attributed to Rilpivirine's high LogP. (*

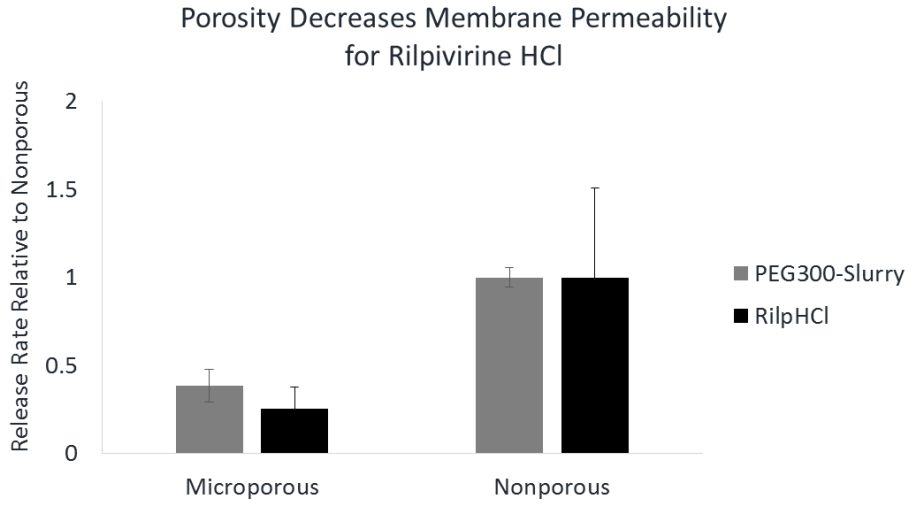

Figure 12 Membrane porosity decreases permeability for highly hydrophobic Rilpivirine HCl (logP 4.86, < 1 µg/ml solubility).)

9.3.3.2. Rilpivirine HCl + PEG300

PEG300 is a known solubilizing excipient for pharmaceutical formulation. Rilpivirine HCl was suspended in PEG300, liquid at room temperature, to create a suspension. PEG300 when dissolved in an aqueous medium may increase Rilpivirine HCl solubility; additionally, Rilpivirine HCl has a significantly higher solubility in PEG300 than in water. [65]These properties may increase rilpivirine solubility and thus reservoir concentration to increase the rate of release.

Rilpivirine HCl as a PEG300 slurry was loaded into TFPDs with 10 or 11 µm thick membranes, and release rates under simulated physiological conditions were evaluated (n=6). Formulation of Rilpivirine HCl as a PEG300 slurry resulted in increased release rates on average 2.7 times higher than those of the unformulated HCl salt, resulting in an achievable release rate in a maximum sized device with a 6 µm thick membrane of 0.6 mg/day. Furthermore, Rilpivirine HCl with PEG300 formulation demonstrated membrane-controlled release indicated by release rates scaling with device surface area and membrane thickness (Figure 50).

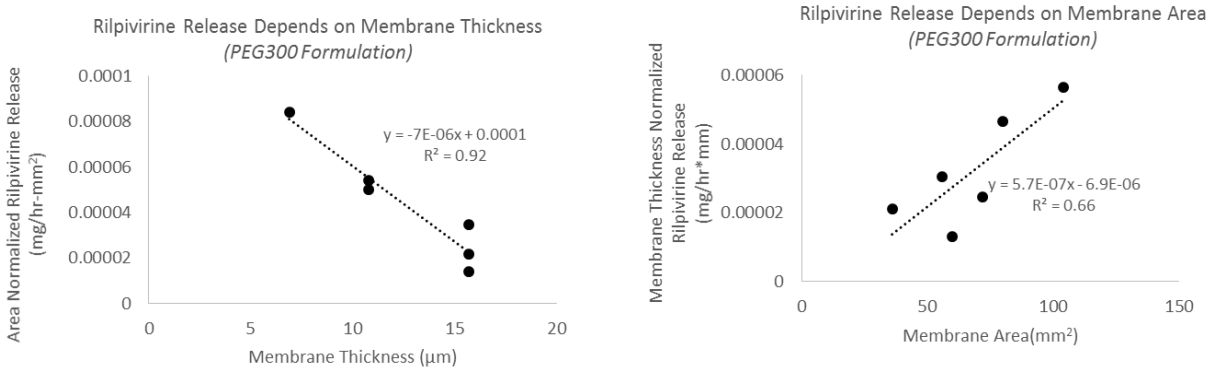

Figure 48 Membrane controlled release of Rilpivirine HCl + PEG300.

9.3.3.3. Rilpivirine + Hydroxypropyl β Cyclodextrin (HP-β-CD)

HP-β-CD is a known solubilizing excipient for pharmaceutical formulation. It is a powder at room temperature and was evaluated for formulation with Rilpivirine HCl by both physically mixing together the two powders as solids as well as by creating a Rilpivirine HCl slurry in a 60% HP-β-CD solution. Better results were obtained with the slurry and are presented here.

Rilpivirine HCl as a slurry in 60% HP-β-CD (aq) was loaded into TFPDs with 7 μm thick membranes, and release rates under simulated physiological conditions were evaluated (n=3). Formulation of Rilpivirine HCl as a slurry in 60% HP-β-CD (aq) resulted in increased release rates on average 2.4 times higher than those of the unformulated HCl salt, resulting in achievable release rate in a maximum sized device with a 6 μm thick membrane of 0.5 mg/day. There was no improvement with HP-β-CD formulation over PEG300 formulation.

With a semi-permeable membrane allowing for the evaporation of water under ambient storage conditions, an aqueous formulation for the device reservoir is not suitable. While a simple physical mixture of HP-β-CD and Rilpivirine HCl did not result in increased release rates, a dehydrated solution of Rilpivirine HCl and 30 or 60% HP-β-CD (aq) did. This suggests that either a spray-dried or lyophilized formulation of Rilpivirine HCl with HP-β-CD would be needed for an appropriate TFPD core formulation. This would add an additional process step, and is not ideal. There are additional concerns with potential toxicity with high levels of HP-β-CD. With no improvement over the PEG300 formulation and with this consideration in mind, device performance with Rilpivirine HCl + HP-β-CD was not investigated further.

9.3.3.4. Rilpivirine + Polysorbate-20 (PS20)

PS20 is a common formulation excipient and is added in low concentrations (1 %) to release media for *in vitro* Rilpivirine release studies to increase solubility and maintain sink conditions. Knowing that PS20 increases Rilpivirine solubility in release media, the use of PS20 as a formulation excipient within the TFPD reservoir was explored.

Rilpivirine HCL as a slurry in PS20, which is a liquid at room temperature, was loaded into TFPDS with 6 µm or 16 µm thick membranes (n=4). While successfully increasing release rates 2.7 times those of the unformulated HCl salt, evaluation of PS20 as a formulation excipient was not carried further, but could be considered as an alternative to PEG300 in future work.

9.3.3.5. Rilpivirine-LA Nanosuspension

Janssen Pharmaceuticals has developed a long-acting rilpivirine nanosuspension for intra-muscular or subcutaneous injection. This formulation leverages a reduction in particle size to increase and control the solubility and dissolution rate. [62] While not an ideal candidate for formulation in the TFPD due to high cost and known cold-chain requirements, two variations of the rilpivirine-LA nanosuspension were evaluated in the TFPD to determine if pursuing a reduction in particle size to achieve increased release was worthwhile.

Two forms of the rilpivirine-LA nanosuspension were evaluated in TFPDs with 5 µm thick membranes, the liquid suspension at a concentration of 300 mg/ml (n=3) and a lyophilized nanosuspension loaded as a powder (n=5). Both formulations resulted in increased release rates compared to the unformulated HCl salt; the lyophilized nanosuspension showed an average 3.8-fold increase in release and the liquid suspension a 2.6-fold increase. While the

lyophilized nanosuspension achieves up to almost 1 mg/day release, release rates obtained for devices loaded with the lyophilized nanosuspension were highly variable and may reflect difficulties in device loading or heterogeneity in lyophilized material. While not investigated further within this evaluation due to considerations of processing complexities, intellectual property, and stability, this preliminary evaluation suggests that a reduction in particle size will effectively increase release rates for rilpivirine HCl from the TFPD.

9.3.4. *Conclusion*

The highest achievable release rates in a maximum sized TFPD with a 6 µm thick membrane for each Rilpivirine HCl formulation investigated are displayed in Figure 51. Adding solubilizing formulation excipients such as PEG300, HP-β-CD, or PS20 to the core reservoir formulation and reducing particle size to the nanometer scale increase release rates up to 3.8 times what is observed with the unformulated microionized rilpivirine HCl powder. However, achievable release rates still fall well short of the estimated 5.5 mg/day needed to maintain effective plasma concentrations for HIV PrEP. The work presented here provides a foundation for understanding the impact of formulation excipients and particle size on release rates from the TFPD as well as a basis for designing rilpivirine devices. While not compatible with the 5.5 mg/day estimates, if future results suggest that rilpivirine plasma concentrations below 40 ng/ml result in effective PrEP or that *in vivo* constant-rate subcutaneous dosing of rilpivirine results in higher than estimated plasma concentrations, the plausibility of achieving effective release rates of rilpivirine from the TFPD may be reconsidered.

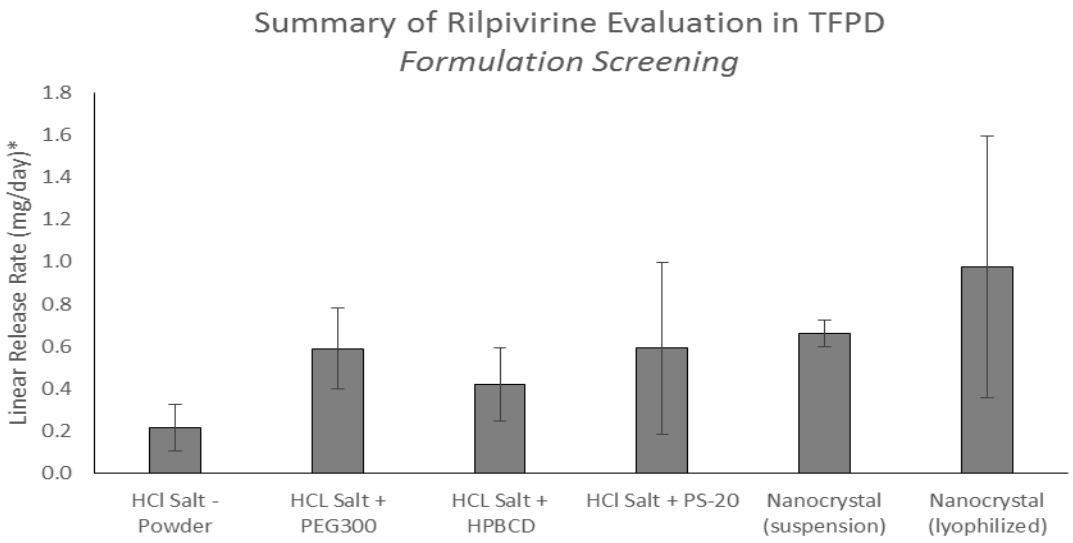

Figure 49 Rilpivirine HCl release rates from TFPD. Release rates are normalized based on surface area to the highest achievable release rate in a maximum sized device with a 6 µm thick membrane. All data sets represent ≥ 3 replicates. Addition of solubilizing excipients and reduction in particle size increase release rates.

9.4. **Tenofovir Alafenimide Fumarate**

9.4.1. Background

When taken daily as an oral dose, tenofovir (TFV)-based antiretrovirals show high efficacy for HIV pre-exposure prophylaxis (HIV PrEP) in men and women, but poor adherence to the regimen drastically decreases effectiveness. [41] Clinical studies with tenofovir disoproxil fumarate (TDF)/emtricitabine (FTC) and TDF alone have highlighted a strong correlation between the level of HIV PrEP effectiveness and product adherence. [42] [43] The iPrEx [44] and Partners PrEP [45] studies investigated the prophylactic effectiveness of orally administered Truvada in gay/bisexual men and heterosexual discordant couples, respectively. In these studies, Truvada reduced the risk of infection by at least 90% when taken regularly, but this level of protection declined to only 44% and 75%, respectively, when lower product adherence resulting in sub-prophylactic dosing regimens were taken into consideration. Outcomes from the VOICE and FemPrEP trials in Sub-Saharan Africa [46] [47] [48] investigating the effectiveness of TDF or TDF/FTC oral dosing regimens -further demonstrated that poor adherence to the product

regimen stands as a barrier to an otherwise efficacious HIV PrEP strategy. In light of these outcomes, there is a strong interest in the development of alternative delivery strategies for antiretrovirals as HIV PrEP, that are less burdensome to the user and do not depend on user compliance.

Here we introduce a tunable biodegradable subcutaneous implant for long-acting constant rate delivery of tenofovir alafenamide fumarate (TAF) for HIV PrEP. TAF, like TDF, is a tenofovir pro-drug (Gilead Sciences, Foster City, CA), but unlike TDF which is converted to TFV upon absorption into the blood stream, TAF is primarily converted to TFV intracellularly, resulting in significantly more potency and lower systemic concentrations of TFV which, when taken systemically and chronically, can have side effects such as reduction in bone demineralization or renal toxicity [66] [67]. Since efficacy of tenofovir-based ARV for HIV PrEP has been confirmed and approved through the oral route [68] [44] it is highly likely that another tenofovir pro-drug, TAF will also be efficacious for HIV PrEP and is currently investigated in clinical studies. [69]

9.4.2. TAF Dosing

In clinical development as an alternative tenofovir antiretroviral for HIV treatment, results show that only 8mg of TAF taken orally is equivalent in the AUC (area under the curve) of intracellular tenofovir as well as in antiviral activity, to 300mg of TDF, the dose commercially available as a standalone and as a TDF/FDC combination product [70]. However, as constant-rate subcutaneous delivery for HIV PrEP has not yet been explored in humans for tenofovir derived APIs, the efficacious dose of TAF from this novel route of administration is as yet unknown. Simply taking into consideration the bioavailability of TAF (35%) [71] and comparing oral TAF efficacy to TDF efficacy, subcutaneous delivery of 2.8 mg/day TAF is estimated as an upper bound for effective PrEP. However, this estimate does not take into consideration the pharmacokinetic benefits of constant rate release nor potential differences in distribution and

tissue sequestration between TDF and TAF. Recently published results for subdermal delivery of TAF delivered from a non-biodegradable constant-rate implant in beagle dogs suggest that human doses as low as 0.15 mg/day may be sufficient to maintain effective concentrations of TFV-diphosphate in peripheral blood mononuclear cells. [72] In order to support device development and testing in pre-clinical models as well as later clinical dose escalation studies, a highly tunable subcutaneous TAF implant with release rates up to 3 mg/day is desired.

9.4.3. TAF release from TFPD

Short term, small scale studies are used to develop an appropriate formulation for overcoming dissolution-limited release and to increase the rate of release. Additionally, these studies investigate the relationships between TAF release and device design parameters, providing an understanding of the achievable range of release and the necessary information to design implants with target specifications. The ability to accurately and reproducibly produce prototype devices targeting specific and relevant release rates based on the results of these small scale studies is demonstrated with the design, fabrication, and in vitro evaluation of relevant prototype devices. Linear release and stability of TAF in these prototype devices is demonstrated up to 90 days. With a simple and flexible fabrication protocol and multiple approaches to tuning release, this implant can be easily tuned to achieve release rates up to 4.4 mg/day in a device comparable in size to commercially available contraceptive implants.

9.4.3.1. Short-term screening studies

In these small-scale studies, release data was collected over 5-10 days. Linear release rates were obtained while solid drug remained in the device reservoir and were compared to device parameters to verify membrane controlled release, to demonstrate the relationship between device parameters and TAF release, to explore the achievable range of release rates, and to develop an empirical model to design devices targeting specific release rates.

9.4.3.1.1. TAF Release

TAF release from 8 different devices was evaluated. In each of these devices TAF was loaded in solid form with no additional excipients into the device reservoir. At the end of the study, all devices still visibly contained solid TAF in the device reservoir and cumulative release profiles appeared linear. Figure 52 illustrates the relationships between release rate and surface area.

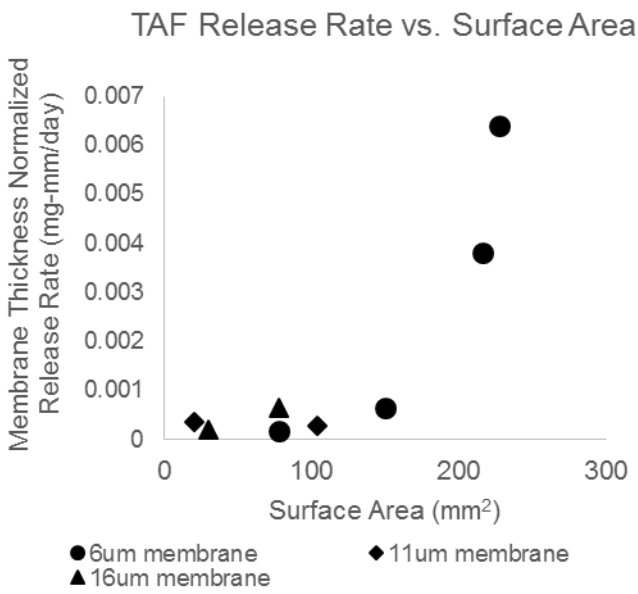

Figure 50 TAF release vs surface area. Linear release rate of TAF from PCL reservoir device has a non-linear dependence on surface area. This is not characteristic of membrane controlled release. Release rates are normalized for membrane thickness and each data point represents an individual device.

For membrane-controlled release, release rates are expected to increase proportionally with membrane surface area. The non-linear relationship between surface area and release rate shown in Figure 52 suggests that membrane controlled release is not achieved and TAF release from the device may be dependent on the rate of TAF dissolution in the device reservoir. Furthermore, based on these preliminary observations, a maximum device area of 250mm^2 and a minimum membrane thickness

of 6um will result in TAF release rates around 1 mg/day. In attempts to achieve membrane controlled release and a broader range of release rates, TAF was formulated in the device reservoir with excipients known to increase solubility and dissolution rate.

9.4.3.1.2. TAF Formulation with PEG300

To investigate the effect of adding PEG300 to the device reservoir and to determine the relationship between TAF release and membrane surface area, TAF release from triplicate rod-shaped devices in three sizes (57 mm^2 +/- 6, 109 mm^2 +/- 18, 260mm^2 +/- 62) loaded with a 2:1 TAF to PEG mass ratio was evaluated for up to 5 days. All devices had a membrane thickness of 8.5µm. Figure 53AA shows the average cumulative release profile for each device size. The average cumulative release profile is only calculated while solid drug remains in all three device reservoirs and the release profile is linear. As expected for membrane controlled release, the rate of TAF release scales proportionally with increasing membrane surface area (Figure 53B).

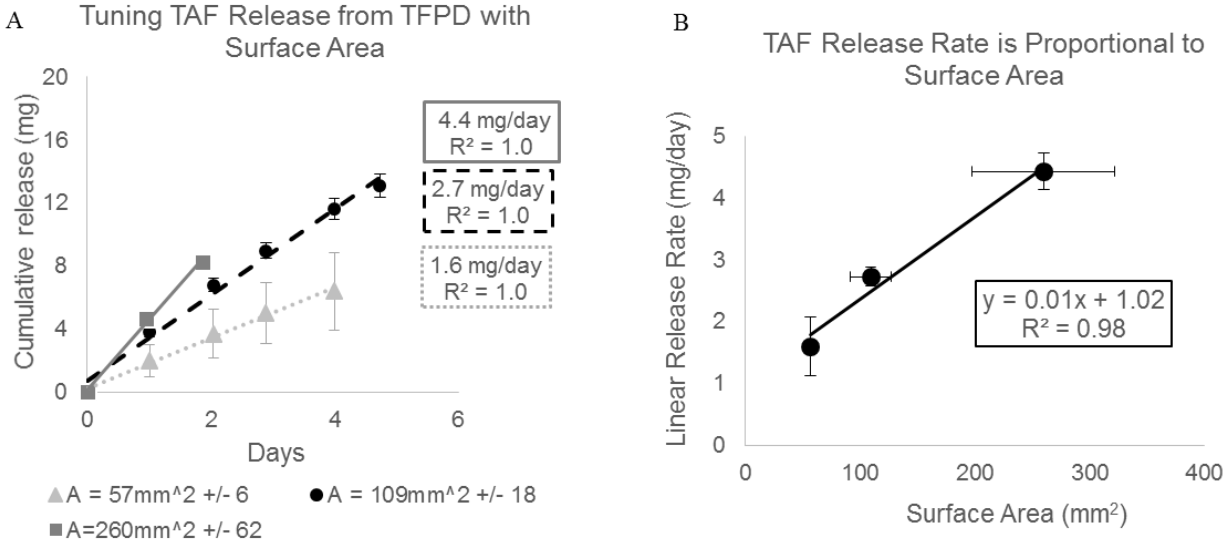

*Figure 51 Membrane controlled release of TAF with PEG300 formulation. (*A) Cumulative release profile of TAF from polycaprolactone thin-film devices loaded with TAF-PEG300 (2:1 w/w ratio). All devices had an 8.5µm thick membrane. Solid trendlines and large data points represent average of triplicate devices with error bars representing 1 standard deviation. Average values are only calculated for time points while all devices retain

solid TAF in device reservoir and release profile is linear. (B) TAF linear release rates taken from the data shown in (A) scale linearly with membrane surface area. Error bars represent 1 standard deviation.

To further investigate the relationship between device design and TAF release, TAF release from triplicate rod-shaped devices, 294 mm^2 +/- 36 surface area, with three different membrane thicknesses (9,15,26 µm) loaded with a 2:1 TAF to PEG ratio was evaluated for up to 7 days. Figure 54A shows the average cumulative release profile for each membrane thickness. The average cumulative release profile is only calculated while solid drug remains in the reservoir of all three devices and the release profile is linear. Figure 54B illustrates the relationship between linear release rate normalized for surface area and membrane thickness, including data represented in A as well as three additional data points taken from the prototype device studies described later in this manuscript (Figure 57). Additionally, release rates from devices with 8.5 m thick membranes loaded with mass ratios of TAF to PEG (2:1 (n=3), 1:1 (n=3) and 1:2 (n=6)) were evaluated to determine if TAF release depends on excipient content within this range. (Figure 54)

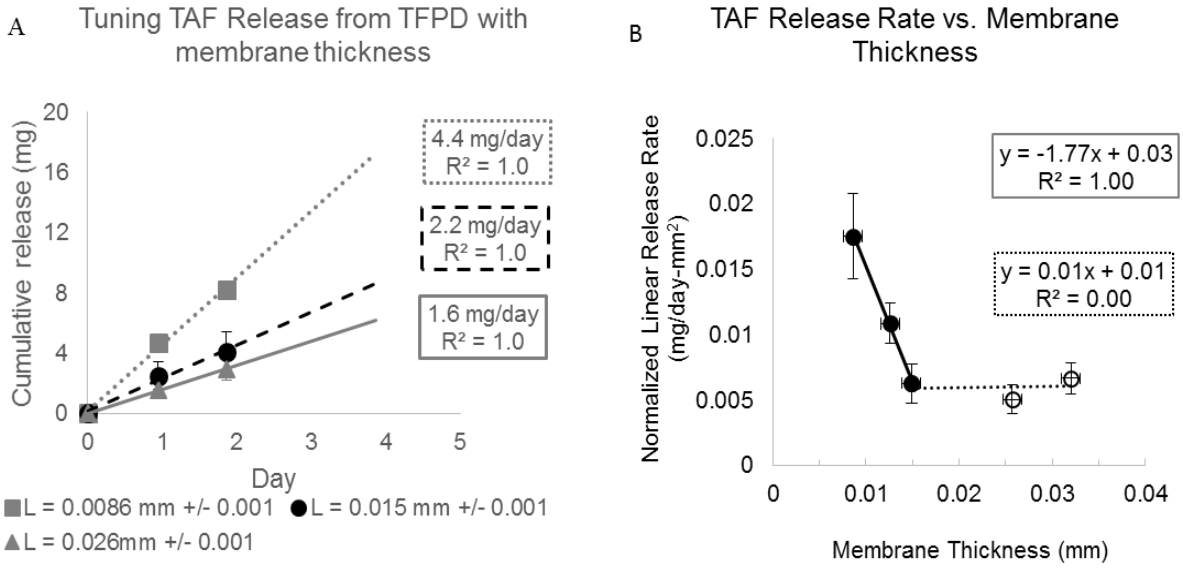

Figure 52 Membrane controlled release of TAF with PEG300 formulation. (A) Cumulative release profile of TAF from polycaprolactone thin-film devices loaded with TAF-PEG300 (2:1 w/w ratio). Solid trendlines and large data points represent average of triplicate devices with error bars representing 1 standard deviation. Average values are only calculated for time points while all devices retain solid TAF in device reservoir and release profile is linear. All devices are roughly 2-2.5mm diameter x 40mm long rods (294 mm^2 +/- 26 surface area). (B) TAF linear release rates taken from the data shown in (A) and from prototype devices in Figure 57

PEG300, a commonly used solubilizing excipient, was evaluated to increase dissolution and solubility of TAF in the device reservoir with the goals of achieving membrane controlled release and of increasing TAF release up to 3 mg/day for a maximum sized (260 mm^2) device. When formulated with PEG300 in a 2:1 mass ratio, we achieved TAF release rates up to 4.4 mg/day in a rod shaped device 2mm in diameter and 4.1cm long with a 260 mm^2 surface area (Figure 53). Furthermore, when formulated with PEG300, we observed membrane controlled release of TAF from the device as exhibited by a proportional relationship between release rat and membrane surface area (Figure 53B). As Figure 54B shows, there was an inverse linear correlation between release rate and membrane thickness until the membrane reaches a critical thickness (0.015 mm) at which point increasing membrane thickness no longer impacts release rate. These results demonstrate that membrane thickness can be used to control the rate of TAF release in a range of 1.6-4.4 mg/day for a maximum sized device.

Release rates for different mass ratios of TAF to PEG300 were explored in order to determine the impact of these different formulations on release rate. While a 2:1 mass ratio is ideal in order to maximize TAF loading capacity, the thick paste is challenging to load by hand into a maximum sized device when loading to full capacity. We therefore explored the use of formulations with more PEG300 which results in a more fluid formulation that is easier to load by hand. Results demonstrate that release rates for

TAF-PEG300 formulations with 2:1, 1:1, and 1:2 mass ratios were not significantly different (p=0.16). (Figure 55)

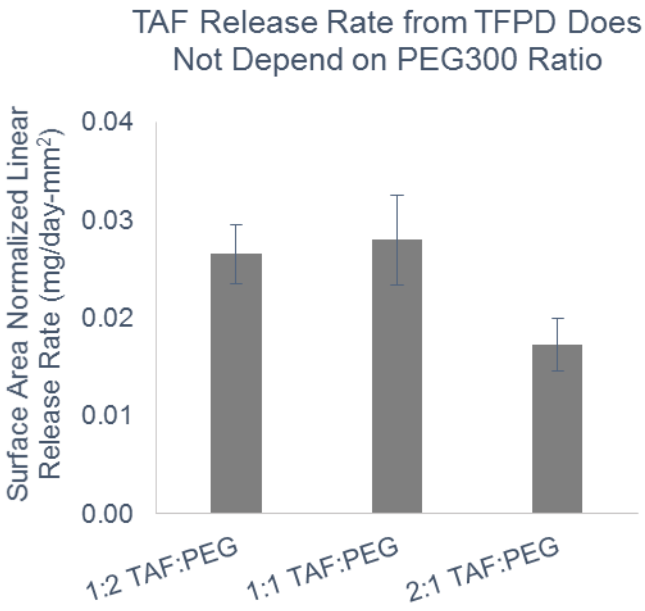

Figure 53 Impact of PEG300 on TAF release from TFPD. Surface area normalized release rates for TAF from PCL TFPD (8.5 µm membrane) with a range of w/w ratios of TAF to PEG300. No statistically significant difference in release rates (p=0.16).

9.4.3.2. Prototype Studies

Using the empirical correlations obtained in the short-term screening studies, three groups of triplicate prototype devices were designed to target three different release rates relevant to the estimated range for effective TAF dosing in humans (2.5 mg/day, 1.4 mg/day, 0.4 mg/day). These devices were fabricated by hand at a lab-scale as previously described. All devices were evaluated for TAF release until device depletion, demonstrating linear release profiles, reproducibility between replicate devices, and accuracy in device designs targeting

specific release rates. Additionally, the chemical stability of TAF remaining in the device reservoir was evaluated at 0, 27, 49, and 89 days.

9.4.3.2.1. Prototype devices targeting specific release rates

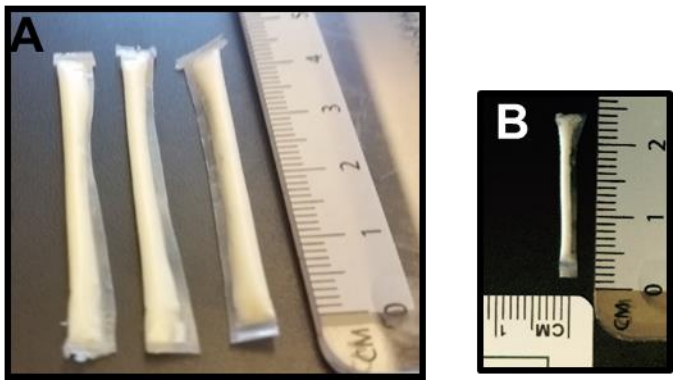

Figure 54 TAF TFPD Prototypes. (A) 2.5mm diameter, 40mm long prototypes loaded with 230mg 1:1 TAF:PEG300 (w/w). (B) 0.6mm diameter, 20mm long prototype loaded with 26mg 1:1 TAF:PEG300 (w/w).

Three groups of triplicate rod-shaped devices were fabricated according to different device designs targeting three release rates. Images of Group II devices and a representative device from Group III are shown in Figure 56. Figure 57A contains the device parameters for each group and the target release rates based on these parameters (2.5 mg/day, 1.4 mg/day, 0.4 mg/day). Devices were loaded with a 1:1 w/w TAF and PEG300 paste and total TAF the total TAF load for each device is presented in Figure 57A. Based on the target release rate and TAF loading, the expected device duration was calculated and provided in Figure 57A. Figure 57B shows the linear release profiles for all three groups of prototype devices until the device approaches depletion. Prototype release rates for Groups I and II are within 15% of target and within 25% of target for Group III. Variability in release rates within each group is less than 10%.

Group	Device Dimensions (Rod, DxL - mm)	Membrane Area (mm^2)	Membrane Thickness (μm)	TAF Load (mg)	Predicted Device Duration (days)	Target Release Rate (mg/day)
I	2.5 x 40	254 +/- 39	13 +/- 1	128 +/- 33	51	2.5
II	2.5 x 40	238 +/- 3	32 +/- 1	115 +/- 10	82	1.4
III	0.6 x 20	40 +/- 0.5	31 +/- 1	13 +/- 6	33	0.4

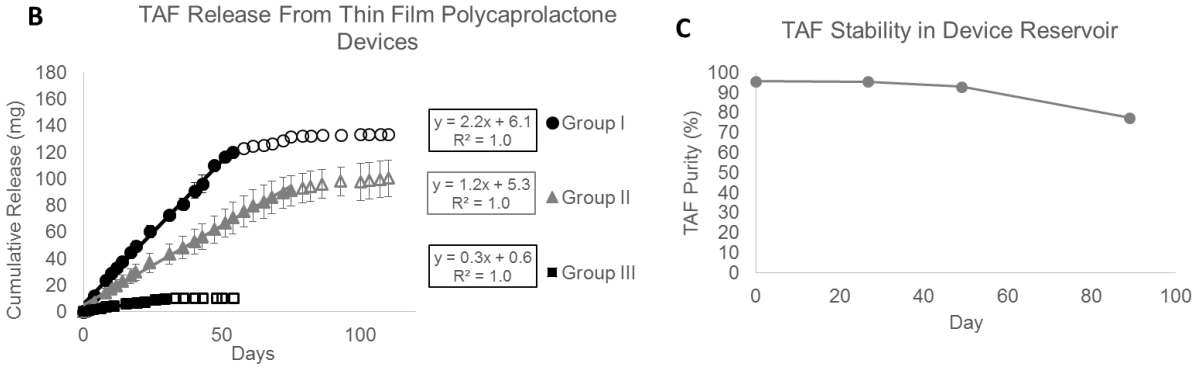

Figure 55 TAF TFPD Prototype Results. (A) Device parameters and predicted release rates for TAF TFPD prototype devices. Each group consists of n=3 devices and measurements represent average values +/- 1 standard deviation. (B) Cumulative release profiles for prototype device groups. Prototype devices are loaded with a 1:1 TAF:PEG300 (w/w) formulation. Release profile is linear (solid data points) until device nears depletion (outlined data points). Linear regression determines average release rate for each prototype group (mg/day). (C) Purity of TAF remaining in device reservoir after incubation under physiological conditions (PBS pH 7.4, 37˚C).

Release profiles from prototype devices demonstrate the potential of this system to deliver relevant constant-rate doses of TAF. TAF release is linear until devices near depletion. When TAF depletes from the device to levels below the solubility of TAF in the device reservoir, there is no longer a constant TAF concentration in the device reservoir and TAF release is proportional to TAF reservoir concentration. This results in the non-linear region of the release profiles represented by open data points in Figure 57B. The mass of TAF released in this non-linear phase will depend on the device size and volume of the device reservoir; larger reservoir volumes will result in larger quantities of soluble TAF. Group I and II prototype devices are maximum sized devices and release on average a total of 10 mg of TAF in the non-linear phase.

All devices presented in this manuscript are fabricated and loaded by hand at a lab-scale. This leads to leads to error in both the accuracy and precision of device fabrication relative to device design. To account for error in the accuracy of device fabrication, target release rates are calculated from the actual device parameters of fabricated devices. This is why target release rates are 2.5 mg/day, 1.4 mg/day, and 0.4 mg/day rather than say 2.5 mg/day, 1.5 mg/day, and 0.5 mg/day. Error in the precision of device fabrication is reported in Figure 57A as +/- 1 standard deviation. Additionally, all prototype devices are loaded with a 1:1 mass ratio of TAF to PEG300 rather than the 2:1 mass ratio used in the screening studies. This is due to the difficulty of fully loading a 40mm long device with the 2:1 formulation due to the high viscosity of the formulation. As the TFPD system is translated from lab scale fabrication to a manufacturing process, accuracy, precision and loading are expected to be improved. In addition to improving accuracy and precision in device fabrication, a manufacturing process with the capacity to fully load devices with a 2:1 mass ratio of TAF to PEG300 will result in significantly higher loading capacities for TAF in the device reservoir. In the prototype devices presented here, the duration of release for each group of devices is dependent on the loading capacity of TAF into the device reservoir. With a 1:1 mass ratio of TAF to PEG300, a fully loaded maximum sized device release 1.2 mg/day has a linear release profile out to 75 days with full device depletion at around 100 days. With a higher loading capacity, the duration of linear release from these devices will be longer.

9.4.3.2.2. TAF Stability in Device Reservoir

A single device from Group I or Group II was sacrificed for analysis of TAF remaining in the device reservoir at 27, 49, and 89 days. Figure 57C shows the purity of TAF remaining in the device reservoir over the course of the in vitro release study out to 89

days. TAF purity remains unchanged within the device reservoir with up to 49 days. Between days 49 and 89, TAF purity decreases by 19% with TFV and monophenyl TFV being the major degradation products.

Results from the analysis of TAF chemical stability in the device reservoir indicate that under physiological conditions in a hydrated device, solid TAF contained in the device reservoir remains stable. (Figure 57) The loss of chemical purity between days 49 and 89 is likely due to the depletion of TAF solid from the device reservoir. The decrease in TAF purity is due to degradation of TAF via hydrolysis to mono-phenyl TFV, a form of TFV that may still be metabolized into active TFV-DP *in vivo*. Future studies will further investigate the *in vivo* activity of TAF released from the TFPD.

9.4.3.2.3. Pre-clinical Prototype Devices

While the *in* vitro prototypes with dimensions and release rates relevant to humans serve as a proof-of-concept, scaled-down devices are necessary for pre-clinical development. One of the benefits of the TFPD system is that it is highly tunable, allowing for easy scale down based on the empirical correlations presented earlier in the *short term screening studies.* This section discusses device design for a pre-clinical rat study to investigate TAF pharmacokinetics for constant-rate subcutaneous delivery at three different doses.

Using body surface area (BSA) based allometric scaling, target doses for a rat were calculated based on the human equivalent doses (HED) of interest. Assuming a standard 70 kg human and a 0.5 kg rat and a Km scaling factor of 6.2 (relating human equivalent dose to a rat equivalent dose), a 0.045, 0.135, and 0.445 mg/day dose in a rat is equivalent to a 3, 10 and 30 mg/day equivalent dose in a human. Device designs based

on empirical correlations (Figure 53, Figure 54) targeting these rat doses are described in Table 14. Table 11 describes the actual device parameters and observed release rates for prototype devices (n=3 per group). Comparing the actual device parameters to target parameters represents the ability to fabricate devices at lab-scale accurately and reproducibly according to a device design; this is dependent on the user and with an improved manufacturing process accuracy and precision are expected to improve drastically. The accuracy in the empirical model is evaluated by comparing the area normalized release rate for all devices is to the predicted value for a 15 µm thick film (Figure 58). No significant difference between the targeted and actual area normalized release rates indicates accuracy in the model. Comparison of the actual release rates in Table 11 to target release rates in Table 13, gives an overall evaluation of the accuracy and precision of both the empirical model and lab scale fabrication capabilities to produce small scale devices relevant for pre-clinical studies in rats. While groups I and II show good correlation between target and actual release rates, the actual release rates in group III are significantly lower than target. This is attributed to large air bubbles in the hydrated devices that can be difficult to avoid when under-loading a device. Based on this observation, it is recommended to fully load devices for pre-clinical studies, even if the full loading capacity is not required for the delivery throughout the study duration.

Table 10 Device designs for pre-clinical rat prototypes.

	Design Targets						
Group	HED * (mg/day)	Membrane Thickness (mm)	Diameter (mm)	Length (mm)	Area (mm^2)	Minimum ARV Load (mg)	Release Rate (mg/day)
I	1	0.015	1	2.2	7	0.9	0.05
II	3	0.015	2	3.3	21	2.8	0.14
III	10	0.015	2	10.3	65	9.3	0.45

Table 11 Device characterization and performance for pre-clinical rat prototypes.

	Actual										
Group	Membrane Thickness (mm)	Diameter (mm)	*SD*	Length (mm)	*SD*	Area (mm2)	*SD*	ARV Load (mg)	*SD*	Release Rate (mg/day)	*SD*
I	0.015	0.6	0.0	3.0	0.0	6	0.0	3.7	1.0	0.06	0.00
II	0.015	1.5	0.4	4.7	0.6	22	7.2	4.5	2.4	0.12	0.03
III	0.015	1.1	0.2	12.0	0.0	42	6.0	9.7	2.6	0.16	0.02

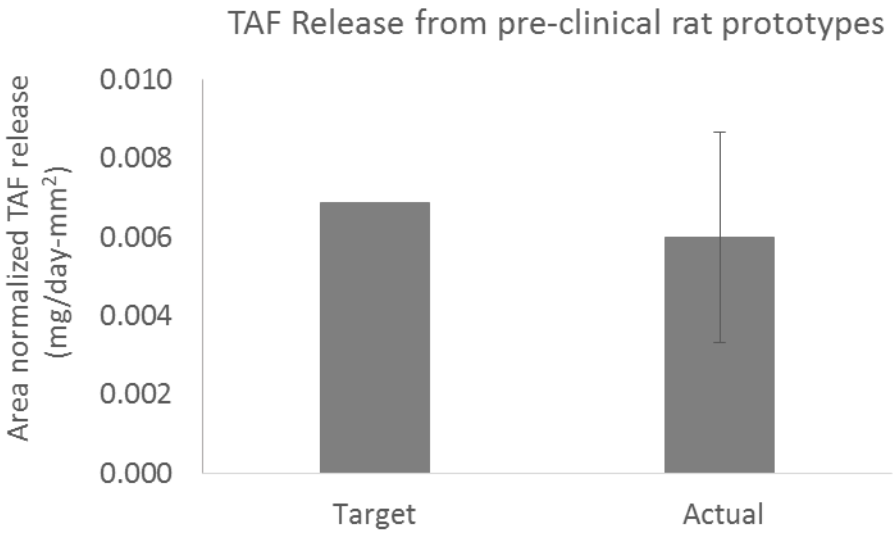

Figure 56 TAF Release from pre-clinical rat prototypes. Target area normalized release for TAF with a PEG300 formulation was calculated for a 15 µm thick film using the empirical correlation presented in Figure 54. Actual area normalized release rates for rat prototype devices (n=9) demonstrate accuracy in the empirical correlation to predict release based on membrane thickness.

9.4.4. Shipping & Terminal (gamma) Sterilization

There are two approaches to producing sterile devices. One is to fabricate and handle devices under aseptic conditions; the other is terminal sterilization. Where permitted, terminal sterilization is the preferred approach as it allows for easier and cheaper fabrication at both the lab and manufacturing scale. However, in order to use terminal sterilization, a sterilization

method must be compatible with both the PCL membrane as well as the drug and excipients contained in the device core. Sterilization must not significantly degrade the polymer membrane nor impact the chemical stability of the API. Additionally sterilization must not affect device performance and integrity. While more in depth studies would be necessary for future development, preliminary shipping and sterilization studies confirm that ambient shipping conditions and terminal sterilization by gamma-irradiation are suitable for pre-clinical studies.

Table 12 Shipping & Gamma Sterilization Study Design

Study Design		
Formulation	**Condition**	**Analytical Plan / Replicates**
TAF-TFPD (powder)	Shipping only	Mass change (n=4); TAF purity (n=1)
	Shipping + Sterilization	Mass change (n=4); TAF purity (n=1)
TAF/PEG300-TFPD (1:1 w/w)	Shipping only	Mass change (n=4); TAF purity (n=1); TAF release (n=3); PCL MW (n=1)
	Shipping + Sterilization	Mass change (n=4); TAF purity (n=1); TAF release (n=3); PCL MW (n=1)
TFPD (empty)	Shipping only	Mass change (n=4); PCL MW (n=1)
	Shipping + Sterilization	Mass change (n=4); PCL MW (n=1)

Table 12 describes the study design to investigate the impact of ambient shipping (transcontinental during the month of June) and gamma-irradiation on polymer and drug stability as well as device performance. Table 16 contains device parameters, physical changes observed upon shipping & sterilization, and TAF purity as measured by RP-HPLC. All devices in both shipping and shipping & sterilization groups, including empty devices, gain on average 11 mg. While not confirmed, this is likely due to moisture uptake by the PCL membrane during

shipping and could be avoided in the future with packaging techniques such as vacuum sealing. Neither this uptake in moisture nor the shipping and sterilization procedure impacted the chemical purity of TAF loaded into the TFPD as either a dry powder or as a PEG300 slurry.

Table 13 Shipping & Sterilization Study Results

Shipping & Sterilization Study Results							
	Surface Area (mm^2) (n=4)		Membrane Thickness (mm) (n=4)		Change in Mass (mg) (n=4)		Purity (n=1) (starting purity, 96%)
Formulation	**Average**	**SD**	**Average**	**Condition**	**Average**	**SD**	**% TAF**
TAF	115	6	0.01	Shipping	10	2	97
TAF	129	11	0.01	Shipping + Sterilization	11	4	96
TAF/PEG300 (1:1 w/w)	125	6	0.01	Shipping	9	0	93
TAF/PEG300 (1:1 w/w)	118	5	0.01	Shipping + Sterilization	12	0	95
Empty	205	40	0.01	Shipping + Sterilization	15	2	
Empty	121	15	0.02	Shipping + Sterilization	9	1	

Gamma-irradiation is expected to degrade PCL, but as Figure 59 illustrates, the PCL molecular weight distribution shifts perceptibly, but only slightly, to lower molecular weight species and average values are not significantly different after shipping or sterilization. Therefore, there is no concern that PCL degradation from this gamma sterilization protocol will impact device performance or integrity.

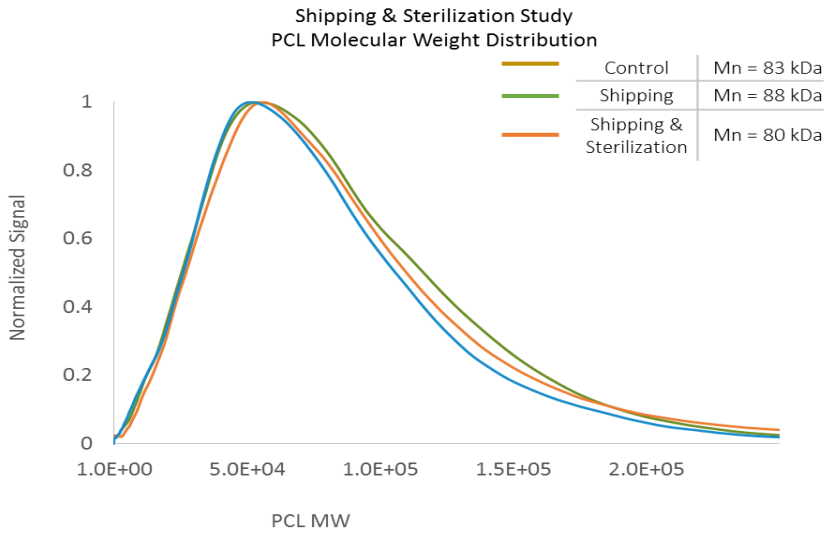

Figure 57 Impact of shipping & sterilization on PCL molecular weight distribution.

As a final evaluation of the impact of shipping and sterilization on the TAF TFPD, device performance was evaluated by comparing *in vitro* release rates and profiles for each group of devices loaded with TAF and PEG300 to a control group that was not subjected to shipping, sterilization, nor storage. Figure 60A shows no significant difference in area normalized release rates between these groups and Figure 60B illustrates the expected linear release profile (until device depletion) for all groups.

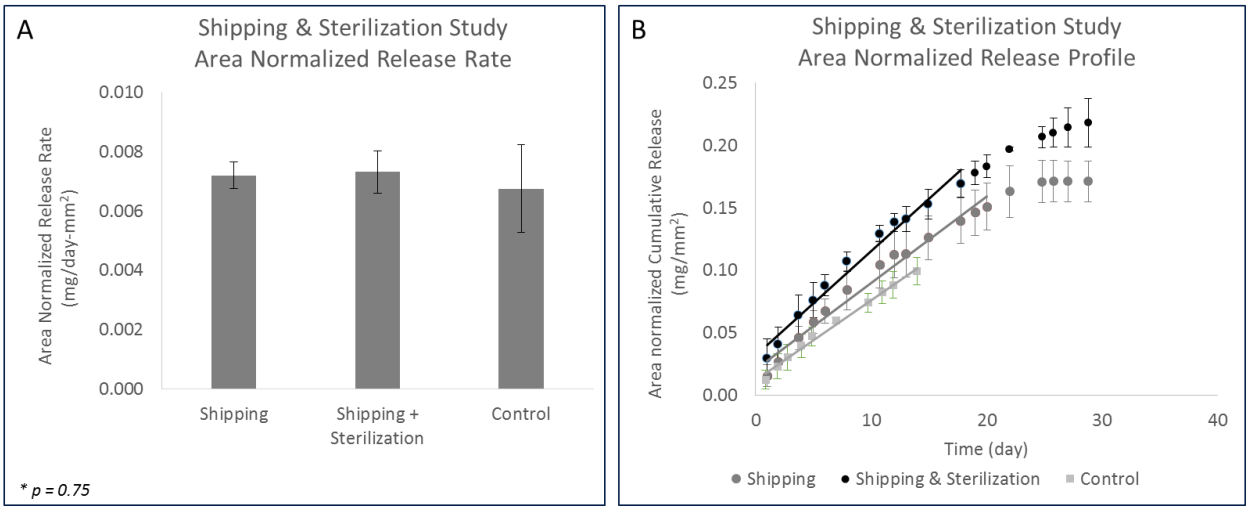

Figure 58 Impact of shipping & sterilization on device performance

9.4.5. Conclusion

Exhibiting membrane controlled release up to 3 months, release rates from the TAF TFPD are highly tunable with membrane surface area and membrane thickness. The device development work here presents a thorough analysis of the relationships between device design and TAF release rates which provides the basis for designing devices to accurately target specific release rates. These results show that without additional solubilizing excipients, TAF release from the TFPD is dissolution limited. However, with PEG300 as a solubilizing excipient, TAF exhibits membrane controlled release and increased release rates.

With this TAF-PEG300 formulation, we demonstrate the ability to target a range of release rates relevant to the estimated effective rates for TAF HIV PrEP subcutaneous delivery based on clinical pharmacokinetic data from oral TAF studies for HIV treatment. The tunability of this device is key to its success in pre-clinical and clinical development. Being able to tune release with both surface area and membrane thickness within this target range allows us to decouple release rate from reservoir volume and thus loading capacity. As a result, we have the potential to maximize our loading capacity and the implant duration or the option to limit the implant duration and loading capacity, but to create a smaller and more desirable implant, all while maintaining the same release rate. Furthermore, we are able to leverage the empirical correlations presented here between device design and TAF release to tune devices for use in future *in vivo* studies to be appropriate for the selected species as well as to consider dose escalation studies. Additionally, ambient shipping and terminal gamma-sterilization were demonstrated to have no deleterious effect on TAF stability nor device integrity and performance.

9.5. **Conclusion**

Development and *in-vitro* testing of a TFPD is presented here as a subcutaneous implant for delivery of the ARVs TAF, Elvitegravir and Rilpivirine for HIV PrEP. As a reservoir device with a thin-film membrane made from PCL, a biocompatible and biodegradable polymer [73] [74], this system should be retrievable throughout the duration of administration if needed, but will not require removal upon drug depletion. This is a highly desirable feature for HIV PrEP in particular due to the possibility of seroconversion after device implantation and the potential for developing resistance with low doses of a single ARV post-seroconversion.

The biodegradable and subcutaneous implant described here offers great potential for user-independent and long-acting delivery of HIV PrEP. With such flexibility in design and potential to tune the device for a broad range of release rates, the device is well suited for use throughout pre-clinical and clinical trials for an API such as TAF, Elvitegravir, or Rilpivirine for which the efficacious constant-rate subcutaneous dose for HIV PrEP has not yet been confirmed in humans.

Based on estimates of target dosing made from available pre-clinical and clinical pharmacokinetic data, TAF, of the three ARVs evaluated, is the most compatible for subcutaneous delivery with the TFPD. While elvitegravir may be suitable pending results of further studies investigating effective HIV PrEP with low elvitegravir plasma concentrations, release rates based on effective dosing for treatment are unattainable with a reasonably sized device. With extremely low solubility, relevant release rates from the TFPD with Rilpivirine are not achieved even with additional formulation efforts. With appropriate formulation, TAF release rates above the estimated upper range of subcutaneous constant rate dosing, based on effective antiretroviral treatment, are achievable in a maximum sized device. Additional studies demonstrated the accuracy and precision of device design and tunability for both human relevant devices and rat sized devices to achieve relevant human

equivalent doses, long-term release profiles and stability of TAF in human sized prototype devices, and stability of TAF loaded TFPD during shipping and terminal sterilization.

10. Case Study III: A TFPD as a Subcutaneous Implant for Contraception

10.1. Introduction

There are a variety of long-acting hormonal contraceptive options commercially available. These contraceptive options have the potential to increase user compliance while also reducing side effects. [76] Multiple routes of administration including transdermal patches, depot injections, sub-dermal implants, and intravaginal rings offer contraception for one month up to a five years. Depot injections and implants are available for users who prefer a long-acting and user-independent systemic option. Commercially available depot injections include Sayana ® Press and Depo-Provera ®, both made by Pfizer, Inc., and Noristerat by Bayer. These injections last 13, 12, and 8 weeks respectively and do not require follow-up for removal. While reversible after the duration of administration, these contraceptive injections cannot be retrieved or removed after administration. In contrast to the injections that are not retrievable and last only a few months, implants are retrievable and are significantly longer in their duration. Two contraceptive implants are currently available: Jadelle® by Bayer, and Implanon ® by Merck. Both implants are delivered subdermal and are non-biodegradable, and thus require follow-up appointments and removal. Jadelle® requires implantation of two rods, both 2.5 mm in diameter and 43 mm long, while Implanon ® is only a single rod, 2 mm in diameter and 40 mm long. Both provide contraception for up to 5 years. One of the major challenges for these contraceptive implants is device retrieval which can be problematic due to difficulties in locating the implant when inserted too deep in the arm (subcutaneously rather than subdermally) or upon weight gain. [76]

There is a gap in the contraceptive market for a systemic user-independent hormonal contraceptive with a mid-range duration of 1 to 2 years. While the concept of contraceptive implants based on similar principles is not novel [77] [78], in fact several examples of polymer-based contraceptive

systems have been explored [79] [80], the thin film membrane and reservoir design of the TFPD platform offers a contraceptive implant alternative delivering levenorgestrel, the same active ingredient in the Jadelle implant, that is biodegradable, significantly smaller than other available implants, and could be designed for durations in the 6-month to 2-year range. This case-study presents a proof-of-principle study describing a levonorgestrel biodegradable TFPD implant based on the fundamentals of TFPD design described previously.

10.2. LNG Dosing

An estimate of effective levenorgestrel dosing from an implant can be made based on clinical pharmacokinetic and drug release profiles from Norplant ®, the precursor to Jadelle ®. Drug release from the Norplant implant is not constant, and decreases over time. Based on the pharmacokinetic profile for Norplant, between 18-24 months after implantation, the average plasma concentration of levonorgestrel is 300 pg/ml. [81] The corresponding average release rate from the Norplant system during this same time frame is 30 µg/day. [82] Furthermore, based on a basic one compartment pharmacokinetic model utilizing parameters from oral dosing of levonorgestrel ($t_{1/2}$ = 25 h, V_{ss} = 100 L, CL_{ss} = 0.7 ml/min/kg) [83] and assuming a 100% bioavailability, a 10 µg/day constant rate release will result in a 300 pg/ml plasma concentration and a 30 µg/day release in 800 pg/ml plasma concentration. Therefore, effective constant-rate dosing of levonorgestrel from an implant is estimated between 10-30 µg/day.

10.3. LNG release from TFPD

10.3.1. *Short term screening studies*

Short term and screening studies, comparable to those described in Case Study II for TAF and Rilpivirine TFPD development were conducted to:

- **a)** Determine if LNG release from TFPD is membrane controlled
- **b)** Determine correlation between membrane thickness and LNG release

c) Determine correlation between surface area and LNG release

d) Determine device size required to achieve target release rate

Figure 61 and Figure 62 show the results of these screening studies. Figure 61 illustrates the proportional relationship between LNG release and membrane surface area for membranes with all the same thickness (7 µm). Figure 62 shows the area normalized release profiles for two sets of devices with different membrane thicknesses. The inversely proportional relationship between membrane thickness and release is evident as the release rate nearly doubles (1.9-fold increase) as the membrane thickness is cut roughly in half (0.6-fold decrease). The expected linear correlations between membrane surface area and thickness and release rates indicate that in the TFPD, LNG release is membrane controlled. Furthermore, as illustrated in Figure 61, devices with 7 µm thick membranes and surface areas around 100 mm^2 result in release rates roughly 10-fold higher than required for effective contraception. This suggests that significantly smaller devices are suitable as contraceptive implants.

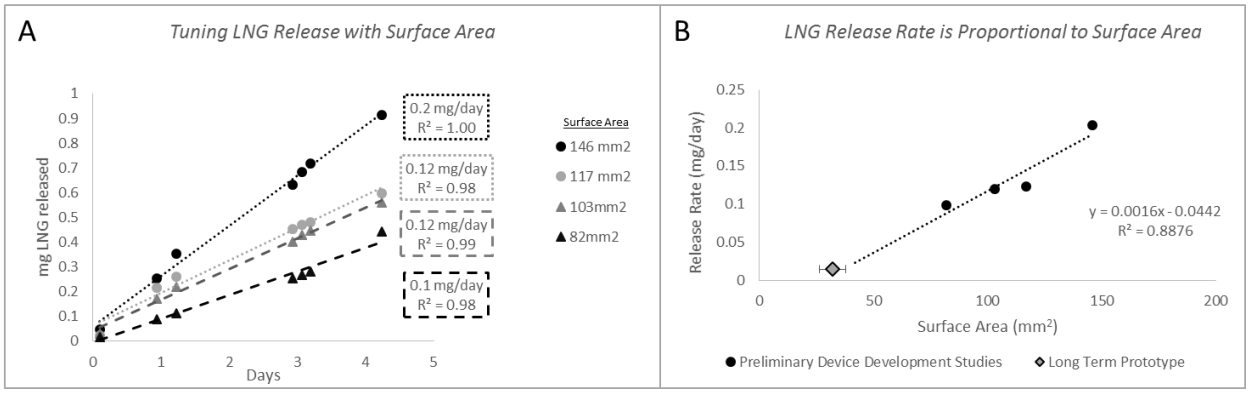

Figure 59 Levonorgestrel release from TFPD is proportional to membrane surface area. All devices described in this figure have 7 µm thick membranes. (A) Individual release profiles for devices with varied surface areas. (B) Release rates calculated from slopes of each series in (A) compared to surface areas illustrate linear correlation. Release rate and surface area for long term prototype devices also displayed, demonstrating accuracy of correlation even at smaller surface areas.

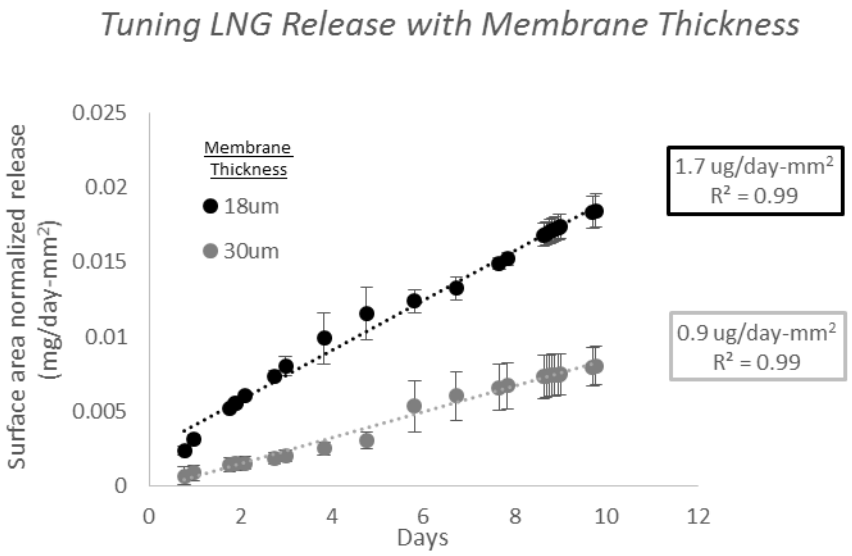

Figure 60 Levonorgestrel release from TFPD is inversely proportional to membrane thickness. When membrane thickness doubles, release rate halves.

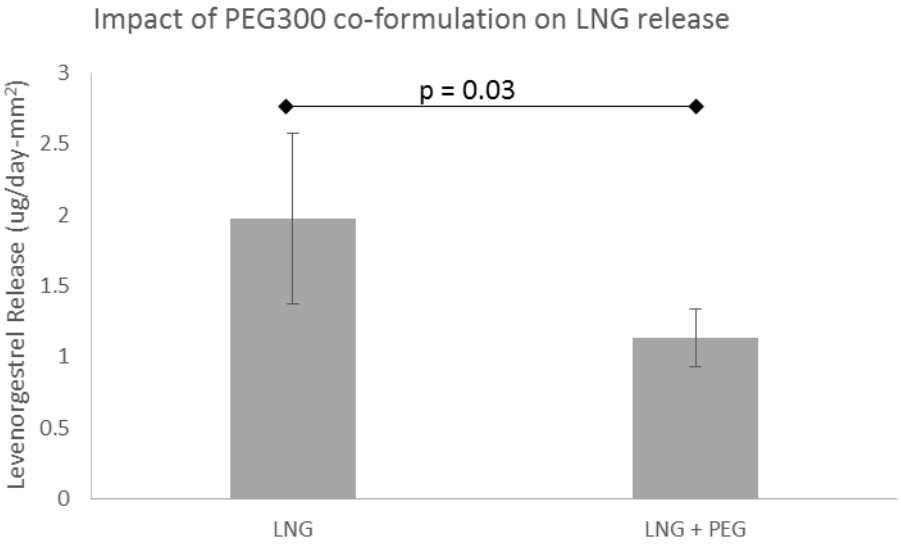

Figure 61 Co-formulation of levonorgestrel with PEG300 (2:1 w/w) slightly decreases release rate from TFPD. Co-formulation is used to facilitate loading of small TFPDs at bench scale.

10.3.2. *Prototype studies*

Based on the empirical correlations in Figure 61 and Figure 62, proof-of-concept prototype devices (n=2) were designed to target 15 µg/day release rates of LNG. PEG300, in a 2:1 w/w slurry with LNG, was used to facilitate loading of these small devices. As Figure 63 shows, the co-

formulation of LNG with PEG300 slightly decreases release rates; however, use of this excipient is necessary to load these small devices at the bench scale and is thus included in these prototype studies. Figure 64A describes the details of these prototype devices, Figure 64B captures an image of the devices, highlighting the small size, and Figure 64C shows the cumulative release profile for LNG out to 80 days; based on LNG loading into these devices, they are expected to continue releasing in a linear fashion until device depletion at around 170 days.[13]

A

Device Parameters (n=2)		
Formulation	2:1 w/w PEG300:LNG	PEG300 used to facilitate loading
Area	32 mm^2 +/- 5	Rod dimensions: • A: 2mm diameter, 6mm long • B: 1.3mm diameter, 7mm long
LNG Load	2.2 mg +/- 0.1 mg	Device duration: 170 days

B

C

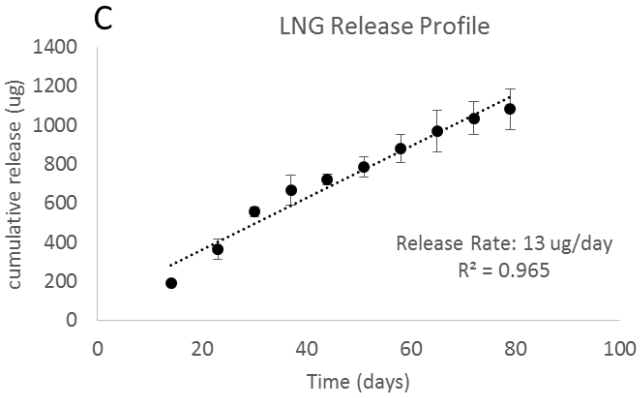

Figure 62 Levonorgestrel TFPD contraceptive implant prototypes. (A) Device parameters; (B) Images of prototype devices highlighting small size; (C) In vitro release profile demonstrating 13 ug/day constant rate release.

[13] Experiment on-going.

10.4. **Conclusion**

The preliminary work presented here demonstrates the potential to develop a contraceptive implant based on the TFPD platform. Benefits of this system over existing contraceptive implants include that it is biodegradable, much smaller than existing implants, exhibits constant rate release, and can be tuned to accommodate target release rates and implant durations. For example, the prototype devices presented here are only 1-2mm in diameter and 6-7 mm long and contain enough LNG for roughly a 6 month duration, a device could be designed with higher drug loading resulting in longer duration of contraception. Such a device could be comparable in size to the prototypes with a higher drug loading achieved with more refined fabrication techniques, or a slightly longer device with a larger reservoir and thus loading capacity could be designed with a thicker membrane to achieve the same target release rates. Additionally, the dimensions of a LNG TFPD contraceptive could be adjusted to be compatible for co-insertion with the ARV TFPD presented in Case Study II to achieve a multipurpose technology implant. The work presented here simply illustrates the potential for developing such systems, but significant work in manufacturing and pre-clinical evaluation would be needed to bring such a system to fruition.

11. References

[1] M. Woodruff and D. Hutmacher, "The return of a forgotten polymer: Polycaprolactone in the 21st century," *Progress in Polymer Science,* vol. 35, no. 10, pp. 1217-1256, 2010.

[2] J. Hu, Y.-C. Zhou, L.-H. Huang and H.-B. Lu, "Development of biodegradable polycaprolactone film as an internal fixation material to enhance tendon repair: an in vitro study," *BMC Musculoskeletal Disorders,* vol. 14, no. 246, 2013.

[3] L. Mei, J. Boa, L. Tang, C. Zhang, H. Wang, L. Sun, G. Ma, L. Huang, J. Yang, L. Zhang, K. Liu, C. Song and H. Sun, "A novel mifepristone-loaded implant for long-term treatment of endometriosis: In vitro and in vivo studies," *European Journal of Pharmaceutical Sciences,* vol. 39, pp. 421-427, 2010.

[4] J. Williams, A. Adewunmi, R. Schek, C. Flanagan, P. Krebsbach, S. Feinberg, S. Hollister and S. Das, "Bone tissue engineering using polycaprolactone scaffolds fabricated via selective laser sintering," *Biomaterials,* vol. 26, pp. 4817-4827, 2005.

[5] C. Pitt, F. Chasalow, Y. Hibionada, D. Klimas and A. Schindler, "Aliphatic Polyesters. I. The degradation of Poly(e-caprolactone) In Vivo," *Journal of Applied Polymer Science,* vol. 26, pp. 3779-3787, 1981.

[6] H. Sun, L. Mei, C. Song, X. Cui and P. Wang, "The in vivo degradation, absorption, and excretion of PCL-based implant," *Biomaterials,* vol. 27, pp. 1735-1740, 2006.

[7] D. Bernards, K. Lance, N. Ciaccio and T. Desai, "Nanostructure Thin Film Polymer Devices for Constant-Rate Protein Delivery," *Nanoletters,* vol. 12, pp. 5355-5361, 2012.

[8] J. Siepmann and F. Siepmann, "Review: Modeling of diffusion controlled drug delivery," *Journal of controlled release,* vol. 161, pp. 351-362, 2012.

[9] J. van Brakel and P. Heertjes, "Analysis of diffusion in macroporous media in terms of a porosity, a tortuosity, and a constrictivity factor.," *Int. J. Heat Mass Transfer,* vol. 17, pp. 1093-1103, 1974.

[10] B. Mitchell, An introduction to materials engineering and science for chemical and materials engineers, Hoboken, NJ: John Wiley & Sons, Inc., 2004.

[11] L. Clark, G. Ye and R. Snurr, "Molecular traffic control in a nanoscale system.," *Phys Rev Lett,* vol. 84, pp. 2893-2896, 2000.

[12] K. Hahn, J. Karger and V. Kukla, "Single-file diffusion observation.," *Phys. Rev. Lett.,* vol. 76, pp. 2762-2765, 1996.

[13] D. Klose, S. F., K. Elkharraz and F. Siepmann, "PLGA-based drug delivery systems: importance of drug and device geometry.," *International Journal of Pharmaceutics,* vol. 354, pp. 95-103, 2008.

[14] R. Rosenberg, W. Devennev and S. D. N. Siegel, "Anomalous release of hydrophillic drugs from poly(e-caprolactone) matrices," *Molecular Pharmaceutics,* vol. 4, pp. 943-948, 2007.

[15] K. Sung, R. Han, O. Hu and L. Hus, "Controlled release of Nalbuphine prodrugs from biodegradable polymer matrices: influence of prodrug hydrophilicity and polymer composition," *International Journal of Pharmaceutics,* vol. 172, pp. 17-25, 1998.

[16] J. Petropoulus, K. Papadokostaki and S. Amarantos, "A general model for the release of active agents incorporated in swellable polymeric matrices.," *Journal of Polymer Science B: Polymer Physics,* vol. 30, pp. 717-725, 1992.

[17] J. Siepmann and A. Gopferich, "Mathematical modeling of bioerodible, polymeric drug delivery systems," *Advanced Drug Delivery Reviews,* vol. 48, pp. 229-247, 2001.

[18] J. Siepmann and F. Siepmann, "Review: modeling of diffusion controlled drug delivery.," *Journal of Controlled Release,* vol. 161, pp. 351-362, 2012.

[19] E. Schlesinger, N. Ciaccio and T. Desai, "Polycaprolactone Thin-Film Drug Delivery Systems: Empirical and Predictive Models for Device Design," *Material Science and Engineering C: Materi Bio Appl,* vol. 57, pp. 232-239, 2015.

[20] A. Jaeger, F. Flesch, J. Kopferschmitt and P. Sauder, "InChem - Timolol," 28 March 1991. [Online]. Available: http://www.inchem.org/documents/pims/pharm/timolol.htm. [Accessed 2014].

[21] D. Wishart, C. Knox, A. Guao, D. Cheng, S. Shrivastava and T. D. , "DrugBank: a knowledge base for drugs, drug actions and drug targets.," *Nucleic Acid Res ,* vol. 36 , no. database issue, pp. D901-6, 2008.

[22] H. Hiratani, A. Fujiwara, Y. Tamiya, Y. Mizutani and C. Alvarez-Lorenzo, "Ocular release of timolol from molecularly imprinted soft contact lenses.," *Biomaterials,* vol. 26, pp. 1293-1298, 2005.

[23] H. Jung Jung and A. Chauhan, "Extended release of timolol from nanoparticle loaded fornix insert for glaucoma therapy," *Journal of Ocular Pharmacological Therapeutics,* vol. 29, pp. 229-235, 2013.

[24] O. Kasilo and C. Nhachi, "InChem - Primaquine Phosphate," March 1990. [Online]. Available: http://www.inchem.org/documents/pims/pharm/primaqui.htm. [Accessed 2014].

[25] C. Dusautois and S. Neves, "Hydroxypropylbetacyclodextrin," *Solid Dosage (www.pharma-mag.com),* vol. May/June, pp. 36-39, 2009.

[26] T. Reintjes, " Solubility enhancement with BASF pharma polymers: solubilizer compendium," BASF SE, Lampertheim, Germany, 2011.

[27] M. Casas, A. Aguilar-de-Levya and I. Caraballo, "Towards a rational basis for selection of excipients: Excipient Efficiency for controlled release," *International Journal of Pharmaceutics,* vol. 494, no. 1, pp. 288-295, 2015.

[28] F. Wang, G. Saidel and J. Gao, "A mechanistic model of controlled drug release from polymer millirods: Effects of excipients and complex binding," *Journal of Controlled Release,* vol. 119, no. 1, pp. 111-120, 2007.

[29] M. O'Roruke, "Next generation ocular drug delivery platforms," *Eye on Innovation, The Official Publication of OIS,* vol. 1, no. 7, 2014.

[30] I. Rupenthal, "Sector Overview: Ocular drug delivery technologies: exciting times ahead.," *www.ondrugdelivery.com,* 2015.

[31] R. Guadana, H. Ananthula, A. Parenky and A. Mitra, "Ocular Drug Delivery," *AAPS J.,* vol. 12, no. 3, pp. 348-360, 2010.

[32] W. Wang, "Protein aggregation and its inhibition in biopharmaceutics," *International Journal of Pharmaceutics,* no. 289, pp. 1-30, 2005.

[33] W. Wang, "Instability, stabilization, and formulation of liquid protein pharmaceuticals," *International Journal of Pharmaceutics,* vol. 185, pp. 129-188, 1999.

[34] Y. Zhou and C. Hall, "Solute excluded-volume effects on the stability of globular proteins: a statistical thermodynamic theory," *Biopolymers,* vol. 38, pp. 273-284, 1996.

[35] T. Arakawa, S. Prestrelski, W. Kenney and J. Carpenter, "Factors affecting short-term and long-term stabilities of proteins," *Advance Drug Delivery Reviews,* vol. 10, pp. 1-28, 1993.

[36] S. Dumitriu and E. Chornet, "Inclusion and release of proteins from polysaccharide-based polyion complexes," *Advanced Drug Delivery Reviews,* vol. 31, pp. 223-246, 1998.

[37] D. Atha and K. Ingham, "Mechanism of precipitation of proteins by polyethylene glycols," *Journal of Biological Chemistry,* vol. 256, no. 23, pp. 12108-12117, 1981.

[38] M. Kumar, "A review of chitin and chitosan applications," *Reactive and Functional Polymers,* vol. 46, no. 1, pp. 1-27, 2000.

[39] B. Karjewska, "Application of chitin- and chitosan-based materials for enzyme immbolizations: a review," *Enzyme and Microbial Technology,* vol. 35, no. 2-3, pp. 126-139, 2004.

[40] J. Ji, J. Liu and Y. Wang, "Compositions and methods useful for stabilizing protein-containing formulations". USA Patent WO2011119487 A2, 29 September 2011.

[41] J. Baeten and C. Celum, "Systemic and topical drugs for the prevention of HIV infection: antiretroviral preexposure prophylaxis," *Annu Rev Med,* vol. 64, pp. 219-232, 2013.

[42] I. McGowan, "An overview of antiretroviral pre-exposure prophylaxis of HIV infection," *Am. J. Reprod. Immunol.,* vol. 71, no. 6, pp. 624-630, 2014.

[43] K. Amico, L. Mansoor, A. Corneli, K. Torjesen and A. van der Straten, "Adherence support approaches in biomedical HIV prevention trials: experienes, insights and future directions from four multisite prevention trials," *AIDS Behav.,* vol. 17, pp. 2143-2155, 2013.

[44] N. I. o. A. a. I. D. (NIAID), "Emtricitabine/Tenofovir Disproxil Fumarate for HIV Prevention in Men (iPrEx)," *clinicaltrials.gov [Internet]. Bethesda (MD): National Library of Medicine (US),* 2000-[cited 2015 Aug 02].

[45] U. o. Washington, "Pre-Exposure Prophylaxis to Prevent HIV-1 Acquisition Within HIV-1 Discordant Couples (Partners PrEP)," *Clinicaltrials.gov [internet]. Bethesda (MD): National Library of Medicine (US).,* 2000-[cited 2015 Aug 02].

[46] J. Marrazzo, G. Ramjee, B. Richardson, K. Gomez, N. Mgodi, G. Nair and e. al., "Tenofovir-based preexposure prophylaxis for HIV infection among African women," *NEngl JMed,* vol. 372, pp. 50-518, 2015.

[47] L. Van Damme, A. Corneli, K. Ahemd, K. Agot, J. Lombaard, S. Kapiga and e. al., "Preexposure prophylaxis for HIV infection among African women," *NEngl JMed,* vol. 367, pp. 411-422, 2012.

[48] N. I. o. A. a. I. D. NIAID, "Safety and Effeciveness of Tenofovir 1% Gel, Tenofovir Disproxil Fumarate, and Emtricitabine/Tenofovir Disproxil Fumarate Tablets in Preventing HIV in Women," *ClinicalTrials.gov [Internet]. Bethesda (MD): National Library of Medicine (US).,* 2000-[cited 2015 Aug 02].

[49] W. Spreen, D. Margolis and J. Pottage, "Long-acting antiretrovirals for HIV treatment and prevention," *Current Opinion in HIV and AIDS,* vol. 8, no. 6, pp. 565-571, 2013.

[50] G. van't Klooster, E. Hoeben, H. Borghys, A. Looszova, M. Bouche, F. van Velsen and L. Baert, "Pharmacokinetics and Disoposition of Rilpivirine (TMC278) Nanosuspension as a Long-acting Injectable Antiretroviral Formulation," *Antimicrobial Agents and Chemotherapy,* vol. 54, no. 5, pp. 2042-2050, 2010.

[51] W. Spreen, S. Ford, S. Chen, D. Wilfret, D. Margolis, E. Gould and S. Piscitelli, "GSK1265744 Pharmacokinetics in Plasma and Tissue After Single-Dose Long Acting Injectable Administration in Healthy Subjects," *J. Acquir. Immun. Defic. Syndr.,* vol. 67, no. 5, pp. 481-486, 2014.

[52] S. Taylor, M. Boffito, S. Khoo, E. Smit and D. Back, "Stopping antiretroviral therapy," *AIDS,* vol. 21, pp. 1673-1682, 2007.

[53] N. C. f. B. I. (NCBI), "PubChem Compound Database," [Online]. Available: https://pubchem.ncbi.nlm.nih.gov/compound/5277135. [Accessed 14 October 2015].

[54] S. Ramanathan, A. Mathias, P. German and B. Kearney, "Clinical pharmacokinetic and pharmacodynamic profile of the HIV integrase inhibitor elvitegravir," *Clin Pharmacokinet,* vol. 50, no. 4, pp. 229-244, 2011.

[55] J. Lee, A. Calmy, I. Andrieux-Meyer and N. Ford, "Review of the safety, efficacy, and pharmacokinetics of elvitegravir with emphasis on resource-limited settings," *HIV/AIDS - Research and Palliative Care,* vol. 4, pp. 5-15, 2012.

[56] J. Adams and e. al, "Pharmacology of HIV integrase inhibitors," *Curr Opin HIV AIDS,* vol. 7, no. 5, pp. 390-400, 2012.

[57] C. Dobard, S. Sharma, U. Parikh, R. West, A. Taylor, A. Martin, C. Pau, D. Hanson, J. Lipscomb, J. Smith, F. Novembre, D. Hazuda, J. Garcia-Lerma and W. Heneine, "Postexposure protection of macaques from vaginal SHIV infection by topical integrase inhibitors," *Sci Transl Med,* vol. 6, no. 227, 2014.

[58] J. Radzio, W. Spreen, Y. Yueh, J. Mitchell, L. Jenkins, J. Garcia-Lema and W. Heniene, "The long-acting integrase inhibitor GSK744 protects macaques from repeated intravaginal SHIV challenge," *Science Translational Medicine,* vol. 7, no. 270, 2015.

[59] ACD/Labs Percepta Platform - Physchem Module, "Chemspider," Royal Society of Chemistry, [Online]. Available: http://www.chemspider.com/Chemical-Structure.4441060.html. [Accessed 14 October 2015].

[60] I. Massud, A. Martin, C. Dinh, J. Mitchell, L. Jenkins, W. Heneine, C. Pau and J. Garcia-Lerma, "Pharmacokinetic profile of raltevgravir, elvitegravir, and dolutegravir in plamsa and mucosal secretions in rhesus macaques," *Journal of Antimicrobial Chemotherapy,* vol. 70, pp. 1473-1481, 2015.

[61] A. Jackson and I. McGowan, "Long-acting rilpivirine for HIV prevention," *Curr Opin HIV AIDS,* vol. 10, no. 4, pp. 253-7, 2015.

[62] P. Williams, H. Crawels and B. E., "Formulation and pharmacology of long-acting rilpivirine," *Curr Opin HIV and AIDS,* vol. 10, pp. 233-238, 2015.

[63] R. Verloes, G. van't Klooster, L. Baert and e. al, "TMC278 long acting - a parenteral nanosuspension formulation that provides sustained clinically relevant plasma concentrations in HIV-negative volunteers," in *17th International AIDS Conference*, Mexico City, 2008.

[64] W. Spreen, P. Williams, D. Margolis, S. Ford, H. Crauwels, Y. Lou, E. Gould, M. Stevens and S. Piscitelli, "Pharmacokinetics, safety, and tolerability with repeat doses of GSK1265744 and rilpivirine (TMC278) long-acting nanosuspensions in healthy adults," *J Acquir Immune Defic Syndr,* vol. 67, no. 5, pp. 487-492, 2014.

[65] P. Stevens, J. Peeters, R. Vandecruys, A. Stappers and A. Copmans, "Salt of 4[[4-[[4-(2-Cyanoethenyl)-2,6-dimethylphenyl]amino]-2-Pyrimidinyl]amino]benzonitrile". CA, EP, WO Patent EP1632232B1, CA2577288A1, CA2577288C, EP1632232A1, WO2006024668A1, 11 May 2011.

[66] W. Lee, G. He, E. Eisenberg, T. Cihlar, S. Swaminathan, A. Mulato and C. K. , "Selective Intracellular Activation of a Novel Prodrug of the Human Immunodeficiency Virus Reverse Transcriptase

Inhibitor Tenofovir Leads to Preferential Distribution and Accumulation in Lymphatic Tissue," *Antimicrobial Agents and Chemotherapy,* vol. 49, no. 5, pp. 1989-1906, 2005.

[67] J. Falutz, "Unmasking the bare bones of HIV Preexposure Prophylaxis," *Clinical Infections disease,* pp. 1-3, 2015.

[68] R. Grant, J. Lama, P. Anderson, V. McMahan, A. Liu, L. Vargas and e. al., "Preexposure prophylaxis for HIV prevention in men who have sex with men," *N Engl J Med,* vol. 363, pp. 2587-2599, 2010.

[69] U. o. N. C. C. H. (NCT02357602), "Dose Proportionality of TFV-DP After a Single Dose of GS-7340 in Women," *ClinicalTrials.gov,* 2015.

[70] P. Ruane and et al., "Antiviral Activity and Safety, and Pharmacokinetics/Pharmacodynamics of Tenofovir Alafenamide as 10-day Monotherapy in HIV-1 Positive Adults," *J. Acquir. Immune. Defic. Syndr.,* vol. 63, no. 4, pp. 449-455, 2013.

[71] D. Babusis and et. al., "Mechanism for Effective Lymphoid Cell and Tissue Loading Following Oral Administration fo Nucleotide Prodrug GS-7340," *Mol. Pharm. ,* vol. 10, no. 2, pp. 459-466, 2013.

[72] M. Gunawardana, M. Remedios-Chan, C. Miller, R. Fanter, F. Yang, M. Marzinke, C. Hendrix, M. Beliveau, J. Moss, T. Smith and M. Baum, "Pharmacokinetics of Long-Acting Tenofovir Alafenimide (GS-7340) Subdermapl Implant for HIV Prophylaxis," *Antimicrobial Agents and Chemotherapy,* vol. 59, no. 7, pp. 3913-3919, 2015.

[73] H. Sun, L. Mei, C. Song, X. Cui and P. Wang, "The in vivo Degradation, Absoprtion, and Excetion of PCL-based Implant," *Biomaterials,* vol. 27, pp. 1735-1740, 2006.

[74] M. Woodruff and D. Hutmacher, "The Return of the Forgotten Polymer: Polycaprolactone in the 21st Century," *Progress in Polymer Science,* vol. 35, no. 10, pp. 1217-1256, 2010.

[75] N. C. f. B. I. (NCBI), "PubChem Compound Database," [Online]. Available: https://pubchem.ncbi.nlm.nih.gov/compound/6451164. [Accessed 28 October 2015].

[76] L. Bahamondes and M. Bahamondes, "New and emerging contraceptives: a state-of-the-art review," *International Journal of Women's Health,* vol. 6, pp. 221-234, 2014.

[77] P. Darney, "Subdermal progestin implant contraception," *Curr Opin Obstet Gynecol,* vol. 3, no. 4, pp. 470-6, 1991.

[78] H. Croxatt, "Progestin implants for female contraception," *Contraception,* vol. 65, no. 1, pp. 15-9, 2002.

[79] G. Ma, C. Song, H. Sun, J. Yang and X. Leng, "A biodegradable levenorgestrel-releasing implant made of PCL/F68 compound as tested in rats and dogs," *Contraception,* vol. 74, no. 2, pp. 141-147, 2006.

[80] C. Pitt, "Poly(a-caprolactone) and its copolymers.," in *Biodegradable polymers as drug delivery systems*, New York, Marcel Dekker, 1990, pp. 71-120.

[81] I. Sivin, P. Lahteenmaki, S. Ranta, P. Darney, C. Klaisle, L. Wan, D. Mishell, M. Lacarra, O. Viegas, P. Bilhareus, S. Koetsawang, M. Piya-Anant, S. Diaz, M. Pavez, F. Alvarez, V. Brache, K. LaGuardia, H. Nash and J. Stern, "Levonorgestrel concentrations during use of levonorgestrel rod (LNG ROD) implants," *Contraception,* vol. 55, no. 2, pp. 81-85, 1997.

[82] Wyeth Pharmaceuticals, *Product Label/Insert for Norplant (R) System,* 2008.

[83] Schering LTD, *Package Insert for Miranova,* 2004.

[84] G. van Klooster, E. Hoeben, H. Borghys, A. Looszova, M. Bouche, F. van Velsen and L. Baert, "Pharmacokinetics and disposition of rilpivirine (TMC278) nanosuspension as a long-acting injectable antiretroviral formulation," *Antimicrobial agents and chemotherapy,* vol. 54, no. 5, pp. 2042-2050, 2010.

Publishing Agreement

It is the policy of the University to encourage the distribution of all theses, dissertations, and manuscripts. Copies of all UCSF theses, dissertations, and manuscripts will be routed to the library via the Graduate Division. The library will make all theses, dissertations, and manuscripts accessible to the public and will preserve these to the best of their abilities, in perpetuity.

Please sign the following statement:

I hereby grant permission to the Graduate Division of the University of California, San Francisco to release copies of my thesis, dissertation, or manuscript to the Campus Library to provide access and preservation, in whole or in part, in perpetuity.

Author Signature

12/15/2015
Date